DETERMINATION OF THE SITE OF ULTRASONIC ABSORPTION IN SUSPENSIONS OF LARGE UNILAMELLAR VESICLES

BY

LORALIE DAWN MA

B.S., University of Illinois, 1985

THESIS

Submitted in partial fulfillment of the requirements
for the degree of Doctor of Philosophy in Biophysics
in the Graduate College of the
University of Illinois at Urbana-Champaign, 1988

Urbana, Illinois

ACKNOWLEDGEMENTS

I am deeply grateful to Professor Floyd Dunn for his much appreciated tutelage, along with his kind encouragement throughout this project. I would also like to express my deepest thanks to Professor Richard Magin, without whom the daily obstacles encountered in the course of my work might have been insurmountable. Valerie Maynard is also given my sincere thanks for her many hours of expert advice as I started work on this project, and I would also like to thank Michael Niesman for his assistance in the preparation of biological samples. In addition, I would like to thank Dr. Terrance Smith for his help with the use of the differential scanning calorimeter. Thanks go to Billy McNeil, without whose machining expertise, none of my experiments would be possible, and I would also like to thank Joseph Cobb for his invaluable help with electronics and computers. I would especially like to thank Wanda Elliot and Nancy Dimond for their daily advice on laboratory matters and for their help in manuscript preparation. Thanks also to Robert Cicone for his excellent figures which are throughout this work. This work is dedicated to my husband and family, whose patience, understanding and encouragement made this work possible.

This work was supported by the following grants: GM 12281 and CA 45689 of the National Institutes of Health.

TABLE OF CONTENTS

CHAPTER 1

INTRODUCTION

Ultrasound, a pressure wave with frequencies above the human perception limit, viz., beyond about 20 kHz, is often employed in science and technology [IEEE Centennial, 1984], and as a diagnostic and therapeutic tool in medicine [Kossoff and Fukuda, 1984; Chaussy et al., 1984]. The propagation of ultrasound through various types of media is dependent upon the physical characteristics, e.g., densities, compressibilities, homogeneity and chemical nature, of these media. As ultrasound interacts with, for example, biological media, energy attenuation occurs resulting from a number of factors which can be grouped into two categories, viz., scattering and absorption. Scattering refers to the removal of energy from the wave path by reflection, refraction and diffraction processes associated with structural elements of all sizes having distributions of speed of sound, acoustic impedance, etc. Absorption refers to the conversion of ultrasonic energy to thermal energy and the consequent dissipation of heat.

The observed rate of ultrasound absorption in biological systems is relatively high, is largely determined by the macromolecular content [Dunn and O'Brien, 1976], and is not accounted for completely by theories of classical ultrasound propagation in bulk media [Herzfeld and Litovitz, 1959; Dunn et al., 1969]. The fate of the absorbed energy as heat dissipation or as contributions to conformational or chemical changes in, for example, cells or the cell membrane, is poorly understood, although ultrasound absorption has been studied as a function of protein, water, fat and collagen content in biological tissues [Dunn and O'Brien, 1976, O'Brien et al., 1987]. A deeper understanding of ultrasound absorption in biological media could aid in the identification of the events contributing to ultrasonic interaction with biological media. It is important to understand these mechanisms, to determine not only the safety of diagnostic and therapeutic ultrasound, but also as an aid to their effective application. In addition, with an understanding of ultrasonic interaction with cells, ultrasound may be used as a probe of molecular, cellular, and cell membrane events.

Biological systems are composed of many levels of structure and the ultrasound wave may interact at any level, depending upon its frequency. Ultrasound may interact with biological systems at the level of organs, their tissue structure, and their individual cells and macromolecules. Ultrasound absorption has been studied in tissues, and it can be used to characterize tissues [O'Brien et al., 1987; Olerud et al., 1987]. In order to understand the microscopic or macromolecular interaction of ultrasound with biological media, the understanding of ultrasound interaction with the cell and its various components is necessary. Ultrasound, a mechanical wave process, yields information about the mechanical properties of biological suspensions of cells. Direct measurement of the speed of sound and determination of the ultrasonic absorption coefficient per wavelength, $\alpha\lambda$, (the exponential reduction in the sound pressure amplitude as the acoustic wave travels the distance of one wavelength) can be made in these suspensions. Determinations of $\alpha\lambda$ as a function of temperature and frequency can provide information as to the nature of ultrasound interaction(s) with these systems. Compressibility, determinable by ultrasonic techniques, is related to biological membrane permeability, and viscosity, which contributes to ultrasonic absorption, is related to membrane fluidity [Mitaku and Okano, 1981].

To further simplify this investigation, models are often used in the study of the interactions between ultrasound and suspensions of cells. Biomembrane vesicles (liposomes) are useful models of biological systems for the elucidation of the interaction of ultrasound with cell suspensions, and as a step to answer the fundamental question of how ultrasound affects specific cellular function, in which membranes are found to play an important role. Ultrasound has been used to investigate the mechanical and thermodynamic properties of liposomes, including MLVs (multilamellar vesicles), SUVs (small unilamellar vesicles) and especially LUVs (large unilamellar vesicles), in aqueous suspension as model cell systems [Hammes and Roberts, 1970; Eggers and Funck, 1976; Gamble and Schimmel, 1978; Harkness and White, 1979; Strom-Jensen et al., 1984; Maynard, 1984; Maynard et al., 1985; Mitaku and Sakka, 1987].

Small unilamellar vesicles, formed by intense sonication of phospholipids in aqueous suspension, are spherical unilamellar vesicles with diameters in the range of 20 to 50 nm [Cullis and Hope, 1985]. Multilamellar vesicles, formed by agitation and vortexing of phospholipids in aqueous suspension, are composed of multiple bilayers, whose outside diameter ranges from approximately 1.0 to 3.0 μm [Paphadjopoulos et al., 1972]. Large unilamellar vesicles, formed by the reverse phase evaporation method [Szoka and Papahadjopoulos, 1976] are spherical, as determined by electron microscopy, with diameters in the range of 0.2 to 0.8 μm and are composed of natural or synthetic phospholipids (see Figure 1.1) [Strom-Jensen et al., 1984]. The relatively simple structure and composition of these vesicles, and their association with the suspending medium, could aid in identifying the events contributing to ultrasonic interaction with membranes. The LUV system can be made more complex and biologically relevant by, for example, incorporating within their structure lipid mixtures, proteins and other biomolecules in order to model living cells more closely.

The first ultrasound studies involving liposomes were performed on small unilamellar vesicle (SUV) and multilamellar vesicle (MLV) suspensions and showed that $\alpha\lambda$ exhibited maxima at certain relaxation frequencies [Gamble and Schimmel, 1978; Hammes and Roberts, 1970; Harkness and White, 1979]. The relaxational absorption of ultrasound in the vesicle suspensions was presumed to be due to ultrasonic coupling to movement of phospholipids in the vesicle membrane. It was observed with MLVs that $\alpha\lambda$ exhibited a large increase near the phase transition temperature (t_m) of the phospholipids in the vesicle membrane [Harkness and White, 1979; Sano et al., 1982]. The LUVs, which are structurally more similar to biological cells than are the SUVs or MLVs, also exhibited large increases in $\alpha\lambda$, in the 1-5 MHz range of ultrasound, near the phase transition temperature of the vesicle membrane. The peak in $\alpha\lambda$ was correlated with structural changes in the membrane which led to dramatic increases in the permeability of LUV membranes in the vicinity of the phase transition temperature. For the membrane composition used in these experiments, this increase in permeability, as measured by the release of tritiated Ara-C, occurred 2°C below the t_m of the phospholipid bilayer [Magin and Niesman, 1984]. Further

ultrasonic studies using LUVs of a specific composition (see Figure 1.2) have shown that, at the phase transition temperature of the liposomes, a maximum in $\alpha\lambda$ at 2.1 MHz occurred and represented a relaxation frequency of the LUV suspension [Strom-Jensen et al., 1984]. Such a frequency dependence was also seen in nuclear magnetic resonance (NMR) studies of MLVs, which showed correlation times of 10^{-6} to 10^{-8} seconds for the methylene groups of the fatty acyl chains nearest to and furthest from the phospholipid headgroups [Nagle, 1973].

Ultrasonic studies employing LUVs have shown that the incorporation of biological molecules into the membrane bilayer could affect the temperature dependence of $\alpha\lambda$, as well as its frequency dependence. For example, the incorporation of gramicidin into the phospholipid bilayer broadened the phase transition, possibly by decreasing the cooperativity of the phase transition, and the addition of 5 mole percent gramicidin shifted the relaxation frequency of the suspension from 2.1 to 0.75 MHz at t_m [Strom-Jensen et al., 1984]. These results suggested that certain substances that insert into the hydrophobic membrane are able to affect the time rate of the event responsible for the absorption of ultrasonic energy. It is therefore suggested that it is some event occurring within the hydrophobic phospholipid bilayer, at the phospholipid phase transition temperature, to which ultrasound couples, resulting in the $\alpha\lambda$ maximum at 2.1 MHz.

Ultrasonic absorption measurements have also been performed on LUV suspensions of different sizes, ranging from 0.03 μm to 0.4 μm in diameter, to determine whether LUV size has an effect on ultrasonic absorption [Maynard et al., 1985]. It was found that ultrasonic absorption per wavelength, $\alpha\lambda$, as a function of temperature was not dependent upon LUV size until very small LUV diameters (0.03 μm) were reached, whereupon the absorption versus temperature curve began to appear similar to that of SUVs. In studies of LUVs of different sizes, $\alpha\lambda_{max}$ (at t_m) as a function of frequency did not shift as a function of LUV size for LUVs separated by size in column chromatography or for 0.1 μm, 0.2 μm or 0.4 μm filtered LUVs. Experiments performed in this laboratory using SUVs showed that the relaxation frequency was shifted to low frequencies as might be expected due to the greater restriction of hydrocarbon side-chain motion, due to the small radius of curvature in the SUV

population. This further suggested that the absorption of ultrasound at 2.1 MHz is related to ultrasonic participating in a relaxation process that is not a function of liposome diameter, but rather of membrane mechanical properties.

It is the purpose of this study to determine the site and nature of the interaction of ultrasound with biological membranes. This was accomplished by perturbing LUV membranes, as models of biological membranes, with agents such that the resulting changes in LUV membrane dynamics would be reflected by changes in $\alpha\lambda$ of ultrasound as a function of temperature and frequency. By perturbing different sites of the LUV suspensions, e.g., the aqueous component of the suspension, the hydrophobic bilayer, the membrane-aqueous interface, etc., and by analyses of the resulting changes in ultrasonic absorption, the mechanisms of ultrasound interactions with the liposome membrane may be identified. If ultrasound interacted with a particular site of the bilayer, perturbation of that site (in the LUV suspension) might alter the observed ultrasonic absorption. Conversely, if the perturbation of a specific site, or aspect, of membrane structure did not result in a perturbation of the ultrasonic interaction with the LUV suspension, then that site would most likely not be the site of the observed ultrasound interaction with the LUVs. Changes in $\alpha\lambda$ as a function of frequency and temperature were noted. Analyses were performed to give information on the transition temperature, transition enthalpy and the Van't Hoff enthalpy of the transition, as well as to study the relaxational character of the transition, where the relaxation time is identified by the frequency of maximum ultrasound $\alpha\lambda$. The relaxation time is defined as the characteristic time needed for a reaction system, once perturbed, to reach a new state of equilibrium. Such analyses have been carried out in other media where it has been shown that $\alpha\lambda_{max}$ and the relaxation frequency f_{max} are related to the relaxation strength ($\Delta\kappa_S/\kappa_S$) (κ_S = adiabatic compressibility) of a reaction and could be used to determine the enthalpy and activation energy of a relaxation mechanism [Lamb, 1965]. Further analysis of data would determine whether the absorption changes seen as a function of temperature and frequency represent a thermal relaxation process or a structural relaxation process. A thermal relaxation process can be represented in terms of a single relaxation time or characteristic frequency,

whereas structural relaxation mechanisms usually give rise to a distribution of relaxation times and result in a velocity dispersion of ultrasound in the fluid media. Differentiation between thermal and structural relaxation mechanisms may be ascertained by studying $\alpha\lambda$ as a function of frequency and noting if, over an appropriate range of frequencies, a single relaxation frequency appeared or whether a distribution of frequencies occur.

Specifically, it is hypothesized that the site of ultrasonic interaction with the LUV membrane is at the level of the fatty acyl side chains of the phospholipid bilayer, and that the interaction comprises an event related to the trans to gauche conformational change of the phospholipid fatty acyl side chains occurring at the lipid bilayer phase transition that causes the increased excess ultrasonic $\alpha\lambda$ observed at the phase transition temperature of the LUVs. Therefore, agents that affect the hydrophobic portion of the bilayer should change the frequency dependence of $\alpha\lambda$, while those agents that affect other aspects of membrane dynamics should not.

The perturbing agents in this study were chosen such that each would affect a different aspect of membrane structure, and the corresponding changes in $\alpha\lambda$ as a function of temperature and frequency would give information to identify the aspects of membrane structure and dynamics most important in determining the absorption of ultrasonic energy in biological media. The perturbing agents used in this study were divalent cations (Ca^{2+}, Mg^{2+}), deuterium oxide, and the lipophilic ionophore, A23187, which are now briefly introduced.

Divalent cations, e.g., Ca^{2+} and Mg^{2+}, are known to interact specifically with negatively-charged phospholipids, viz., DPPG, to produce changes in the phase transition temperature and membrane permeability [Muhleisen et al., 1983]. They interact with the headgroups of the phospholipids, thus possibly perturbing the headgroup movements and their interactions with one another and the aqueous medium. As such agents do not interact with the hydrophobic region of the membrane bilayer, they should not perturb the kinetics of ultrasonic interaction with that bilayer.

Deuterium oxide, D_2O, is used as a specific variation on water structure in order to determine the sensitivity of ultrasonic absorption to perturbations of the membrane-water interaction. The D_2O is specfically different from water in such molecular properties as mass, density, dielectric constant, dipole moment, melting and boiling points, critical temperature and pressure, triple point temperature and pressure, and index of refraction [CRC, 1987]. These differences are a consequence of the difference in mass between these two aqueous types, as the molecular weight of D_2O is 10% greater than that of water. In this study, D_2O is used in place of H_2O (in specified proportions) as the main component of the aqueous hepes buffered saline, in order to investigate the importance of the aqueous component in the interactions of ultrasound with LUV membranes. The differences in the interaction of D_2O as compared to H_2O with LUV membranes may not be complex. However, because of its 10% greater mass (MW = 20.028), D_2O may interact with individual phospholipids differently than does H_2O with respect to the phospholipid membrane.

The third perturbing agent in this study is the antibiotic, Ca^{2+} - specific ionophore, A23187 ($C_{29}H_{37}N_3O_6$, m.p. = 181-182°C). The A23187 is a small molecular weight, viz., 523.6 daltons, ionophore which forms stable complexes with divalent cations, thus making these ions soluble in ordinary organic solvents. It has been shown to partition into the phospholipid bilayer of phosphatidylcholine liposomes [Vidaver and Lee, 1983]. Such hydrophobic agents have been studied previously and have given varying results as to changes in $\alpha\lambda$ as a function of temperature and frequency [Strom-Jensen et al., 1984]. The structure of this ionophore is shown in Figure 1.3.

The A23187 complexes consist of two molecules per divalent cation complexed. However, A23187 is not well defined in its effect on membrane structure. It should partition into the hydrophobic membrane as it is readily soluble in organic solvents [Houslay and Stanley, 1982]. The insertion of A23187 may affect the cooperative unit of the transition, as can be detected by measurements of $\alpha\lambda$ as a function of temperature. However, it is not known whether it may affect movement in the phospholipids and/or their carbon side chains.

Also, it is possible that the ionophore may not partition homogeneously into the membrane. If it does not, two or more peaks may be seen by the determination of $\alpha\lambda$ as a function of temperature or frequency. Note that, as A23187 does interact with the hydrophobic bilayer, $\alpha\lambda$ as a function of frequency in these LUV suspensions may be perturbed.

This thesis is organized in the following manner. Chapter 2 addresses the acoustic theory of ultrasonic absorption in fluid media with specific attention to the microscopic absorption mechanisms of an ultrasound wave in fluid media, and also addresses the theory of the acoustic interferometer. Chapter 3 deals with the biochemical materials and the methods used to synthesize liposomes, and includes details on the structure and operation of the acoustic interferometer. The addition of increasing concentrations of divalent cations to LUV suspensions, and its effects on $\alpha\lambda$ as a function of temperature and frequency are presented and discussed in Chapter 4. The effects of replacing increasing portions of the aqueous content of LUV suspensions with D_2O on $\alpha\lambda$ and on differential scanning calorimetry (DSC) measurements are discussed in Chapter 5, as are the implications for ultrasound interaction with the aqueous portion of LUV suspensions, and the effects of the addition of A23187 to LUV membranes on $\alpha\lambda$ are discussed in Chapter 6. The replacement of DPPC by per-deuterated DPPC, and its effect on $\alpha\lambda$ as a function of temperature and frequency are also discussed in Chapter 6. Chapter 7 includes a final discussion of the experiments presented in Chapters 4, 5 and 6, summarizes the results from the three phases of experimentation in this thesis, proposes mechanisms for ultrasound absorption in LUV membranes and also addresses future directions in this field.

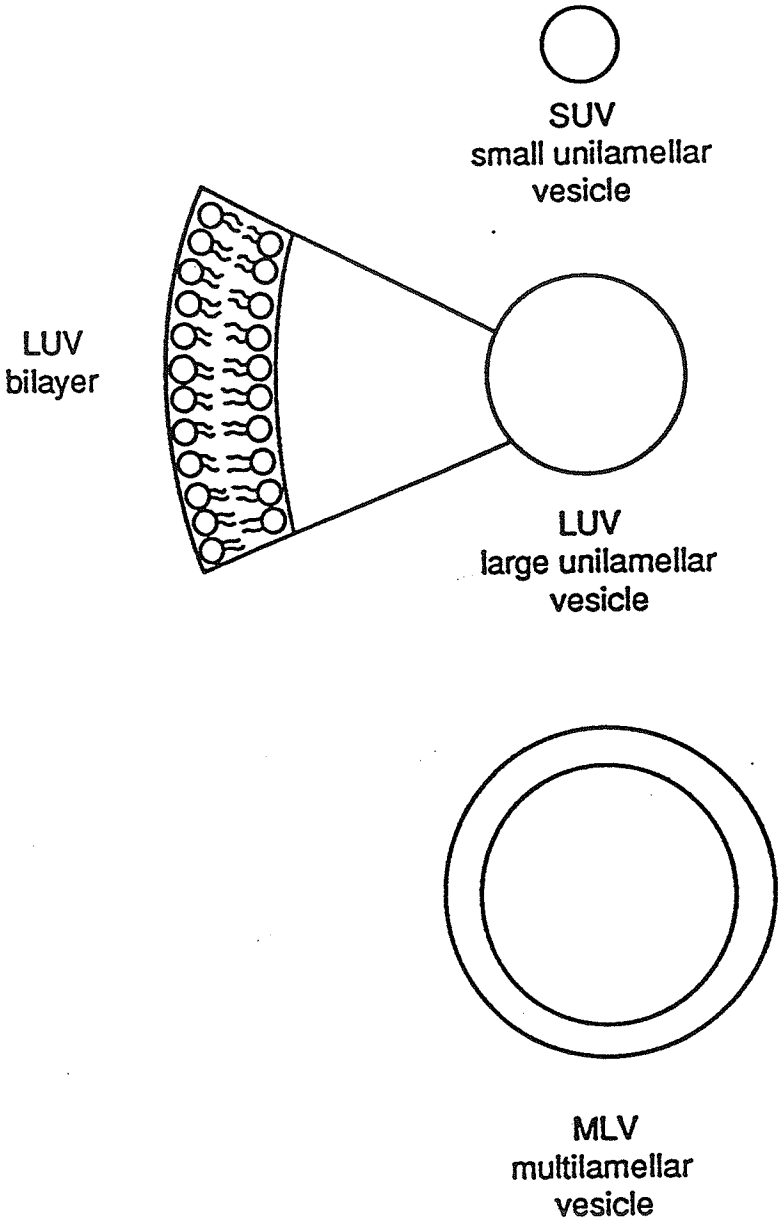

Figure 1.1 Three categories of liposomes with an enlargement of the bilayer portion. The negative headgroups indicate the 20% of the molecules which are DPPG (cf. Fig. 1.2) [Maynard, 1984].

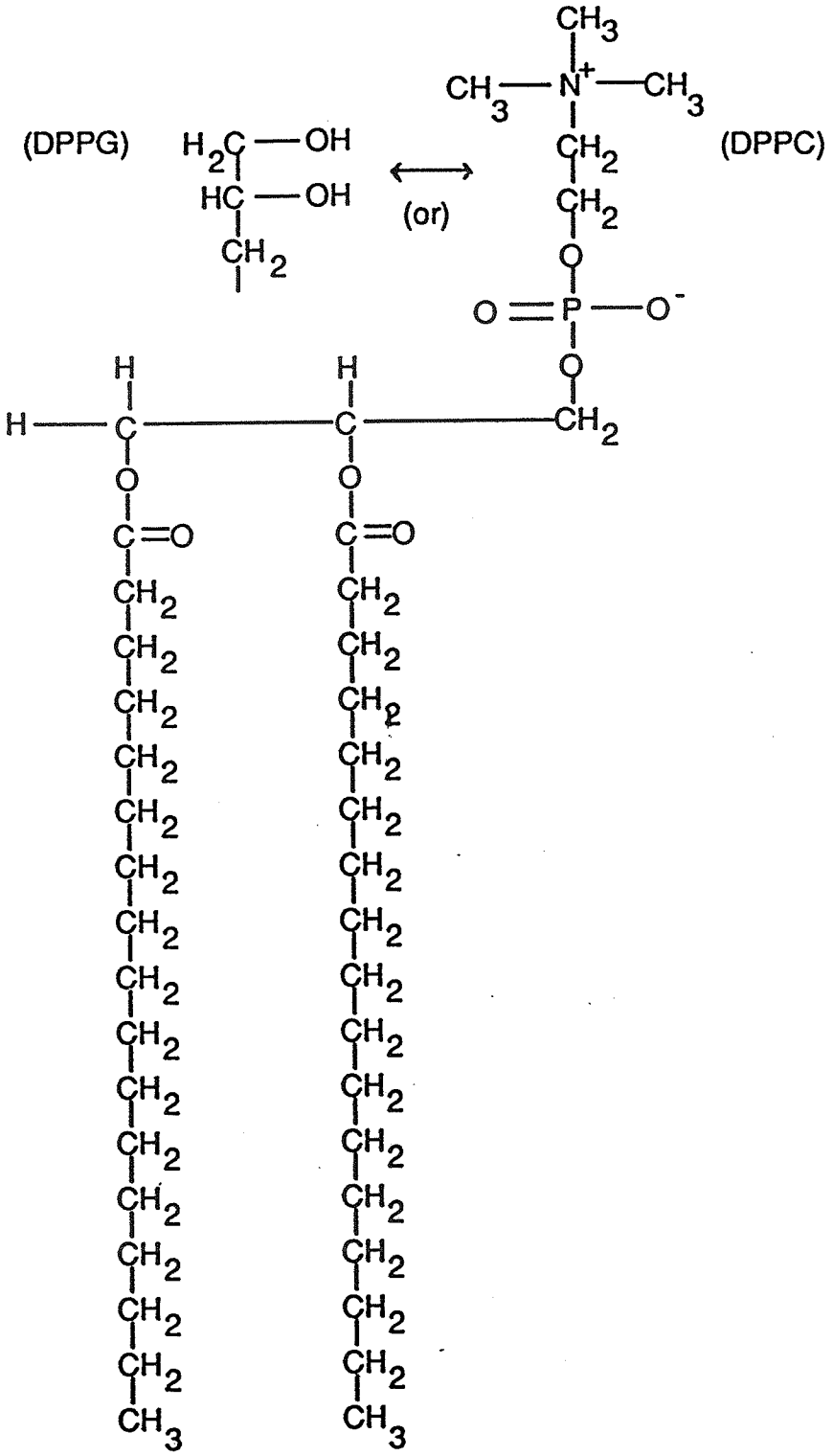

Figure 1.2 Molecular constituents of the liposomes used in this study, viz.,
(DPPC) dipalmitoylphosphatidylcholine
(DPPG) dipalmitoylphosphatidylglycerol
These molecules differ only in the headgroup structure.
The LUVs in this study are of the composition (4:1 w/w DPPC:DPPG)
[Maynard, 1984].

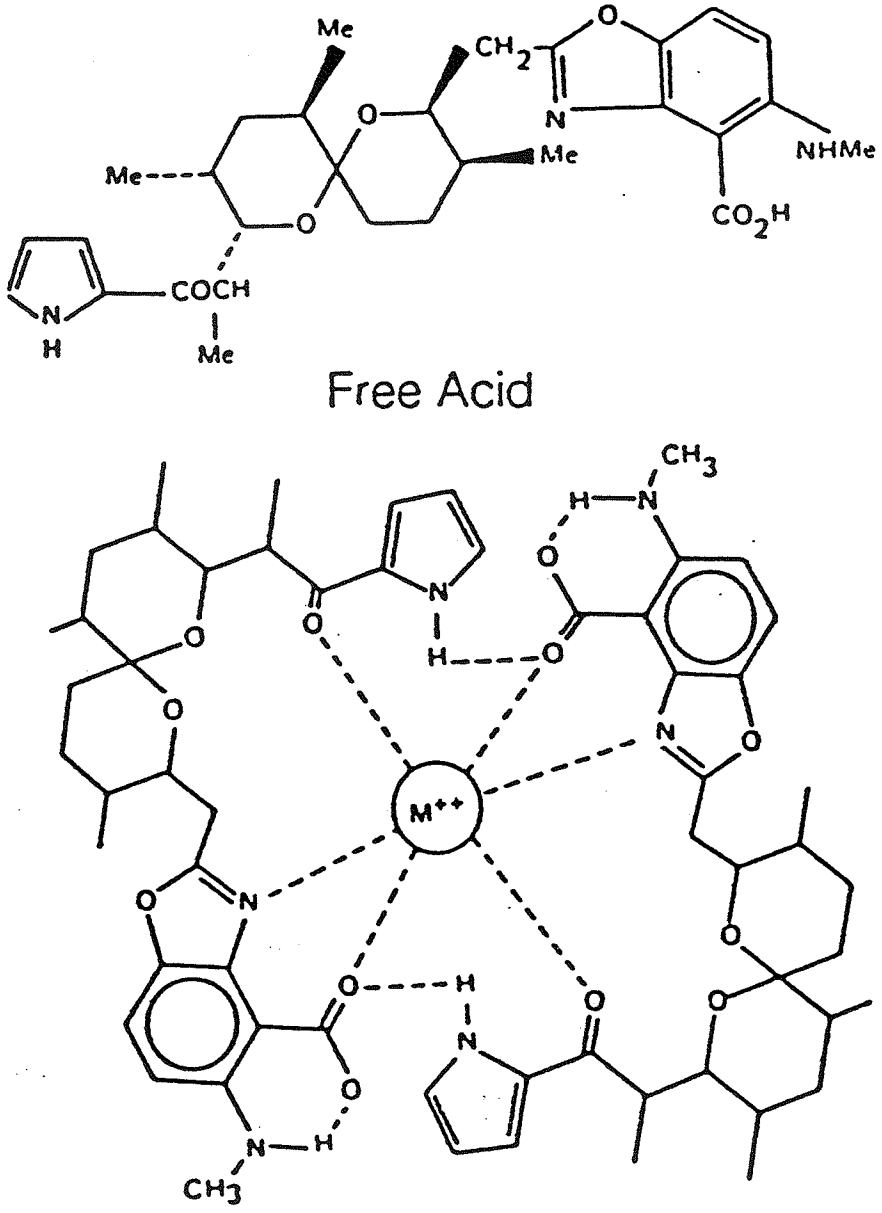

Figure 1.3 Chemical structure of A23187 in its free acid form and its complexed form.

CHAPTER 2

ACOUSTIC THEORY

2.1. Introduction

The propagation of a sound wave in a fluid medium may be described by variables such as p (pressure), t (temperature), and c (velocity). When a small amplitude sound wave travels through a fluid medium there occurs a small alternating increase and decrease in the pressure (Δp) which is superimposed on the medium's static pressure (p_o). The changes in pressure are accompanied by changes in the volume of a small element of the fluid medium, thus bringing about density and temperature fluctuations. Such small changes are interrelated in a way determined by the equation of state of the fluid and by the type of thermodynamic process that takes place. If one assumes an unlimited medium in which a given plane is subjected to a simple harmonic motion produced by the periodic ultrasound wave, and if it is also assumed that the "perfect" fluid possesses no viscosity and no thermal conduction, then the pressure and density changes take place reversibly and a plane sound wave propagates through the fluid medium with an undiminishing pressure wave amplitude. In the case of such ideal wave propagation, the equation representing the propagation of a plane acoustic wave may be written:

$$p = p_o e^{i(\omega t - kx)} \tag{2.1}$$

where ω = the frequency of the wave and k is the wave number.

2.2. Macroscopic Absorption Mechanisms

In contrast to the above ideal propagation, as a real sound wave travels in a real homogeneous fluid its energy is eventually dissipated as heat. Absorption refers to the processes by which energy losses occur in the medium in which ultrasound energy is converted to thermal energy. The mechanisms of such energy absorption may be broadly classified into two categories: macroscopic mechanisms and microscopic mechanisms.

Macroscopic mechanisms of absorption of an acoustic wave consist of those absorption phenomena dependent upon the macroscopic variables of a fluid, such as the viscosity and the compressibility of a fluid. Such phenomena were treated in the last century and consist of two main types of phenomena: viscosity and heat conduction [Kinsler et al., 1982]. Viscosity refers to the relative motion between adjacent portions of a medium, and is analogous to a frictional force [Kinsler et al., 1982]. Heat conduction refers to the conduction of thermal energy between higher temperature condensations and lower temperature rarefactions of a sound wave. These two phenomena result in the dissipation of heat and result in attenuation of the propagating acoustic wave. They also give rise to an absorption that is described by the classical absorption coefficient, α_{class}, which is the equation

$$\alpha_{class} = \left(\frac{2}{3}\right)\left(\frac{\omega^2}{c^3 \rho_o}\right)\left(\eta + \left(\frac{3}{4}\right)(\gamma - 1)\frac{\lambda}{C_p}\right) \qquad (2.2)$$

where η = viscosity of the fluid medium, γ = the ratio of the heat capacities, λ = the wavelength of the sound wave and C_p = the heat capacity of the fluid at constant pressure.

2.3. Molecular Mechanisms of Ultrasound Absorption

2.3.1. Introduction to Relaxation Phenomena

Classical absorption does not account for all of the absorption observed in fluid media. Ultrasound also couples to molecular relaxation processes and this also contributes to the absorption of ultrasonic energy in fluid media. This absorption is represented by a term, η_V, the volume viscosity. The volume viscosity is a measure of the mechanical energy lost by a fluid subjected to pure compression or dilatation [Kinsler et al., 1982], represents relaxation processes which may be thermal and/or structural in character, and may be determined by comparing the observed ultrasonic absorption coefficient α_{obs} and α_{class}. The exact relation [Lamb, 1965] is:

$$\alpha_{obs} - \alpha_{class} = (\frac{3}{4}) \frac{\eta_v \alpha_{class}}{\eta_s} \qquad (2.3)$$

where η_s = shear viscosity and can be measured by subjecting a fluid to shearing forces.

In order to describe further thermal and structural relaxation processes, and their interaction with a propagating ultrasound wave, the definition of a relaxation process will first be given. A thermodynamic system ($A \rightleftharpoons B$) will be studied where states A and B may represent reactants and products, two structural states, etc., and where k_1 is the forward rate of the reaction and k_2 is the rate of the backward reaction at equilibrium. At equilibrium, this system may be subjected to a sharp variation in some physical parameter, upon which the value of the equilibrium constant, $k = k_2/k_1$, is dependent. The system must then change to a new state of chemical or structural equilibrium, and the rate of this change may be followed. If the displacement of the chemical or molecular equilibrium is small enough, the rate of restoration of equilibrium can be assumed to follow first order kinetics. Such a process is characterized by a time constant, the "relaxation time," which, for a one-step reaction under defined external conditions, can be simply related to the rate constants [Eigen and deMayer, 1963]. That is $-dc_A/dt = dc_B/dt = k_1c_A - k_2c_B$, where c_A = the concentration of substance A and c_B = the concentration of substance B. For small perturbations from equilibrium, if x_o is the initial value of the displacement of a system parameter from equilibrium, and x is the value of this displacement at any time t after the initial disturbance, x may be assumed to vary with time as

$$x = x_o e^{-t/\tau}, \qquad 1/\tau = k_1 + k_2, \qquad (2.4)$$

where τ is defined as the chemical or molecular relaxation time for the reaction system.

If the time course of the perturbation, i.e., the ultrasound wave, is described by a forcing function f(t), then f(t) may be included in the differential equation of motion to obtain [Eigen and deMayer, 1963]

$$dx/dt + x/\tau = f(t)/\tau. \qquad (2.5)$$

This yields the general solution for the response of the system parameter x(t)

$$x(t) = \frac{e^{-t/\tau}}{\tau} \int_0^t e^{t'/\tau} f(t')dt'. \tag{2.6}$$

If the forcing function can be written as a complex exponential of the form $f(t) = Ce^{pt}$ (of which $f(t) = Fe^{i\omega t}$ is an example) then the stationary relation between x(t) and f(t) is expressed by

$$x(t) = Tf(t), \tag{2.7}$$

where T represents a time-independent function called the transfer function [Eigen and deMayer, 1963]. The solution of the integral in Eq. (2.6) is [Eigen and deMayer, 1963]:

$$x(t) = \frac{Fe^{i\omega t}}{1 + i\omega\tau}, \tag{2.8}$$

Therefore the transfer function, T, is equal to $1/(1 + i\omega\tau)$, and can be written in the form,

$$T = T_{real} + T_{imag} = 1/(1 + \omega^2\tau^2) + i(-\omega\tau)/(1 + \omega^2\tau^2). \tag{2.9}$$

Having described the transfer function for a system under forced harmonic oscillation, one may turn to rewriting the wave equation for the propagating ultrasound wave in fluid media, considering only the effects of chemical relaxation upon such propagation. The expression for the adiabatic compressibility is [Eigen and deMayer, 1965],

$$\kappa_S = \kappa_S^{\infty} + \kappa'_S T. \tag{2.10}$$

where κ_S' is complex and corresponds to the adiabatic compressibility relating to the effects of the reaction $A \rightleftharpoons B$, and κ_S^{∞} corresponds to relaxations at frequencies much greater than those referred to in these studies. As the propagation velocity, $c = (\rho_O\kappa_S)^{-1/2}$, c is also complex and may be expressed as

$$1/c = 1/c_{re} - i\alpha/\omega, \tag{2.11}$$

where c_{re} = real phase velocity, α = absorption coefficient. Also, since $c = (\rho_0 \kappa_S)^{-1/2}$,

$$\rho_O\kappa_S = [(\frac{1}{c_{re}})^2 - (\frac{\alpha}{\omega})^2] - i(\frac{2\alpha}{\omega c_{re}}). \tag{2.12}$$

The real and imaginary values of κ_S are related to velocity and absorption as

$$c_{re}^2 = \frac{-2Re(\kappa_S)}{\rho[Im^2(\kappa_S)]}\{1 - [1 + (Im(\kappa_S)/Re(\kappa_S))^2]^{1/2}\} \tag{2.13}$$

and

$$\frac{\alpha c_{re}}{\omega} = \frac{Re(\kappa_S)}{\rho Im(\kappa_S)}\{1 - [1 + (Im(\kappa_S)/Re(\kappa_S))^2]^{1/2}\} \tag{2.14}$$

where Re and Im are the real and imaginary parts of κ_S. If the assumption is made that the $Im(\kappa_S) << Re(\kappa_S)$, then

$$c_{re} = [\rho Re(\kappa_S)]^{-1/2} \tag{2.15}$$

and

$$\frac{\alpha c_{re}}{\omega} = \frac{1}{2}[Im(\kappa_S)/Re(\kappa_S)]. \tag{2.16}$$

Therefore,

$$c_{re} = (\rho_o \kappa_S^\infty)^{-1/2}\{1 - \frac{\kappa_S'}{2\kappa_S^\infty}(\frac{1}{1 + \omega^2\tau^2})\} \tag{2.17}$$

and

$$\frac{\alpha c_{re}}{\omega} = \frac{\kappa_S'}{2\kappa_S^\infty}(\frac{\omega\tau}{1 + \omega^2\tau^2}), \tag{2.18}$$

where α is the frequency-dependent absorption coefficient due to the reaction ($A \rightleftharpoons B$). If this absorption coefficient can be assumed to add algebraically to the classical absorption then it becomes

$$\alpha\lambda = \frac{A\omega\tau}{1 + \omega^2\tau^2} + B\omega \tag{2.19}$$

where A and B are the amplitude coefficients for the relaxational and the classical absorption processes, respectively. Note $\alpha\lambda$ is the value determined in these studies. When relaxational

absorption occurs, there is a flow of energy from the mechanical energy mode to the internal energy mode of the equilibrium that is being perturbed by the variation in the variables, viz., pressure and temperature. This flow will be significant when the period $T \geq \tau$.

2.3.2. Thermal Relaxation Processes

When an ultrasound wave sinusoidally perturbs a liquid, sinusoidal perturbations in pressure and temperature occur. Perturbations in temperature are discussed first. As noted by Lamb [1965], propagation of a compressional wave through a liquid is essentially an adiabatic process at the frequencies used in this study. The excess pressure at any point in the liquid alternates sinusoidally about the ambient pressure, p_o, in the medium. Because $C_p > C_v$, there will be a corresponding cyclical variation in temperature, and relaxation processes arise from these temperature variations accompanying the ultrasonic wave. Thermal relaxation mechanisms are those for which absorption arises from a perturbation in a molecular equilibrium due to temperature alternations in a compressional wave. If the oscillation in temperature is on a timescale of microseconds to nanoseconds, it is possible to excite, and to study, reactions in liquids and in biological samples in suspension that take place on such time scales. Such molecular exchanges of energy may involve the following processes: conversion of the kinetic energy of molecules into stored potential energy, internal rotational and vibration energies in polyatomic molecules, and energies of association and dissociation between different ionic species and complexes in ionized solutions.

Thermal relaxation gives rise to a measured absorption which can be represented by an equation of the form:

$$\left(\frac{\alpha}{f^2}\right) = B' + \frac{A'}{[1 + (f/f_r)^2]}, \tag{2.20}$$

where f = frequency, f_r = characteristic frequency of the relaxation process and $B' = B/2\pi c$ and $A' = A/2\pi c$. In these studies, it has been found that a single relaxation occurs in LUV suspensions, in the frequency range of 1 - 5 MHz. As this relaxation is observed at the

phase transition of the phospholipid bilayer of these suspensions, it is possible that the observed relaxation is thermal in character and is related to the "melting" process undergone by phospholipids at their gel to liquid-crystalline phase transition. However, as volume changes, and thus, reordering of phospholipids occur at this transition, it is also possible that the observed relaxation is structural in nature.

2.3.3. Structural Relaxation

The second type of molecular relaxation mechanism, structural relaxation, based on the exposition of Litovitz and Davis [1965], is discussed. Structural relaxation in liquids arises from changes in liquid structure due to (in this case) ultrasonic perturbation of a structural molecular equilibrium. Ordinary liquid structure may be described as consisting of small regions (5 - 50 or more molecules) of short-range order which are continually breaking up and reforming. When the pressure and temperature are changed in such a system, the degree of order and potential energy, which describes the geometric state of the liquid, are also changed, thus requiring energy to be added to or taken from the system. If the perturbation in pressure is on a time scale greater than or equal to the time required for a molecular rearrangement to occur, then the relaxation time of the structural rearrangements due to changes in pressure and temperature may be observed, as well as the energy loss due to these structural rearrangements. Such structural rearrangements occur in biological molecules often on the time scale of milliseconds to nanoseconds and thus may be detected by ultrasound. In these studies, η_V comprises the structural component of volume viscosity of the liquid media.

Two theories of the analysis of structural volume viscosity will be discussed briefly, although it must be noted that the theories apply only to very simplified systems and cannot be used directly to discuss biological suspensions. The first is Hall's [1948] two-state theory of structural viscosity. In this theory, it is proposed that the absorption properties of water are due to the coexistence of two structure types in the liquid, each of which exhibits a different molar volume and exists at certain mole fractions in the liquid. Here, the

relaxational thermal expansion and the relaxational isothermal compressibility are defined for the differences in the two states, whose change in volume is defined as Δv. Using these equations, and the equilibrium constant for the two states: $(x_1/x_2) = e^{-F/RT}$ the equations for relaxational thermal expansion and relaxational isothermal compressibility may be defined in terms of thermodynamic variables and analyzed to obtain η_V. For a more detailed discussion the reader is referred to [Hall, 1948] or [Litovitz and Davis, 1965].

The second theory of structural viscosity discussed is the hole theory of viscosity [Hirai and Eyring, 1958]. Here it is proposed that at equilibrium a certain number of holes exists in a group of molecules, and that when an external pressure is applied, the equilibrium is shifted to fewer holes, through rearrangement of the liquid molecules. The rate of compression is determined by the rate of molecular rearrangement. For a more detailed discussion on this theory the reader is referred to Hirai and Eyring, [1958].

2.3.4. Differentiation between Thermal and Structural Relaxation

One may differentiate between structural and thermal relaxation in the following manners. One difference between these phenomena is that the former exhibits only one characteristic frequency of relaxation, while the latter exhibits a distribution of characteristic frequencies. Another difference may be found in the ratio of η_V to η_S. In thermal relaxation phenomena, which are the major causes of volume viscosity in non-associated liquids, η_V/η_S is dependent on temperature, and may be quite large [Lamb, 1965]. However in structural relaxation mechanisms, η_V/η_S is relatively independent of temperature and is limited by $20 > \eta_V/\eta_S > 0.1$ [Litovitz and Davis, 1965]. This may allow one to determine, using measurements of the volume viscosity versus shear viscosity as a function of temperature, the character of the relaxation mechanism studied. It also gives information of the character of structural relaxation mechanisms. The relation between η_V and η_S in structural relaxation mechanisms may occur because of the similarity of molecular movement in shear versus structural relaxation processes. Shear viscous flow theoretically involves "jumps" of a molecule from one lattice position to another in the direction of shear flow [Litovitz and

Davis, 1965]. Structural or compressional rearrangement processes also seem to involve a jump of one or more molecules from one site to another, however, in the direction of closer packing. Therefore, in both shear and structural compressional processes, molecules change their lattice positions, and it is therefore the bonds that are broken in these processes, thus closely relating their activation energies. It is important to note, however, that the volume viscosity due to structural relaxation in the liquid medium is related to entropy changes that occur during fusion. This was found in molten salts, and the relation is expressed by:

$$\ln(\eta_V/\eta_S) = C - D(S_F/R) \qquad (2.21)$$

η_V/η_S has also been found to be related to ΔS_F, change in entropy, in alcohols, although the coefficients, C and D are different for these systems. This relation of η_V/η_S to the entropy of fusion indicates that the structural relaxation flow occurring in liquids is not a process in which a series of "jumps" from one lattice site to another occurs, but is instead a cooperative phenomenon. In such a situation, a cooperative group of molecules in the quasi-crystalline state would melt or randomize in structure, before flow could occur, during which molecules could change their positions in order to reach a new equilibrium. As the relaxation seen in studies of LUV suspensions is also at the phase transition or "melting" of the phospholipid bilayer, it is quite possible therefore that a single molecular relaxation is not being observed, but instead that a cooperative phenomenon of repacking of the phospholipids or of some region of the side chains, upon undergoing the gel to liquid-crystalline phase transition, is being detected.

It has been suggested in this discussion that thermal and structural relaxation mechanisms in fluid media may be investigated using ultrasound. The ultrasound determination of $\alpha\lambda$ and f_r allow a single relaxation to be analyzed for thermodynamic properties of a reaction or conformational change. These properties include the enthalpy of a process, the activation energy of a process, and the change in compressibility characteristic of the relaxation process. However, in structural relaxation mechanisms, analysis of $\alpha\lambda$ as a function of frequency is difficult, as a distribution of relaxation times occurs. Here, only the average relaxation times may be obtained, and in certain cases, crude estimates of activation

energies. The determination of η_V/η_S as a function of temperature can be used to determine whether an observed relaxation is structural or thermal in character.

Ultrasound determinations of $\alpha\lambda$ and f_{max} as a function of temperature and frequency in liposome suspensions have shown maxima as a function of temperature and frequency and these data in model cell systems suggest that ultrasound indeed does interact with biological samples at the molecular level, specifically at a microsecond to nanosecond time scale. It has not yet been determined whether these phenomena are thermal or structural in character. In order to do so, η_V and η_S determinations might be carried out, as could $\alpha\lambda$ determinations as a function of frequency, over a wide range of frequencies. Also, structural relaxation phenomena show velocity dispersion [Lamb, 1965], which could be used as a test to differentiate between the two non-classical absorption processes.

In these studies, $\alpha\lambda$ as a function of frequency has been determined at the phase transition temperature of LUV suspensions of specific composition, where $f_{max} = 2.1$ MHz (see Figure 2.1). The $\alpha\lambda/c$ versus frequency curves at t_m for a number of LUV suspensions were analyzed in the following manner. A baseline curve was fit to the $\alpha\lambda/c$ points which did not include the peak (defined by $(\alpha\lambda/c)_{max}$) by a least squares linear regression. The average uncertainty in these baselines was approximately 0.002 ml/g, and the average peak is approximately 0.020 ml/g above the baseline at this frequency. Therefore the signal to noise ratio (S/N) of the detection of this peak is approximately 10, which is considered significant. The best determination of this relaxation as thermal or structural can only be made if the frequency range of the ultrasound $\alpha\lambda$ determination is increased beyond its present range of 0.58 to 6 MHz. A discussion on the frequency range of the interferometer is given in Chapter 3.

2.4. Theory of the Acoustic Inteferometer

2.4.1. Introduction

The theory of the CW two-transducer, fixed-path acoustic interferometer is discussed. This discussion pertains to the use of the interferometer in the determination of the ultrasound

absorption coefficient per wavelength, $\alpha\lambda$, in fluid media. The fluid media under study consist of biological solutes (e.g. proteins, phospholipids, liposomes, etc.) dissolved in biologically compatible solvents. The acoustic interferometer is well-suited to such measurements because of its sensitivity and because it requires relatively small samples for study. The acoustic interferometer, based on the design of Labhardt and Schwarz [1976], requires only milliliters of sample, compared to the liters needed for other techniques used to measure ultrasound absorption in liquid media.

2.4.2. Physical Description of the Acoustic Interferometer

The CW two-transducer, fixed-path acoustic interferometer consists of a cylindrical cavity (called a "cell"), whose ends are bounded by X-cut quartz transducers (X-cut specifies that the thickness is along the X-crystallographic axis), and whose side walls consist of an inert material which ideally does not interact with the fluid sample or the transmitted sound wave. A schematic of this situation is shown in Figure 2.2.

The quartz plates are piezoelectric transducers which transmit and receive the ultrasound waves. Specifically, one of the transducers, the "transmitting" transducer, is driven by a tunable frequency synthesizer. The transducer has a diameter much greater than the wavelength of the sound in the quartz plate and in the liquid specimen. The wave is then reflected back and forth between the two transducer faces, while the transmitting transducer continually propagates sound into the medium. The theory describing the operation of the interferometer assumes that the transducer surfaces are perfectly planar and parallel, due to the large number of reflections that a sound wave must undergo before being damped to 1/e of its original value [Strom-Jensen, 1984]. If the plates are not parallel, propagation of the sound wave out of the resonator axis direction would result in an energy loss so large that absorption by the fluid would be obscured. The resultant pressure wave in the medium drives the receiving transducer, which develops a voltage signal output at the terminals of the receiving transducer. The system may be modelled as three adjacent media whose interfaces are perfectly planar and are perpendicular to the axis of wave propagation. As the quartz

transducers have impedances greater than that of the fluid medium (characterisitic impedance of quartz = 15.3 x 10^6 Pa s/m, characteristic impedance of water = 1.48 x 10^6 Pa s/m), the propagated wave is reflected at the fluid-quartz boundary in phase, and with a pressure reflection coefficient of ~ 0.84.

2.4.3. Resonance Frequencies of the Acoustic Interferometer

The acoustic interferometer is employed to observe the resultant pressure wave in the medium, and to identify its peak power frequencies and half-power frequencies. The method takes advantage of the fact that the peak power frequencies of the wave occur when the driving frequency of the transmitting transducer is such that an integral number of half-wavelengths exist in the space between the two transducers. It is at one of these frequencies, called a "resonance" frequency, that the interference between the sound waves travelling in the positive and negative x-directions (x chosen as the coordinate axis along the axis of wave propagation) is constructive at the receiver transducer interface. The resulting standing wave has a maximum pressure amplitude at the transducer faces, which in turn develops maximum force at the receiving transducer. The resulting voltage output is thus also maximum, and is manifest as a voltage peak appearing at the transducer electrical terminals. The driving frequency corresponding to such a voltage peak is referred to as f_o, while the frequencies above and below f_o, at which the power of the wave falls to half its peak value, are termed f_+ and f_-, respectively. Defining the peak power frequency and a half power frequency allows two equations for power of the sound wave to be found, each of which is directly related to the other by the relation

$$\text{power at } f_o + \Delta f = 1/2 \text{ power at } f_o, \quad \Delta f = (f_+ - f_-). \tag{2.22}$$

The above comparison of the two equations will then yield the absorption per wavelength of the sound wave in the fluid medium, in terms of f_o, f_+ and f_-. The derivation of the equation for the absorption per wavelength of sound ($\alpha\lambda$) in a fluid medium for this situation is given by Maynard [1984].

2.4.4. Resonance Theory

Resonance conditions may be described by a quality factor, Q, where

$$Q = 2\pi(\text{Energy stored in system})/(\text{Energy dissipated per cycle}). \quad (2.23)$$

In order to use this equation the energy associated with an acoustic wave must be given in acoustic parameters. The energy transported by an acoustic wave may be described by E' = E/v, energy density, where E is the energy transported by the wave and v volume. Expressed in terms of equilibrium density and the positive and negative particle velocities,

$$E'(\text{energy density}) = \rho_o(U_+^2 + U_-^2). \quad (2.24)$$

The energy transported by the wave process across a unit area in a unit time is the energy density times the propagation velocity, called the intensity,

$$I = cE' = \rho_o c\,(U_+^2 + U_-^2), \quad (2.25)$$

or in terms of acoustic pressure,

$$I = p^2/\rho_o c. \quad (2.26)$$

As the sound intensity decays exponentially,

$$I = I_o e^{-2\alpha x}. \quad (2.27)$$

To find an expression for energy dissipation per cycle, first one may calculate $\partial I/\partial x$, which yields the energy loss per volume per unit distance:

$$\partial I/\partial x = -2\alpha I_o e^{-2\alpha x} = -2\alpha I. \quad (2.28)$$

If the energy dissipated per cycle is much less than the total energy, E, of the wave, then I is not signficantly changed in one period T. Therefore, Eq. (2.28) becomes

$$\partial I/\partial x \sim -2\alpha I_o \quad (2.29)$$

and the energy dissipated per cycle is given by $-2\alpha I_o(v1/f)$ where the acoustic resonator volume is v and wave period 1/f. Therefore,

$$Q = 2\pi\rho_o\,(U_+2 + U_-2)v/2\alpha\rho_o c\,(U_+^2 + U_-^2)v(1/f) \quad (2.30)$$

which may be simplified to:

$$Q = \pi f/\alpha c \quad \text{or } \alpha\lambda = \pi/Q. \quad (2.31)$$

It is known that the mechanical quality factor of a resonance is expressed by the quantity

$$Q = f_o/\Delta f \quad (2.32)$$

where f_o is the resonance frequency and Δf is the half-power bandwidth of the resonance. Combining Eq. (2.31) and Eq. (2.32), one obtains

$$\alpha\lambda = \pi\Delta f/f_o. \tag{2.33}$$

2.5. Discussion of $\alpha\lambda$ Determination

In the determination of $\alpha\lambda$ in the case of a suspension of biological material, an absolute value cannot be found. The $\alpha\lambda$ directly determined is the result of many absorption and other attenuation mechanisms. Specifically, the measured absorption in a homogeneous fluid medium within the interferometer may be attributed to solute (LUVs), diffraction, scattering of sound from the side walls of the cylinder, imperfect reflection at transducer surfaces, and absorption by solvent. If these modes of attenuation can be assumed to be algebraically additive, then it is possible to isolate the absorption due to the solute, i.e., biological sample, by making a measurement of $\alpha\lambda$ in a reference fluid whose absorption and other physical and acoustic properties are known. Such suitable reference liquids as water, hepes buffer, etc., must be of nearly the same density and impedance as the sample in order to be able to account for the effects noted above. In this case the "excess" absorption per wavelength, $\alpha\lambda_{excess}$, is given by the following equation:

$$\alpha\lambda_{excess} = \pi(\Delta f_{susp} - \Delta f_{ref})/f_o. \tag{2.34}$$

These are the equations needed for the analyses in the following chapters.

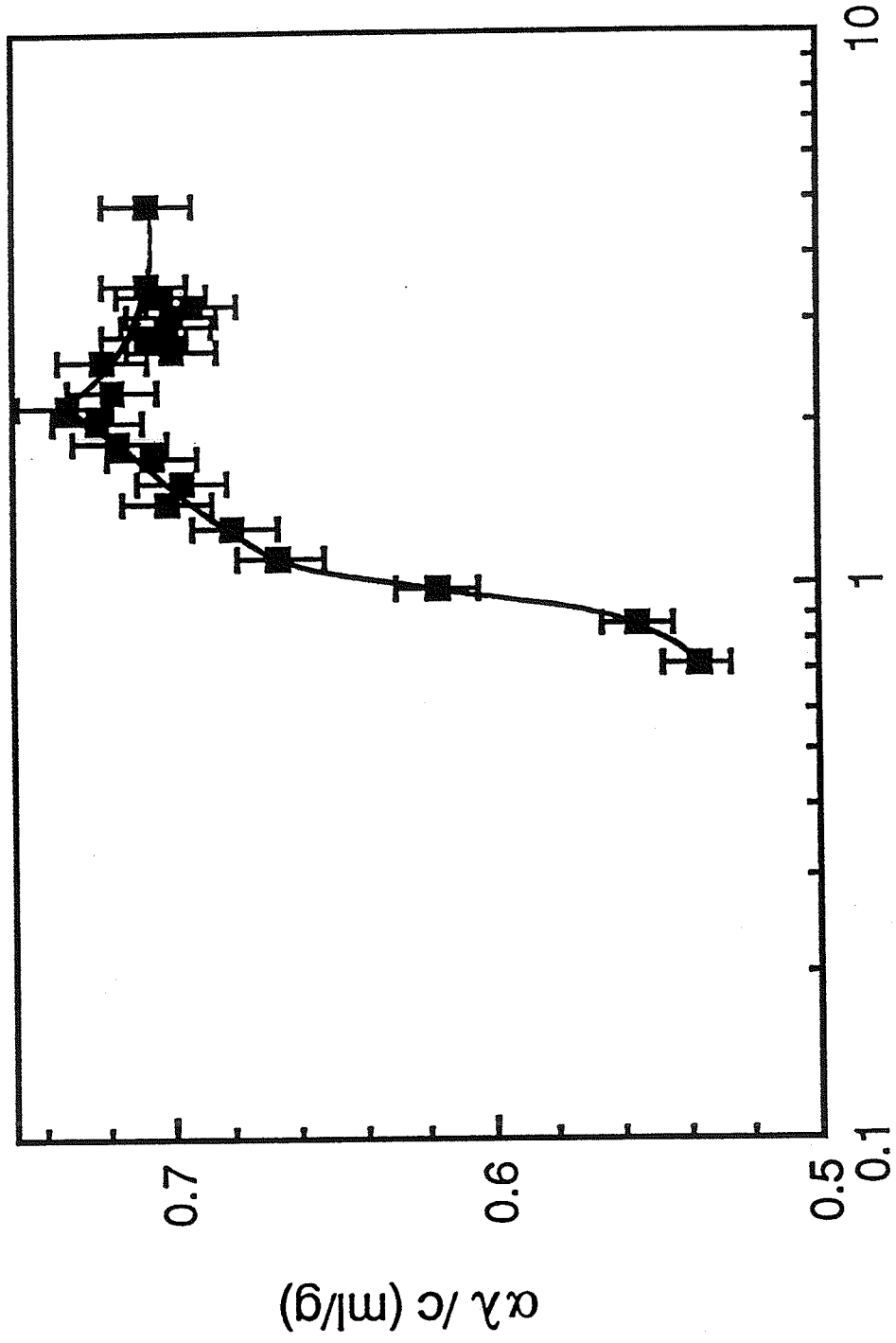

Figure 2.1 $\alpha\lambda/c$ versus frequency in standard LUV suspensions.

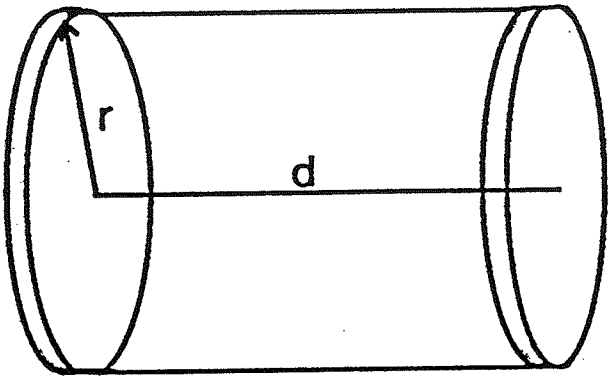

Figure 2.2 Schematic of the resonator cavity.

CHAPTER 3

MATERIALS AND METHODS

3.1. Liposome Suspensions

3.1.1. Chemical Materials

All standard liposome preparations were made from mixtures of dipalmitoylphosphatidylcholine (DPPC) and dipalmitoylphosphatidylglycerol (DPPG), in a 4:1 (w/w) DPPC:DPPG ratio. All lipids were obtained from Avanti Biochemical Co. (Birmingham, AL, USA). The DPPG, whose head group has a net negative charge at pH 7.4, is thought to inhibit liposome aggregation and fusion due to surface repulsion of liposomes [Maynard et al., 1985]. Samples of DPPC and DPPG (100 mg) gave single spots on thin-layer chromatograms (silica gel G developed with $CHCl_3/CH_3OH/H_2O$, 64:24:4, visualized with I_2 vapor). Crystalline 1-β-D arabinofuranosylcytosine (Ara-C) and N-2-hydroxyethylpiperazine-N'-2-ethanesulfonic acid (Hepes) were purchased from Sigma Chemical Company (St. Louis, MO, USA). Ethylenebis(oxy-ethylenenitrilo)tetraacetic acid (EGTA) was purchased from Sigma Chemical Co. Hepes buffer was composed of 10 mM hepes, 139 mM NaCl, 6 mM KCl, and distilled water, using 10 N NaOH to adust the pH to 7.4 at room temperature. Ninety-nine point eight mole percent deuterium oxide was purchased from Sigma Chemical Company. Nitroxides, 5- and 12-DS (4,4 - dimethyl-oxazolidine-N-oxyl derivative of 5- and 12-ketostearic acid); and CAT_{16} (2,2,6,6-tetramethyl piperidine-N-oxyl-[N,N dimethyl-N-hexadecylammonium]) were purchased from Molecular Probes (Junction City, ORE, USA) and PC-12-DS (1-palmitoyl-2-(12-doxyl stearoyl) phosphatidylcholine) was purchased from Avanti Polar Lipids (Birmingham, AL, USA). A23187 was purchased from Boehring Diagnostics (Calbiochem, Los Angeles, CA, USA).

3.1.2. Liposome Preparation

3.1.2.1. Standard preparation LUV suspensions

All standard large unilamellar vesicle (LUV) preparations were made from mixtures of DPPC:DPPG in a 4:1 (w/w) ratio, and were prepared by the reverse phase evaporation method based on the work of Szoka and Papahadjopoulos (1978). Dry lipids (100 mg DPPC, 25 mg DPPG) were dissolved in an organic solution of 8 ml isopropyl ether and 4 ml chloroform. At a temperature (50°C) well above the t_m of 42.0°C, 4 ml of the buffer dilution (30 milliosmolar hepes fixed to 300 milliosmolar with Ara-C) were added. The mixture was then sealed under N_2 gas and sonicated for approximately two minutes, forming an emulsion. The emulsion was transferred to a rotary evaporator, where reverse phase evaporation, i.e., preferential removal of the organic phase, took place, with vigorous foaming and venting. The aqueous phase which was evaporated was then replaced to result in 5 ml of suspension, and the suspension was dialyzed at approximately 9°C.

This process resulted in distributions of liposomes having an average diameter of 0.20 ± 0.05 μm (SE) and ranging in size from 0.06 to 0.43 μm, as determined from electron micrographs of suspensions. The resultant average concentration of phospholipid in the preparation was found to be 21.0 ± 0.1 mg/ml (SE), using the Bartlett phosphorus assay. Samples of the original suspensions were diluted to 2 mg/ml phospholipid in hepes buffer for acoustic measurements. This was hereafter referred to as a standard LUV suspension.

3.1.2.2. D_2O LUV suspensions

The only difference in the preparation of D_2O LUVsuspensions as compared to LUV suspensions was that the H_2O in the aqueous component of the suspension was replaced with deuterium oxide. In the subsequent dilution to 2 mg/ml, varying ratios of D_2O:H_2O were used. Note also that in ESR experiments (described in a later section) various ESR probes (i.e. 5-doxyl stearate and 12-doxyl stearate) were added after liposome preparation, (at a phospholipid:probe ratio of 100:1). This was accomplished by drying the probe on the bottom and sides of a culture tube (with N_2 gas), and then adding the freshly prepared

liposomes and vortexing to ensure complete mixing. The probe partitioned into the organic phase of the LUV suspension, as was shown by the broad ESR spectrum thus obtained from the probe, typical for a nitroxide spin label in a membrane (see Chapter 5).

3.1.2.3. A23187 LUV suspensions

The A23187 LUV suspensions were prepared in the same manner as standard LUV suspensions with the exception that varying amounts of A23187 (MW = 523.6 daltons) Ca^{2+}-ionophore were added to the organic phase (chloroform, ether, lipid, A23187) before performing the reverse phase evaporation process. This resulted in LUVs in which A23187 was a specific portion of the lipid bilayer, as A23187 is hydrophobic. The A23187 was shown to be in the LUV suspension by absorption spectrophotometry measurements, which clearly showed the A23187 spectrum superimposed upon the normal LUV spectrum. It was also shown that A23187 was in the hydrophobic portion of the LUV suspension, as the supernatant of A23187 LUV suspensions showed, in the absorption spectrophotometer, less than 1% of the A23187 absorption than was seen in the corresponding LUV suspension. The mole percents of A23187 in the phospholipid bilayer of the LUVs used in these studies were 1, 2 and 5 mole %. These were referred to as A23187 LUV suspensions.

3.1.2.4. LUV suspensions with per-deuterated DPPC

The LUV suspensions with per-deuterated DPPC were prepared in the same manner as standard LUV suspensions, with the exception that varying amounts of DPPC were replaced with per-deuterated DPPC (DPPC with the side chain hydrogens replaced by deuterium). Further details on the characteristics of such LUV suspensions are given in Chapter 6.

3.2. Ultrasonic Apparatus

3.2.1. Introduction

The acoustic interferometer used in this study was based on the design of Labhardt and Schwarz [1976] and consists of two identical X-cut quartz transducers (diameter = 1 inch,

f_{fund} (fundamental frequency of the transducers) = 4.0 MHz), positioned coaxially and parallel 5.5 mm apart (plexiglass interferometer, 5.1 mm stainless steel interferometer) [Maynard, 1984], forming the end walls of the measuring cell. One transducer is excited electrically at a predetermined frequency to transmit CW ultrasonic waves through the fluid medium. The other transducer receives the sound wave and converts it into an electrical signal. The electrical input to the transmitting transducer is obtained from a synthesized signal generator (HP 8660B, Hewlett-Packard, Palo Alto, CA, USA), and the stable power drive is maintained by the HP 86601A RF section. The electrical output from the receiving transducer is monitored by a spectrum analyzer (HP 85521, HP 8553B). Ultrasonic intensities of less than 1 $\mu W/cm^2$ are used [Maynard et al., 1985], which is many orders of magnitude below that needed to produce cavitation or a significant temperature increase due to absorption processes [Maynard et al., 1985]. The entire system resonates acoustically at certain frequencies. The mechanical quality factory Q of this resonance is related to the acoustic absorption per wavelength by [Maynard, 1984]:

$$\pi/Q = \pi\Delta f/f_o = \alpha\lambda \tag{3.1}$$

where α is the absorption coefficient per unit path length, $\alpha\lambda$ is the absorption per wavelength, λ is the wavelength, Δf is the 3 dB bandwidth of the resonance curve, viz., the difference in the two frequencies for which the output power of the signal is one-half that at the resonance frequency f_o, and Q is the quality factor $f_o/\Delta f$.

The excess absorption due to the presence of LUVs in the suspension is obtained by subtracting the absorption coefficient of the reference buffer from that of the entire ensemble, viz., reference buffer plus LUVs. For the situation pertaining herein, for which the suspension acoustic velocity and impedance are virtually the same as that of the reference buffer, diffraction correction is unnecessary. The excess absorption is:

$$(\alpha\lambda)_{excess} = \pi(\Delta f - \Delta f_{ref})/f_o. \tag{3.2}$$

3.2.2. Structure

A schematic of the interferometer is shown in Figure 3.1. As the stainless steel

interferometer was thoroughly described elsewhere [Maynard, 1984], only a brief overview is given here, with special note of the structural changes made in the design of the plexiglass interferometer, built October, 1985. The body of the interferometer used before September, 1985 consisted of two identical stainless steel halves. A new interferometer, constructed in October, 1985 consists of two plexiglass halves. The stainless steel interferometer, though less susceptible than the previous (brass) interferometer to corrosion by the ionic solvent of the liposome suspensions, still experienced eventual corrosion, and this was the reason for the design of a plexiglass interferometer.

The two plexiglass halves of the interferometer are assembled to form the integrated unit by three plexiglass bolts with brass nuts. Previously four stainless steel bolts and nuts were used, but one bolt was consistently ineffective (loose) after parallelization and changes in its position produced uncertainty in the state of parallelization of the interferometer. A lucite spacer, forming the side walls of the cylindrical cell, is situated between the two plexiglass halves. Lucite is chosen because its optical transparency makes it possible to see bubbles adhering to the end walls of the cell during the filling procedure, and because its characteristic acoustic impedance is nearer to that of the sample than are the impedances of other materials that could have been chosen for this purpose [Maynard, 1984]. This approximate impedance matching minimizes reflection of acoustic energy departing from the ideal plane wave propagation.

A cylindrical opening, with an inserted 18 guage needle and attached tube, at the bottom of the spacer functions as a port for filling and emptying the cell. An identical port at the top of the spacer allows the maintenance of the atmospheric pressure over the liquid, which is desirable during the filling procedure. Flat rubber neoprene rings between the lucite spacer and the plexiglass halves provide a liquid-tight seal and allow the slight angular displacements of the two halves of the interferometer required for the parallelization procedure. The end walls of the cell are the piezoelectric transducers which are supported in the polished recesses of the plexiglass body by RTV sealant and neoprene rings. Vacuum grease was used to hold the transducers in place in the stainless steel interferometer.

The transducers are X-cut quartz with overtone polish to a degree of flatness of 1-10 λ of light (Valpey-Fisher Div., Hopkinton, MA, USA). The plates are one inch in diameter having a fundamental thickness resonance frequency of 4 MHz. The electrodes are evaporated gold on chromium. The ground potential electrode of each transducer covers the entire face in contact with the liquid sample. The electrode on the opposite face is coaxial having a diameter of 7/8", so chosen such that electrical contact with the grounded steel does not occur. As this is no longer a concern with the plexiglass interferometer, electrical contact from the transducer to these electrodes is made via 34 guage platinum wires, soldered to female BNC connectors and bent into a slight hook shape. The pressure applied by the wires to the transducers is minimal producing no mechanical strain. Holes are drilled through the plexiglass body to equalize the pressure, on the back sides of the transducer, with the ambient pressure. The inside diameter of the spacer is 29 mm, and that of the neoprene rings is approximately 31 mm. The distance d between the inside faces of the transducers may be calculated from the frequency separation of two adjacent resonances, $f_n - f_{n-1}$, near $f_{fund}/2$ for a liquid with an accurately known acoustic velocity (c), viz., distilled water at a known temperature. It will then be 1/2 of an acoustic wavelength

$$d = c/(2(f_n - f_{n-1})). \tag{3.3}$$

As the spacer is 3 mm wide (stainless steel interferometer), the cell volume (v) is given by the equation:

$$v = \pi r^2 d \tag{3.4}$$

where r is the radius of the inside diameter of the spacer and d is the distance between the inside faces of the transducers.

The holder is set on the base of an L-shaped lucite support (Figure 3.2) [Maynard, 1984]. A stainless steel piston, tightly fitted into a cylinder with O-rings and machined such that pressure could be controlled for sample input and removal, is attached to the vertical side of the lucite support. Access to the cylinder is via a bleeder valve which is connected to an outlet whose dimensions are identical to those of the cell ports. Polyethylene tubing (1.19 mm i.d., 1.70 mm o.d.) connects the top port of the interferometer to the outlet. Tubing also

connects the bottom port to a reservoir (glass syringe) suspended above the interferometer, which is used to introduce samples into the interferometer.

3.2.3. Assembly

As the assembly of the stainless steel interferometer was covered thoroughly in Maynard [1984], only those aspects which were changed in the plexiglass interferometer assembly are described. The BNC connectors were mounted into the center of each steel or plexiglass half, into threaded bores. RTV sealant was then applied to the nonelectroded area of a transducer. The transducer was then set on the recessed ring in the body and was pushed in by using the 'ringing' method, as detailed in Maynard [1984]. In the plexiglass interferometer, the flat neoprene rings also held down the transducer along its perimeter, so as to insure a more secure seal. The ground connection between the gold electrode on the transducer face and the BNC connector was made with a flat gold foil ring with attached wire which lined the perimeter of the transducer and was connected the BNC connector. Thus, a minimum resistance of approximately 1 ohm was established.

The interferometer was assembled by the concentric stacking of the two halves of the interferomter body with the lucite spacer between them [Maynard, 1984]. This was completed with the use of the three bolts, threaded into the holes in the body halves. Each bolt was tightened the same number of turns to ensure approximate tightness and symmetry of the space between the halves. To parallel the halves, first the bolts were further tightened until the two halves were equally spaced to $\pm$ 0.01 cm around the entire circumference of the body, as determined by caliper measurements [Maynard, 1984]. Then a fine-tune parallelism procedure, as described in Section 3.2.7. was performed to complete the parallelism procedure.

3.2.4. Filling

The sample (LUV suspension) is pipetted into the reservoir. The reservoir is then placed approximately one foot above the interferometer, in order to facilitate gravity flow

from the reservoir into the sample chamber. In order to start the gravity flow, the piston is first moved up slowly to reduce pressure inside the cell below the ambient pressure in order to draw liquid into the cell. Once the fluid flow begins the piston is disengaged and gravity flow is allowed to proceed until the sample chamber is filled, at which time the reservoir fluid level is lowered to the same level as that of the interferometer. The gravity flow may also be stopped by engaging the piston, and this is done in order to stop the gravity flow that occurs as the interferometer, in its plastic bags, is lifted and put into the temperature controlling water bath.

3.2.5. Temperature Control

The temperature is controlled as the resonance frequency of the cell and the sample is a very strong function of temperature [Maynard, 1984]. The interferometer and lucite holder are placed in two plastic bags and set on the lucite support. The entire ensemble is suspended in a temperature controlled bath (Exacal 500, Endocal 350 refrigeration unit, Neslab, Portsmouth, NH, USA). The temperature is stable to $\pm$ 0.05°C for days at a given temperature and to $\pm$ 0.01°C during a particular bandwidth measurement.

3.2.6. Electronic Instrumentation

As stated in Maynard [1984], a synthesized signal generator (8660B with 86601A RF section, Hewlett-Packard) drives the transmitting quartz transducer via a length of RG 58A/U coaxial cable and a BNC connector. The receiving transducer is connected via cable and a BNC to a spectrum analyzer (8553B RF section, 8552A IF section, 140B oscilloscope, Hewlett-Packard). The signal generator is capable of selecting frequency to the nearest hertz. The frequency is adjusted until acoustic resonance is reached, as evidenced by a peak on the screen of the spectrum analyzer.

3.2.7. Parallelism Adjustment

The transducers forming the end walls of the acoustic interferometer ideally must be

perfectly parallel. As the sound wave is reflected a large number of times before being damped to, for example, 1/e of its initial value, deviation from parallelism causes loss in the amplitude of the ultrasound wave and would contribute to the measurment of $\alpha\lambda$. The number of reflections, m, before the amplitude is reduced to 1/e of its initial value for the perfectly parallel case, is dependent upon the distance between the transducers (d) and the attenuation coefficient, α, of the fluid in the cavity [Maynard, 1984]. The equation relating these variables is $md = 1/\alpha$ [Maynard, 1984]. The example given in Maynard (1984), is for water at 39°C where the frequency of the ultrasound wave is 1 MHz. Here $\alpha = 2 \times 10^{-4}$ cm^{-1} and d = 0.55 cm, thus giving $m \sim 10^4$ reflections [Maynard, 1984]. Eggers et al. [1978] state that the planarity of the two transducers must be able to be controlled to $\sim \lambda/m$, where λ is the wavelength at which $\alpha\lambda$ is determined. For the frequency range of ultrasound used in these experiments (1 - 5 MHz) the quantity $\lambda/m = 0.15$ μm. The interferometer body can be adjusted to 0.40 μm given the ability to perform 1/1000 turn on a screw of 64 threads per inch [Maynard, 1984]. Therefore the transducers may be adjusted to approximately 0.40 μm x (distance between two bolts/diameter of the transducer) = 0.10 μm, for the plexiglass interferometer, which results in a resolution greater than the 0.15 μm adjustment required.

After completing the preliminary parallelism procedure, the cell is filled with distilled water, and a resonance frequency near 1 MHz is found. The bolts are adjusted to increase the amplitude of the peak on the spectrum analyzer screen. The amplitude of the resonance peak is determined by the sum of the constructive and destructive interference of the standing wave within the cell. The nearer the cell is to perfect parallelism, the smaller will be the amount of the destructive interference effects of non-parallelism. Therefore the greatest peak amplitude is observed when the transducers of the cell are perfectly parallel. Retuning of the driving frequency to a resonance condition is performed after all parallelism adjustments.

At shorter wavelengths, the transducer displacement is a larger fraction of a wavelength, thus increasing the destructive interference effects of nonparallelism. Therefore the parallelism procedure is more sensitive at higher frequencies, and must be repeated at several such frequencies in order to tune it. With the plexiglass interferometer, above 6

MHz, it is not possible to align the transducers finely enough to produce a peak whose f_o and Δf are able to be determined.

A resonance condition occurs theoretically when the space between the transducer faces an integral number of half-wavelengths. In actuality, each of the observed resonances is the first mode of a spectrum of resonance modes which result in satellite peaks at closely neighboring frequencies (within 10 kHz). The observed spectrum is due to nonideal plane wave behavior, resulting in image sources, imposed by the cylindrical cavity [Labhardt and Schwarz, 1976; Maynard, 1984]. The amplitude of the largest satellite peak is used to determine relatively the degree of parallelism of the transducer faces, as the ratio of the amplitude of the satellite peak to the first mode peak increases as the parallelism decreases. Examples of the relative amplitudes of the main resonance (amplitude = 1) to the largest satellite are given in Table 3.1 from [Maynard, 1984] for the stainless steel interferometer and also for the plexiglass interferometer.

TABLE 3.1

SATELLITES OF RESONANCES IN TWO INTERFEROMETERS

	relative satellite amplitude	
f_o (MHz)	plexiglass interferometer	stainless steel interferometer
1	0.05	----------
2	0.09	0.11
3	0.18	0.24
5	0.33	0.30

It has been shown that this alignment, performed at room temperature, is maintained throughout the temperature range of 4°C to 51°C at least within the uncertainty with which the system can measure absorption, viz., approximately ± 5% [Strom-Jensen, 1983; Maynard, 1984].

The frequency range of the plexiglass interferometer is 0.6 to 6.0 MHz. The quality of the resonances near 2 and 3 MHz is greater than at other frequencies, as is shown in Maynard, 1984. Specifically, the behaviour of the interferometer is closest to ideal at the antiresonant frequencies of the transducers which, for these studies, includes 2 and 6 MHz [Maynard, 1984]. At lower frequencies, precision and accuracy are lost due to diffraction. This is due to the imperfect planar character of the wave originating from the transducers, increasing as the ratio of the wavelength to transducer diameter increases (see Figure 3.3). For the more highly absorbing liquid, the bandwidth minimum occurs at a lower frequency and the diffraction-caused increase in bandwidth at lowest frequencies is not as great [Maynard, 1984]. Precision and accuracy also lost at higher frequencies, starting near 5 MHz, due to asymmetric peaks, probably representing the destructive effects of non-parallelism (see Figure 3.3). This loss at higher frequencies helps to determine the high frequency limit of the interferometer. Another limiting factor in the frequency range is the inability to obtain data within ± 0.5 MHz of the fundamental frequency of the transducers. This is due to non-ideal behavior of the resonance peaks in this frequency range.

3.3. Data Acquisition

3.3.1. Ultrasound Measurements

The equation used to calculate the absorption coeffiient per wavelength, $\alpha\lambda$, is:

$$\alpha\lambda = \pi(\Delta f - \Delta f_{ref})/f_o \qquad (3.5)$$

where f_o is a given resonance frequency, Δf is the half power bandwidth at that frequency, which includes the losses of the interferometer containing the liquid and the losses due to the specific interactions of the sample with the propagating ultrasound wave. The Δf_{ref} is the corresponding bandwidth for a system with the same acoustic properties including $\alpha\lambda$ as the solvent, not including that of the sample (LUVs) under study.

The interferometer system is comprised of the interferometer, containing the LUV suspension, suspended in a water bath of a specific temperature. In this system the

resonance frequencies and their bandwidths are recorded. The signal generator frequency is adjusted until a standing wave is produced at a characteristic frequency, as evidenced by a peak of maximum amplitude, as detected by the spectrum analyzer. The Δf is obtained by tuning the signal generator to give voltage outputs to the spectrum analyzer which are 0.707 of their values at f_o. The same procedure is also employed with the reference buffer (at equivalent resonant frequencies). The Δf and Δf_{ref} are shown in Figure 3.4. as a function of temperature for LUV suspensions. The results are for data acquisition as $\alpha\lambda/c$ versus temperature, to correct the absorption for concentration. The estimated 1σ error of the Δf measurement is 1%. The estimated error in f_o is 0.3%. Thus, a generous estimate of 1 standard deviation error in the calculation of $\alpha\lambda$ is approximately 2%. Note that the uncertainty in c is 5%, given the uncertainty in the initial lipid concentration, pipetting procedure, dilution procedure and sample input procedure, but as this uncertainty is constant over all $\alpha\lambda/c$ determinations for an experiment, it represents an offset and need not be considered in the error of the shape of the $\alpha\lambda/c$ versus temperature curve.

3.3.2. Differential Scanning Calorimeter (DSC) Measurements

The DSC-2 (Perkin-Elmer, St. Louis, MO, USA) is used to obtain the heat capacity at constant pressure c_p versus temperature on 50 µl samples of LUVs. This is done because the temperature dependence of $\alpha\lambda$ at ultrasound frequencies near the relaxation frequency in LUV suspensions is qualitatively similar to that of excess c_p versus temperature, as determined by DSC, a static thermodynamic technique [Dunn and O'Brien, 1976]. It is important to note however, that DSC measures only the static thermodynamic variables of this system while ultrasound measurements provide information on the relaxation times and therefore the kinetics of the system under study. The LUV suspensions ranged in phospholipid concentration from 25 mg/ml to 60 mg/ml and are discussed more thoroughly in Chapters 4, 5 and 6.

3.3.3. Electron Spin Resonance (ESR) Measurements

Electron spin resonance measurements were performed at X-band (9.5 GHz) on a Varian E-109 ESR spectrometer. The temperature of the sample was controlled by a Varian gas flow system using nitrogen. Spectra were recorded in a standard first derivative mode with 100 kHz modulation and a microwave power of 5 mW. Data were collected and stored as arrays of 1024 points per spectrum with a PC computer [Morse, 1987]. The hyperfine splittings, i.e. the positions of the peaks were determined by expanding the spectral feature of intrest using the computer (estimated error $\pm$ 0.3 G for 100 G scans).

Interferometer

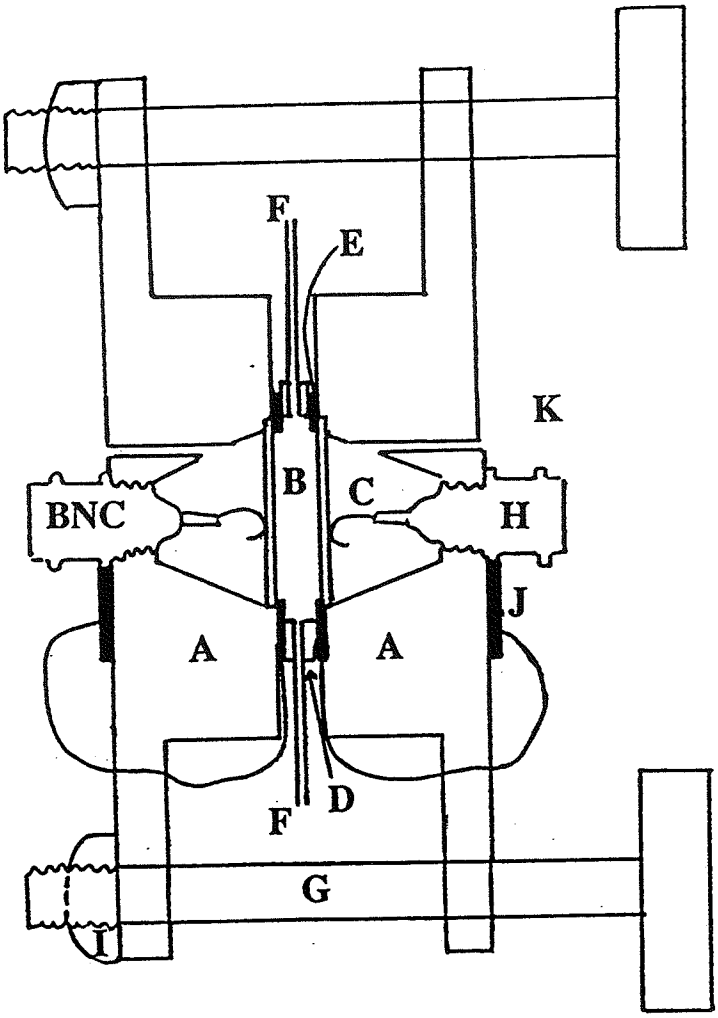

A. Plexiglass Interferometer
B. X-cut Quartz Transducers
C. Platinum Wire Spring Contact
D. Lucite Spacer
E. Flat neoprene rings
F. Filling and Emptying Ports
G. Plexiglass Bolts
H. BNC Connectors
I. Brass Nuts
J. Ground connection

Figure 3.1 Schematic of the plexiglass interferometer.

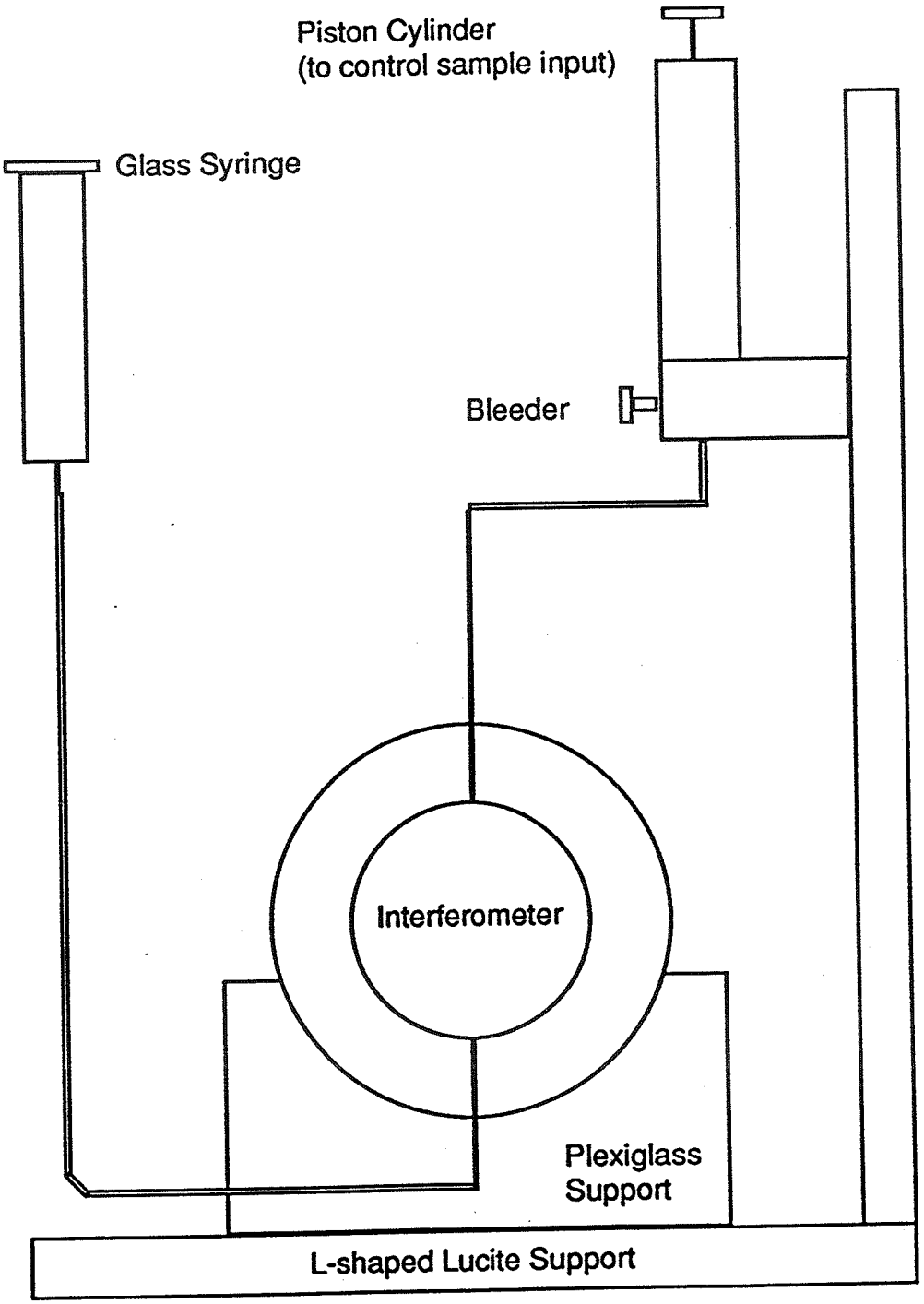

Figure 3.2 Schematic of the interferometer and its lucite support (adapted from Maynard [1984]).

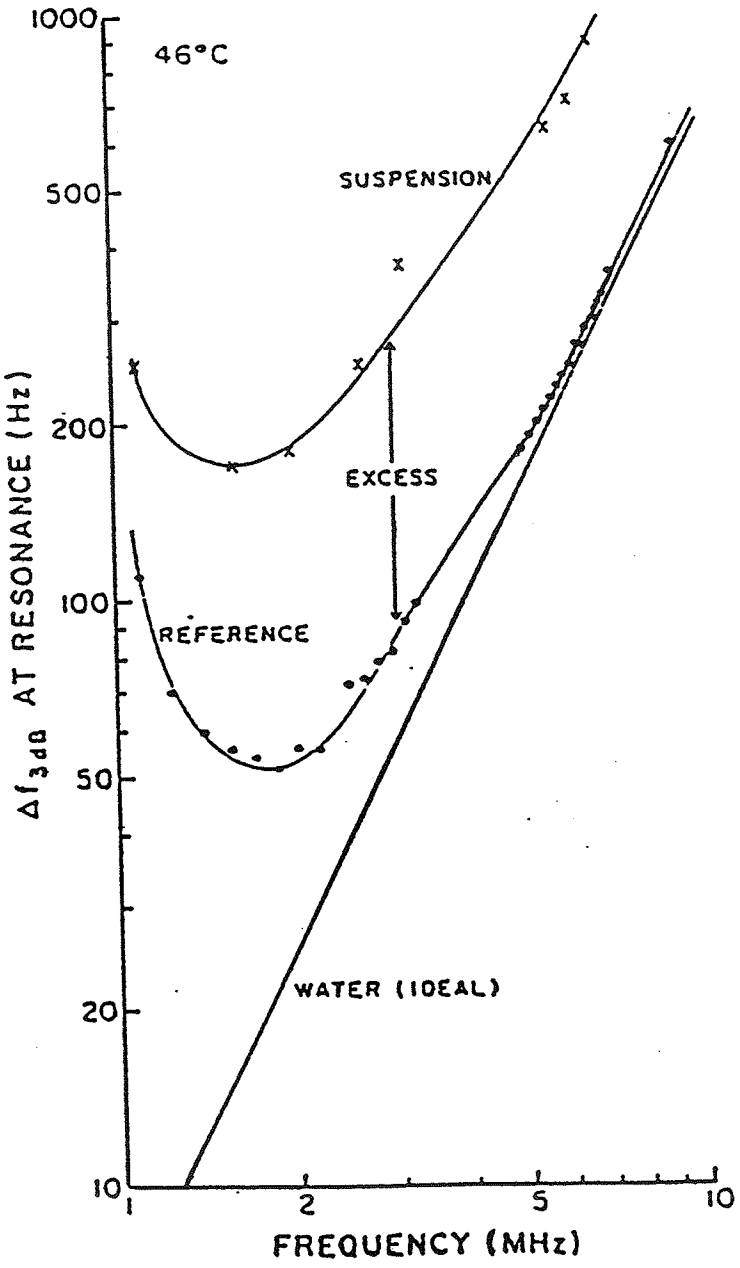

Figure 3.3 Δf as a function of frequency in distilled water, at 25°C, showing diffraction effects at low frequencies and the effects of imperfect reflection at high frequencies [Maynard, 1984].

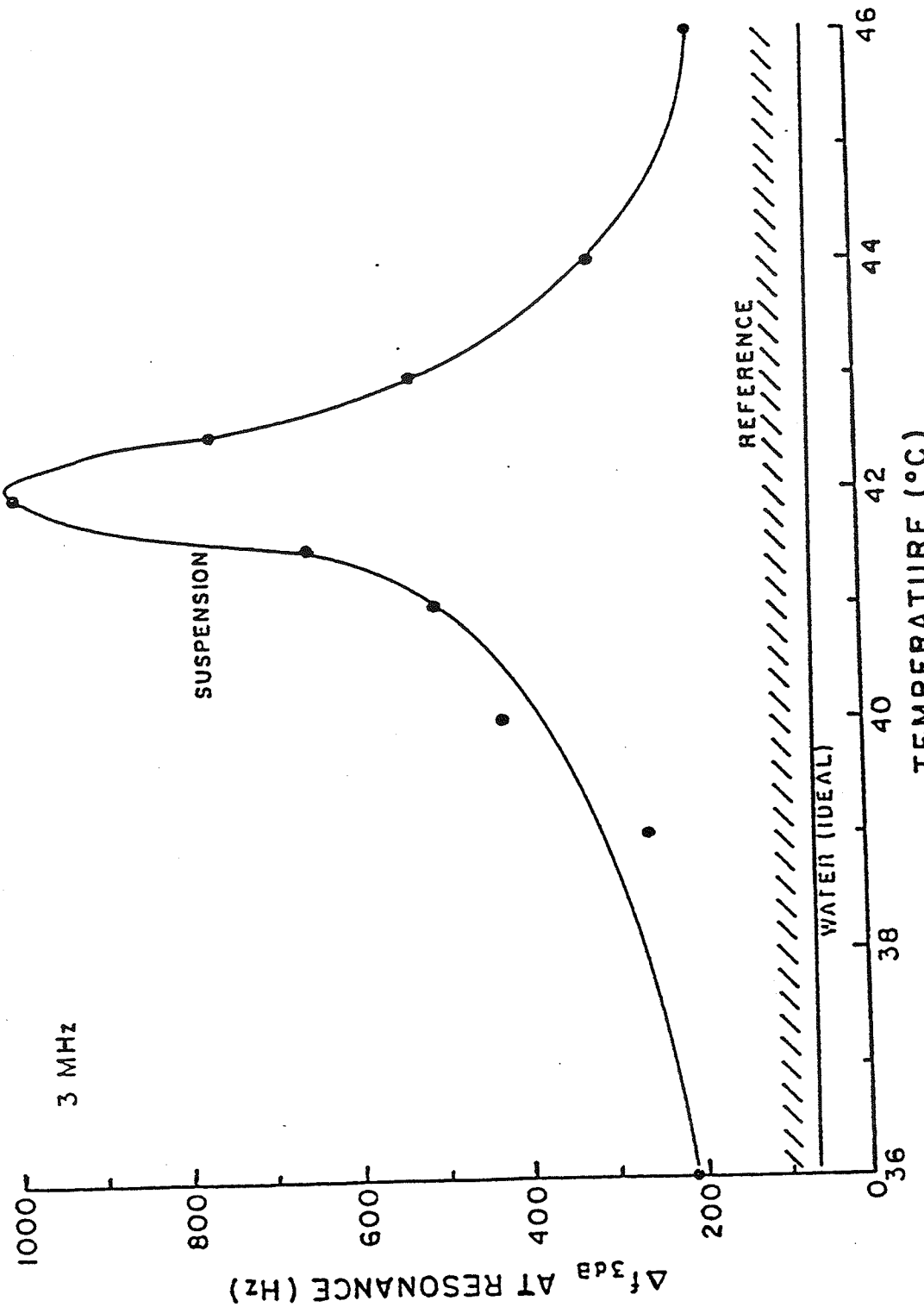

Figure 3.4 Δf and Δf_{ref} are shown as a function of temperature for LUV suspensions [Maynard, 1984].

CHAPTER 4

DIVALENT CATION EXPERIMENTS

4.1. Introduction

In order to test the importance of kinetics at the level of the polar headgroups in the phospholipid bilayer, divalent cations, which are known specifically to interact with negatively-charged headgroups of phospholipids [Muhleisen et al., 1983], were added to LUV suspensions. Specifically, Ca^{2+} and Mg^{2+} were added in increasing concentration to LUV suspensions to determine their effects upon the ultrasonic absorption coefficient per wavelength, $\alpha\lambda$, as a function of temperature and frequency. It was hypothesized that since the phospholipids of vesicle membranes in suspension contribute to the temperature dependent ultrasound absorption coefficient, the addition of cations to a liposome suspension should influence that absorption coefficient. This would be evidenced by a shift in $\alpha\lambda_{max}$ as a function of temperature. However, as the relaxational absorption of ultrasound in membranes is hypothesized to occur at the level of the fatty acyl side chains of the phospholipids (DPPC and DPPG), it could be expected that $\alpha\lambda_{max}$ as a function of frequency, with a peak at 2.1 MHz, would not be affected.

The importance of divalent cations, especially Ca^{2+}, in biological systems is well known, as many biological processes, e.g., exocytosis and neuronal transmission processes, involve Ca^{2+} interactions with cell membranes [Muhleisen et al., 1983]. Such Ca^{2+} interactions may involve Ca^{2+}-induced changes in the permeability of the membrane. In LUV suspensions (4:1 w/w DPPC:DPPG), the addition of Ca^{2+} produced a Ca^{2+}-concentration dependent increase in the temperature at which a significant rise in permeability occurs [Chan, 1986]. It was then hypothesized from the results of these permeability studies that the peak of $\alpha\lambda/c$ as a function of temperature may be shifted to higher temperatures. As the Ca^{2+} interacts with individual phospholipids, other characteristics of the phase transition curve ($\alpha\lambda$ versus temperature) may be changed, as

indicated by, for example, a change in the calorimetric enthalpy (ΔH_{cal}) or in the Van't Hoff enthalpy (ΔH_{VH}) of the lipid bilayer phase transition.

4.2. Procedure

The excess absorption coefficient of LUV suspensions, with and without divalent cations added, was determined as a function of temperature mainly at the frequency of 3.1 MHz. A determination of $\alpha\lambda/c$ (c = concentration of phospholipid) versus frequency (0.7 - 5.1 MHz) was also made at the phase transition temperature of the LUV suspension, because only at t_m was ultrasound absorbed greatly and at a characteristic frequency. The calorimetric transition enthalpy was determined by measuring the area under the $\alpha\lambda/c$ versus temperature curve and comparing this area with the area of a transition of known calorimetric enthalpy, as determined by DSC. It must be noted that this assumes a correlation between the enthalpy of the static thermodynamic transition and that of the ultrasonic transition. The Van't Hoff enthalpy, ΔH_{VH} (cal/mole), of the transition was calculated using the thermal width of the ultrasonic absorption coefficient by [Maynard, 1984]:

$$\Delta H_{VH} = 6.9\ T_m^2/\Delta T_{1/2}. \qquad (4.1)$$

These enthalpy values may be used to determine the cooperative unit of the transition, equal to the ratio of the Van't Hoff enthalpy to the calorimetric enthalpy [Strom-Jensen et al., 1984].

Before adding divalent cations to the LUV suspension, $\alpha\lambda/c$ was determined over the temperature range 37°C to 45°C, at 3.1 MHz, and was compared with that of standard LUV suspensions to ensure that the suspension consisted of LUVs (as opposed to being qualitatively similar to an SUV or MLV curve). This is the most convenient method to determine the composition (LUVs, MLVs or SUVs) of the suspension. Other methods include the use of DSC and permeability studies. The temperature of the specimen was then set to its measured phase transition temperature, t_m, and and the fluid in the cell was forced out of the acoustic interferometer and into the attached reservoir, which is also immersed in the temperature bath. Four to 40 µl of 250 mM $CaCl_2$ solution were then added to the

suspension, resulting in the final sample $CaCl_2$ concentrations of 0.1 mM and 1.0 mM. Similar amounts of $MgCl_2$ were added to LUV suspensions when later measurements were made in which Mg^{2+} was studied. The mixture was then allowed to equilibrate thermally for at least five minutes in the reservoir and to allow complete mixing of the suspension. Through gravity feed, the fluid was allowed to re-enter the cell, and another $\alpha\lambda/c$ determination, over approximately the same temperature range, was made. Once the t_m's of such suspensions were found, a determination of $\alpha\lambda/c$ versus frequency was made in order to determine the characteristic frequency of the ultrasonic absorption.

The addition of such small quantities of divalent cation solutions of greater than 300 milliosmolarity was calculated to not increase the osmolarity of the solution outside the liposomes by more than 5%, and thus should not have disturbed the isosmolarity condition across the LUV bilayers. It is important to note that other investigators have reported that the addition of divalent cations caused aggregation, and subsequently fusion, of LUVs and that sufficiently large additions of these cations caused membrane disruption [Papahadjopoulos et al., 1978]. However, except for the 10 mM $MgCl_2$ solution, the concentrations of divalent cations used in this study were below those for which fusion has been reported [Papahadjopoulos et al., 1978]. Some aggregation of the LUVs may have occurred, as evidenced by (1) observed decrease in $\alpha\lambda/c$ over the temperature range and, (2) the necessity for remixing after the addition of the divalent cation, approximately every six hours, by flushing out the contents of the cell and gravity-feeding the content back into the cell. Nonetheless, after mixing the observed $\alpha\lambda/c$ versus temperature curve was still characteristic of LUVs. After $\alpha\lambda/c$ was determined, a Ca^{2+} chelater (EGTA) was added to the LUV suspensions containing $CaCl_2$, at the t_m of the suspension. In each case $\alpha\lambda/c$ as a function of temperature (35°C - 45°C) was determined in order to observe the effect of the divalent cation chelator on the system. Data presented below show that, under suitable conditions, the LUVs could be returned to their standard state and this was considered evidence that intact LUVs were present.

For DSC experiments, the LUV suspensions ranged in phospholipid concentration from 25 mg/ml to 60 mg/ml. A first set of experiments employed $CaCl_2$ and $MgCl_2$ concentrations of 0, 2.5, and 25.0 mM. A second set of DSC measurements involved LUVs with internal aqueous phase of 50 mM EGTA, while maintaining isosmolarity and pH across the bilayer. The latter set of experiments employed $CaCl_2$ concentrations of 0, 2.5, 8.0 and 20 mM. The conditions of isosmolarity across the lipid bilayer, in each of these suspensions, were not violated as no greater than 10% difference in osmolarity existed between the aqueous phases inside and outside the LUV bilayers.

4.3. Results

4.3.1. Effects of $CaCl_2$

Figure 4.1 shows the acoustic absorption per wavelength per unit concentration as a function of temperature, for suspensions of standard preparation LUVs. With the addition of $CaCl_2$ to the LUV suspension, the peak is shifted toward higher temperatures, decreases in amplitude, and exhibits broadening. However, the relaxation frequency of the ultrasonic absorption does not change with increasing concentrations of divalent cations. That is, $\alpha\lambda/c$ versus frequency always has a peak at 2.1 MHz, even with the addition of $CaCl_2$ (see Figure 4.2). Figures 4.3 and 4.4 show that under suitable conditions, the LUVs can be returned nearly to their standard t_m, upon the addition of EGTA.

4.3.2. Effects of $MgCl_2$

The addition of $MgCl_2$ to LUV suspensions yields similar results, though with some important exceptions (Figure 4.5). The shift seen in t_m as a function of divalent cation concentration is not as great as that for $CaCl_2$ additions. Also, the decrease in amplitude of the $\alpha\lambda/c$ versus temperature peak is much less than for $CaCl_2$ addition. Convenient extrapolations of these curves show that ΔH of the transitions remains approximately the same at $CaCl_2$ concentrations of 0.1 mM and 1.0 mM, as does the ΔH of $MgCl_2$ at

concentrations of 0.1 mM and 1.0 mM. However, at 10 mM Mg^{2+} concentration, the ΔH of the phase transition does increase (see Table 4.1).

4.3.3. DSC Measurements of LUV Suspensions with Divalent Cations

The DSC measurements exhibit a peak in the heat capacity of the suspension which appears qualitatively to be similar to the ultrasound results. However, the DSC temperature measurement is performed on a time scale of minutes, compared with the time scale of hours required for the ultrasound measurement to be fully accomplished. This may be of importance in studying the kinetics of Ca^{2+} interaction with the LUVs, as is seen Figure 4.6. Note however that DSC still measures only the static thermodynamic variables of this system, while ultrasound absorption measurements give determinations of the relaxation kinetics of the system.

While the ultrasound $\alpha\lambda/c$ versus temperature measurements exhibit a single peak shifting to a higher t_m when divalent cations are added, DSC measurements exhibit two peaks (Figure 4.6B). One peak is characteristic of the t_m of standard preparation LUVs, while the other peak has a t_m shifted toward higher temperatures, depending upon the divalent cation concentration in the suspension. Each of these peaks on the first heating is approximately half the magnitude of the peak seen with a normal LUV suspension. However, as successive temperature cycles are conducted on the same sample, the first peak decreases in magnitude, eventually becoming insignificant, and finally leaving only a single peak at the higher t_m (Figures 4.6C and 4.6D). A slower rate of heating the sample may have overcome this effect, as equilibration of Ca^{2+} concentration inside and outside of the LUV bilayer could have occurred. This could indicate that, becauses the divalent cation is added to the suspension at room temperature for the DSC measurement, the divalent cations first bind to the outer lipid bilayer (or other lipid subpopulation), and then near t_m, due to increased permeability of the membrane, have access to the inner lipid bilayers of the LUVs as well.

Attempts were made to demonstrate that this hypothesis should hold for the removal of calcium as well as for its addition. The $CaCl_2$ was added to liposomes whose internal aqueous phase consisted of a high concentration of EGTA (50 mM), while still maintaining conditions of isosmolarity and pH across the bilayer. This experiment could also have been done such that calcium was encapsulated in LUVs. However, calcium tends to change many properties of the lipid bilayer, and may at high concentrations even disturb the bilayer's integrity; the reason for not making LUVs in this manner.

It was hypothesized that if calcium was added to such a suspension, in concentrations less than or equal to that of the EGTA, two populations of liposomes would be detected by DSC measurement upon a first heating through the transition. One population should be bound to the Ca^{2+} while another population should not. Subsequent heatings should allow for an equilibrium of EGTA and Ca^{2+} across the bilayer, thus diminishing the DSC peak of the bound lipid and increasing the amplitude of the peak at the normal t_m of the unbound lipid. However, the results suggest that this system is more complicated than originally believed.

The results show that at a 2.5 mM $CaCl_2$ concentration, the EGTA simply overwhelms the Ca^{2+}; two distinct peaks never being seen. This suggests that during the first run through the phase transition temperature, enough EGTA leaks out effectively to chelate the Ca^{2+}, and effect an equilibrium, as subsequent heatings showed no change in the DSC peak.

At 8.0 mM $CaCl_2$ concentration very different results are observed, as shown in Figure 4.7. Two peaks are observed, but the peak representing "bound" lipid, at a higher t_m, is much smaller than the peak representing "unbound" lipid. This suggests again that EGTA leaks out of the liposomes at the phospholipid phase transition. Upon subsequent heatings however, an effective chelation of the Ca^{2+} by the EGTA is not seen. The peak representing phospholipid bound to Ca^{2+} becomes increasingly larger. It appears that although EGTA may modulate the effects of Ca^{2+}, it does not negate them, and the normal mode of Ca^{2+} affecting the outside and later the inside bilayers of the LUVs still occurs. The same effects

were observed with a 20 mM $CaCl_2$ solution. Note that the temperature at which the second peak occurs, representing bound lipid, increases with the concentration of $CaCl_2$.

Therefore, the DSC measurements suggest that Ca^{2+} binding to the membrane may be preferable to its binding with EGTA, and that some rapid equilibration in the system may occur. However, it is not possible to show that the inside/outside effects of Ca^{2+} addition to LUVs can be observed with its removal.

4.4. Discussion

The results suggest that the acoustic absorption per wavelength ($\alpha\lambda$), as a function of temperature, in LUV suspensions with added divalent cations was quantitatively different from that seen for standard LUV suspensions, that ultrasound may interact with the membrane bilayer, and that ultrasound is sensitive to the divalent cations' interaction with the bilayer. The evidence suggests further that the ultrasound wave is sensitive to movements of the individual phospholipid molecules of the bilayer since the cooperative unit of the transition, as measured using ultrasound, decreases with increasing divalent cation concentration. However, as the relaxation time of the event responsible for the absorption of ultrasound does not change with the addition of divalent cations, the event absorbing ultasound energy has not itself been changed, except in the activation energy needed for its occurrence, or more specifically with the activation energy needed for the lipid bilayer phase transition to occur.

The interaction of the divalent cations with the LUVs may, tentatively, be modeled as follows: The divalent cations introduced to the LUV suspensions interact with the negatively-charged headgroups of the DPPG molecules and, in some manner as yet undetermined, constrain the movement of DPPG and DPPC molecules, and/or their carbon side chains. While the normal activation energy for the conformational change characteristic of the lipid bilayer phase transition, is 3 kcal/mole [Cullis and Hope, 1985], the binding of divalent cations to the negatively-charged bilayer surface could produce an increase in the activation energy over that characteristic of the phase transition, thus causing the phase

transition temperature to be increased. Support for the cations' interacting directly with the membrane phospholipids comes from the reduced values of ΔH_{VH}. While the enthalpies, ΔH, of the transitions remain approximately the same for 0.1 mM and 1.0 mM concentrations of the divalent cations, the Van't Hoff enthalpy decreases with increasing divalent cation concentration. Therefore, the cooperative unit, $\Delta H_{VH}/\Delta H$, of the transition also decreases as a function of divalent cation concentration. This supports the view of divalent cations interacting with phospholipid headgroups, perhaps even inserting themselves between the headgroups.

The fact that the addition of cation chelator to the suspensions produces a shift of the phase transition temperature back toward that characteristic t_m of LUVs, and reduction in the width of the $\alpha\lambda$ versus temperature, implies that the divalent cation interaction with the negatively-charged phospholipid bilayer is not completely irreversible, and that the bilayer structure of the LUVs was not altered irreversibly. The DSC measurements suggest that the binding of the divalent cations to the negatively-charged headgroups is dependent upon the temperature at which the cation is added and, thereby, the membrane permeability.

The absorption of ultrasound at a relaxation frequency of 2.1 MHz at t_m indicates a dynamic interaction between the phospholipid bilayer and the ultrasound wave. It is clear that the relaxation frequency is not perturbed by the addition of Ca^{2+}, which interacts with phospholipid headgroups. This indicates that while ultrasonic absorption is sensitive to changes in the lipid bilayer phase transition, the kinetics of its interaction with phospholipid molecules is not directly sensitive to the effects of divalent cations on the bilayer. Therefore, the site of the ultrasonic energy absorption probably is not in the region of the phospholipid headgroups but perhaps lies elsewhere in the bilayer. Such a site may be the phospholipid carbon side chains were, at t_m, the trans to gauche conformational change occurs, as well as the ultrasosnic absorption peak at 2.1 MHz. Support for this exists in which gramicidin, which inserts into the hydrophobic portion of the bilayer, changes the relaxation frequency of the ultrasonic energy absorption [Strom-Jensen et al., 1984].

TABLE 4.1

ENTHALPY OF LIPID PHASE TRANSITIONS DETERMINED FROM ULTRASONIC ABSORPTION MEASUREMENTS

The Van't Hoff enthalpy was calculated from the width of the ultrasonic peak at one-half its maximum height. The cooperative unit size was estimated from the ratio of the Van't Hoff enthalpy to the calorimetric enthalpy ΔH_{cal}. Estimates of error in the measurements are given for each value.

LUV Composition DPPC:DPPG (4:1 w/w)	0mM Ca^{2+}	0.1mM Ca^{2+}	1.0mM Ca^{2+}	0mM Mg^{2+}	0.1mM Mg^{2+}	1.0mM Mg^{2+}	10.0mM Mg^{2+}
t_m (°C)	42.0 ± 0.1	42.7 ± 0.1	44.0 ± 0.1	42.0 ± 0.1	42.3 ± 0.1	43.2 ± 0.1	44.0 ± 0.1
$\Delta t_{1/2}$ (°C)	1.6 ± 0.2	1.8 ± 0.2	2.9 ± 0.2	1.8 ± 0.2	2.1 ± 0.2	2.5 ± 0.2	2.8 ± 0.2
ΔH_{VH} (kcal/mol)	428 ± 21	382 ± 19	239 ± 12	380 ± 19	327 ± 16	276 ± 14	248 ± 12
ΔH_{cal} (kcal/mol)	7.5 ± 0.1	7.5 ± 0.1	7.5 ± 0.1	13.9 ± 0.1	13.9 ± 0.1	13.9 ± 0.1	18.4 ± 0.2
Cooperative Unit Size	57 ± 4	51 ± 3	32 ± 2	27 ± 2	23 ± 2	20 ± 1	14 ± 1

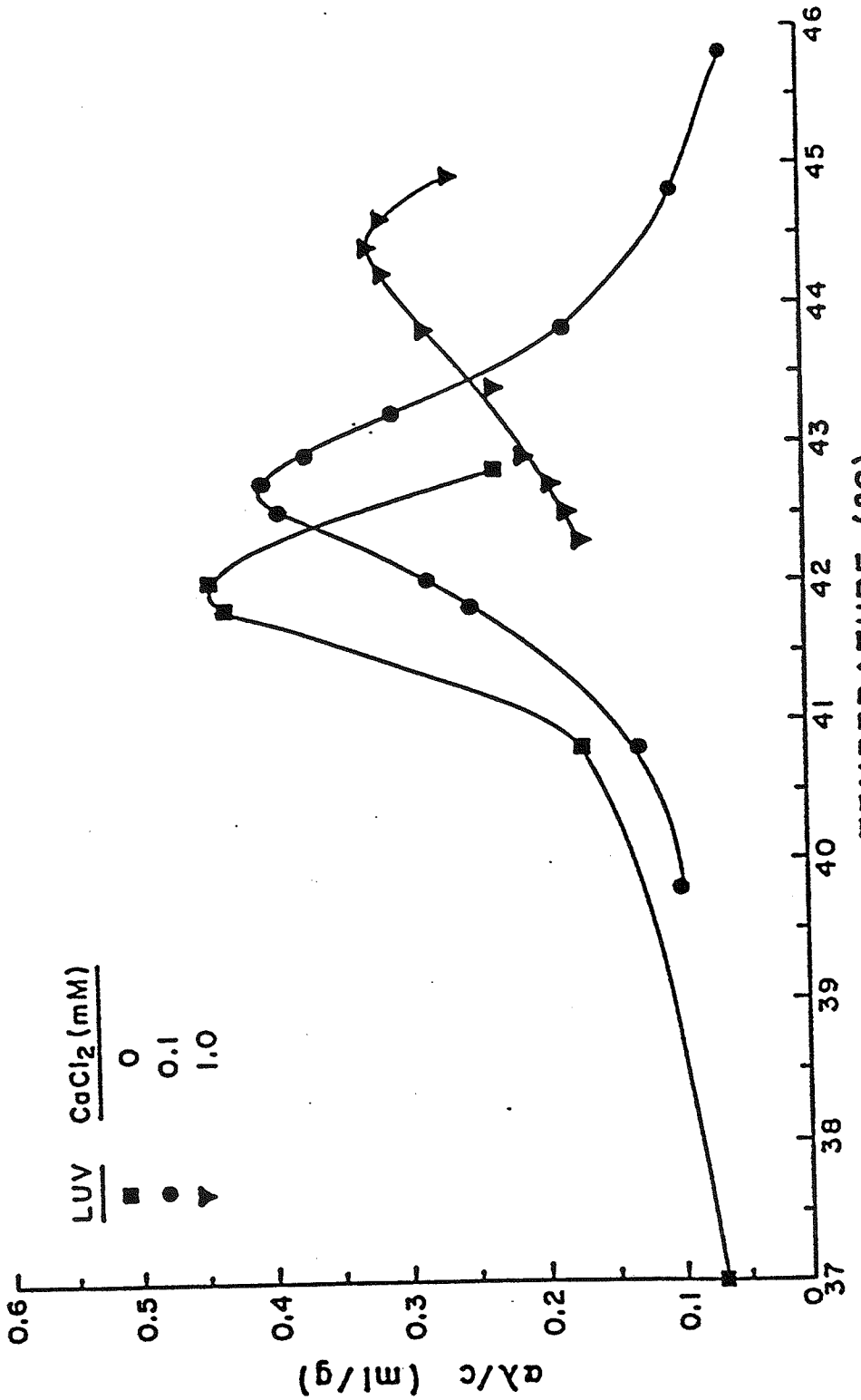

Figure 4.1 Effects of $CaCl_2$ (0 mM, 0.1 mM, and 1.0 mM) on $\alpha\lambda/c$ versus temperature in LUV suspensions.

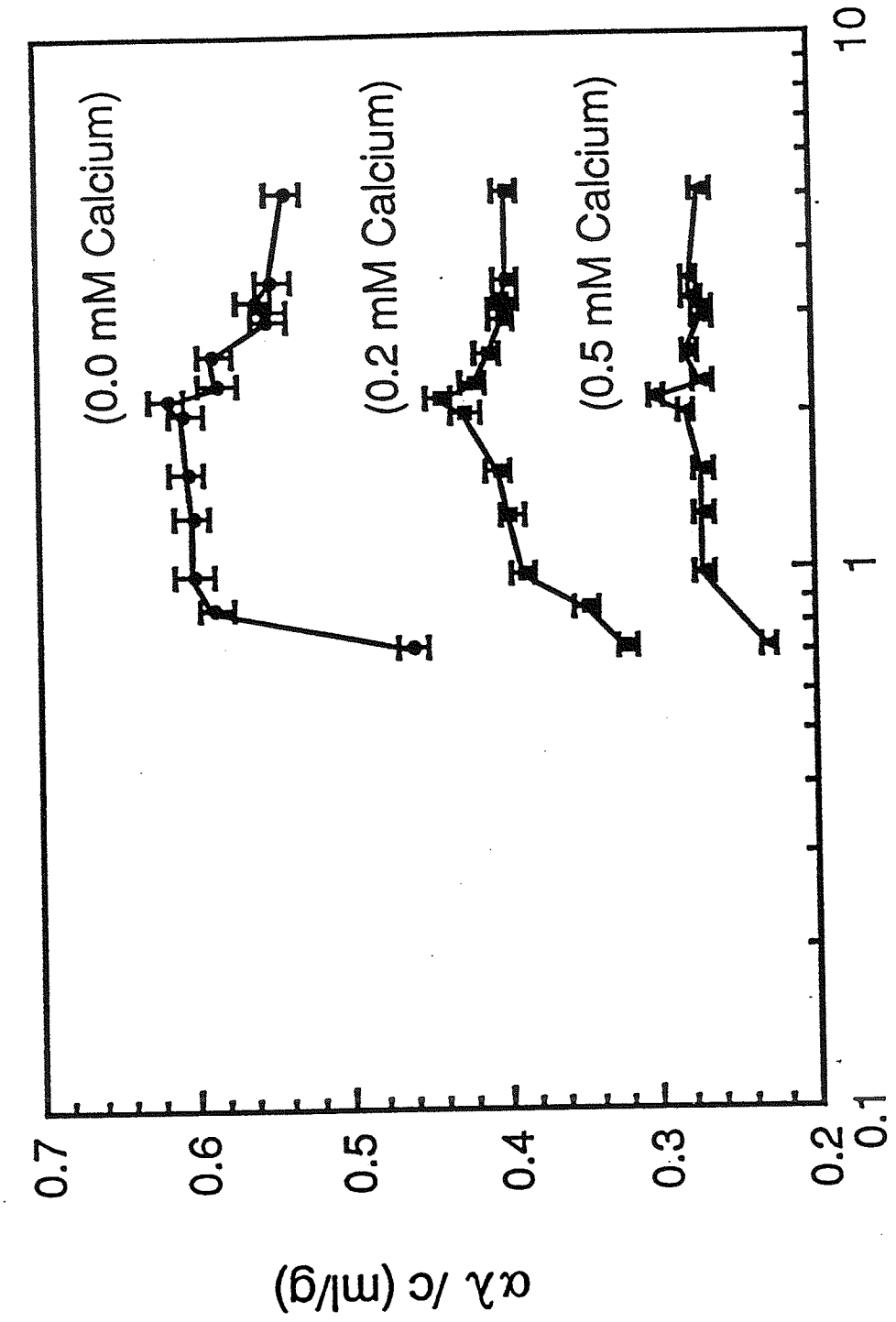

Figure 4.2 $\alpha\lambda/c$ as a function of frequency for LUV suspensions with and without added $CaCl_2$.

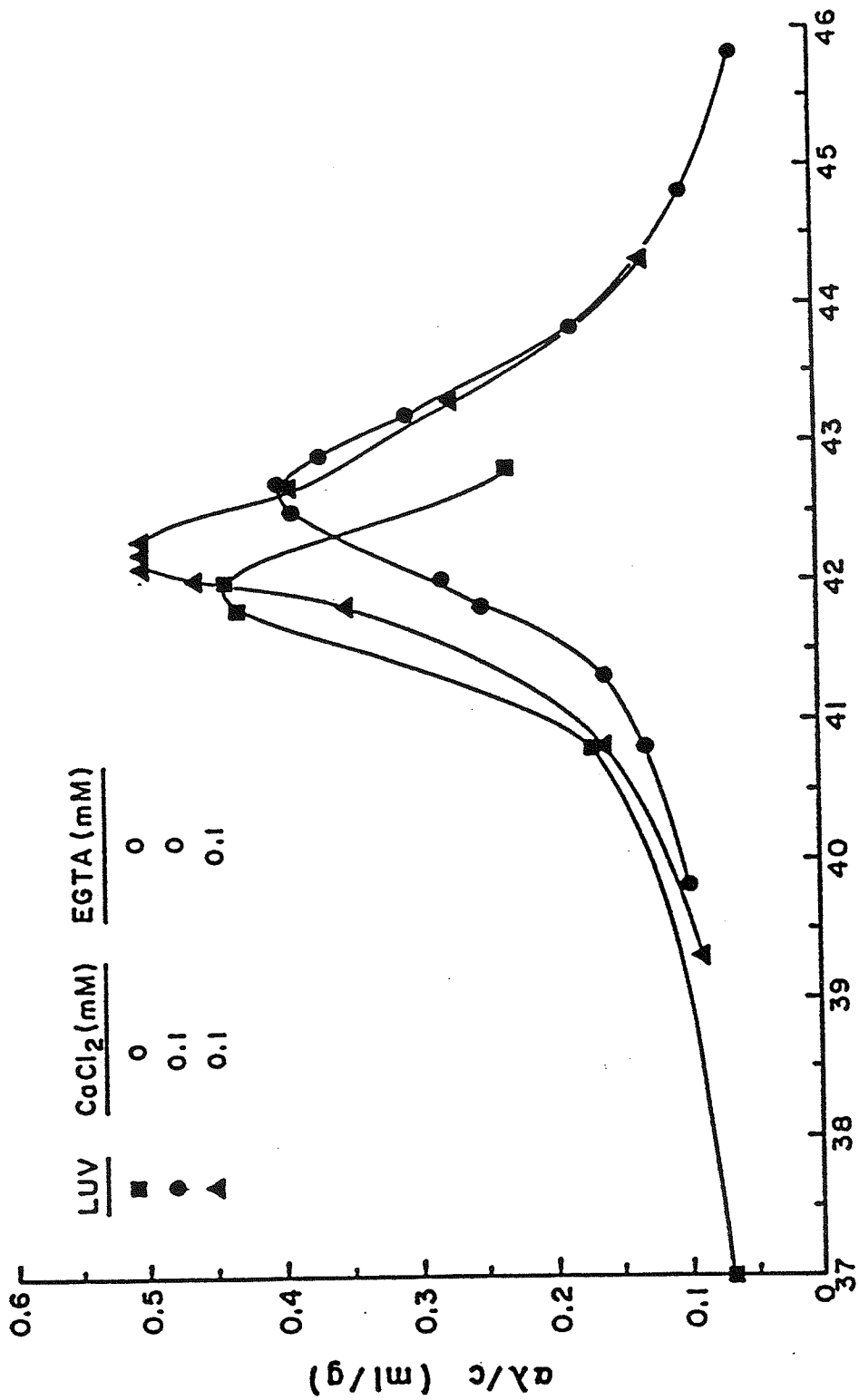

Figure 4.3 Addition of EGTA partially offsets the effects of $CaCl_2$ on LUV suspensions (0.1 mM $CaCl_2$, 0.1 mM EGTA).

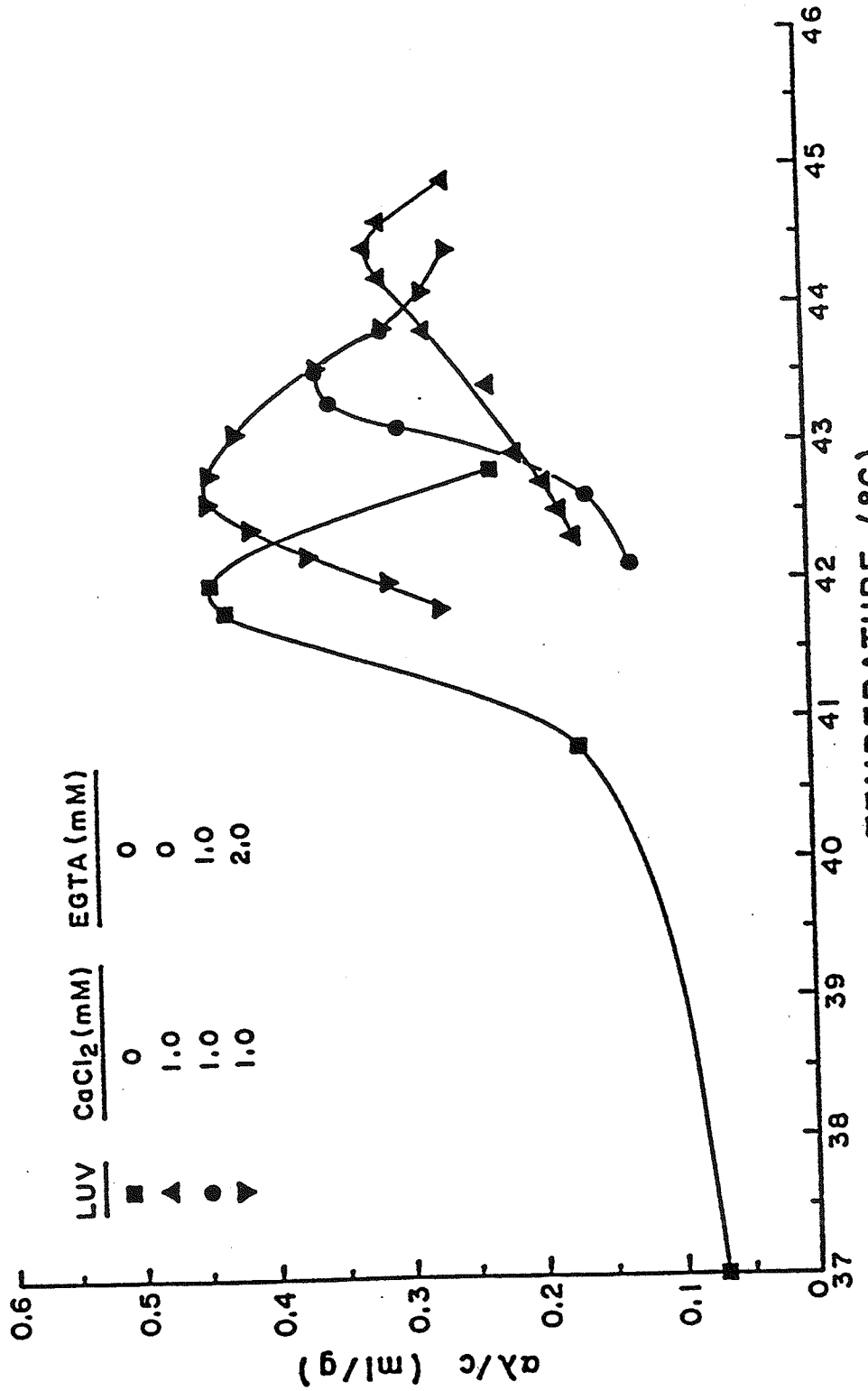

Figure 4.4 Addition of EGTA (1.0 mM, 2.0 mM) partially offsets the effects of 1.0 mM $CaCl_2$ on $\alpha\lambda/c$ versus temperature in LUV suspensions.

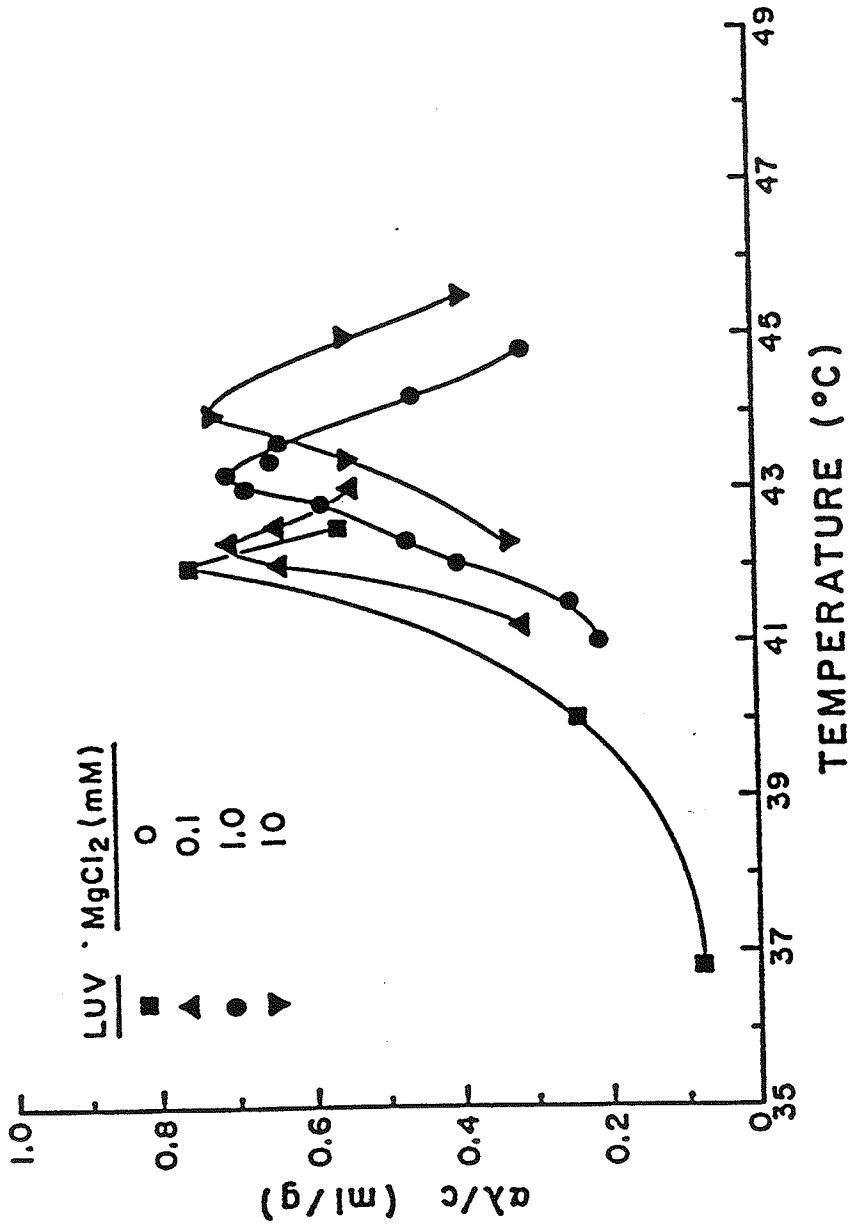

Figure 4.5 Effects of $MgCl_2$ (0 mM, 1.0 mM, and 10.0 mM) on $\alpha\lambda/c$ versus temperature in LUV suspensions.

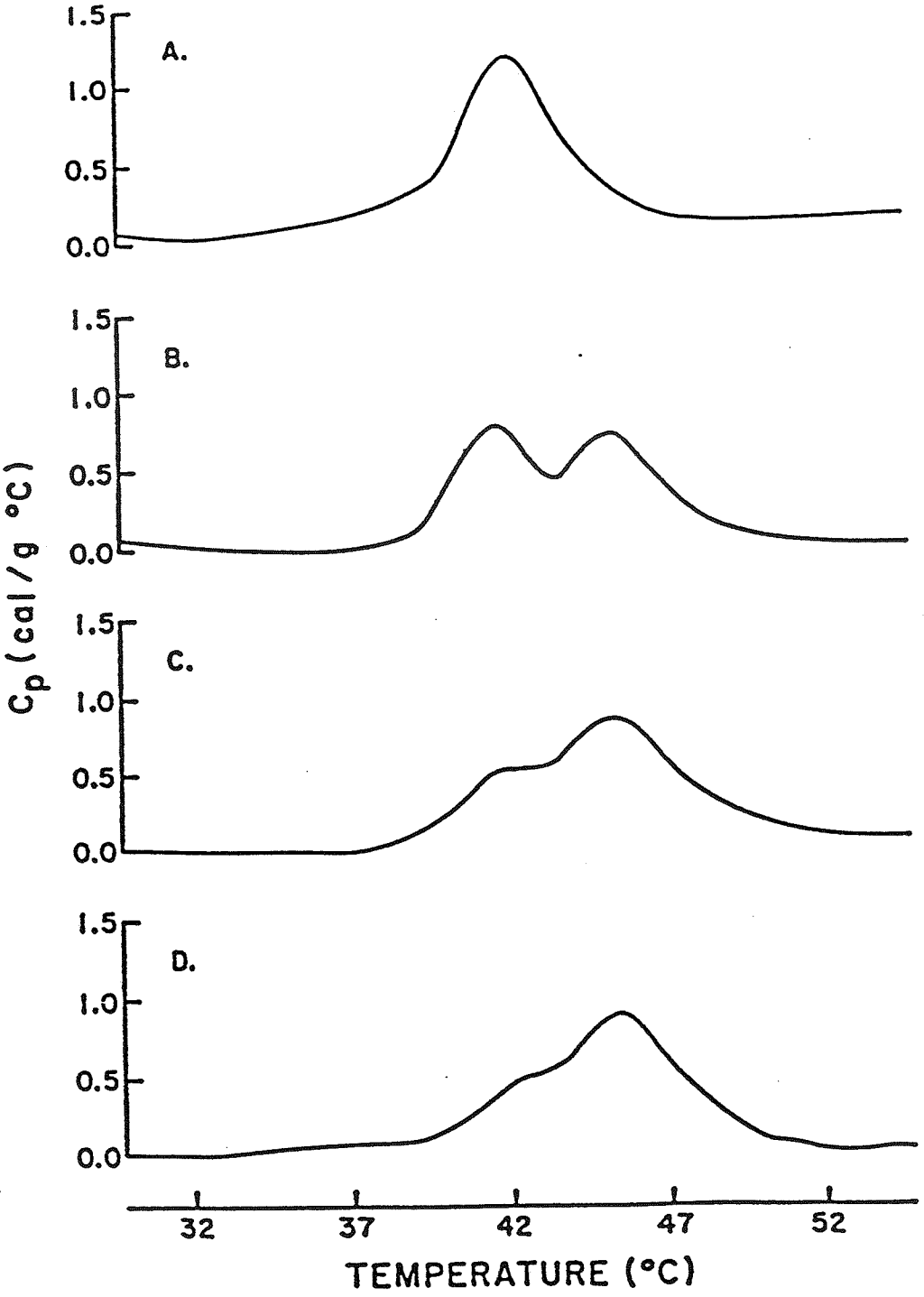

Figure 4.6 (A) C_p versus temperature in an LUV suspension.

(B) Effects of $CaCl_2$ (2.5 mM) on LUV suspensions, as measured by DSC (Note: two peaks), first heating.

(C) The second heating gives a DSC curve where the first peak is reduced in amplitude while the second peak increases in amplitude.

(D) The third heating of the sample by DSC exhibits further reduction of the first peak (at the lower temperature) and further increase in amplitude of the peak at higher temperature.

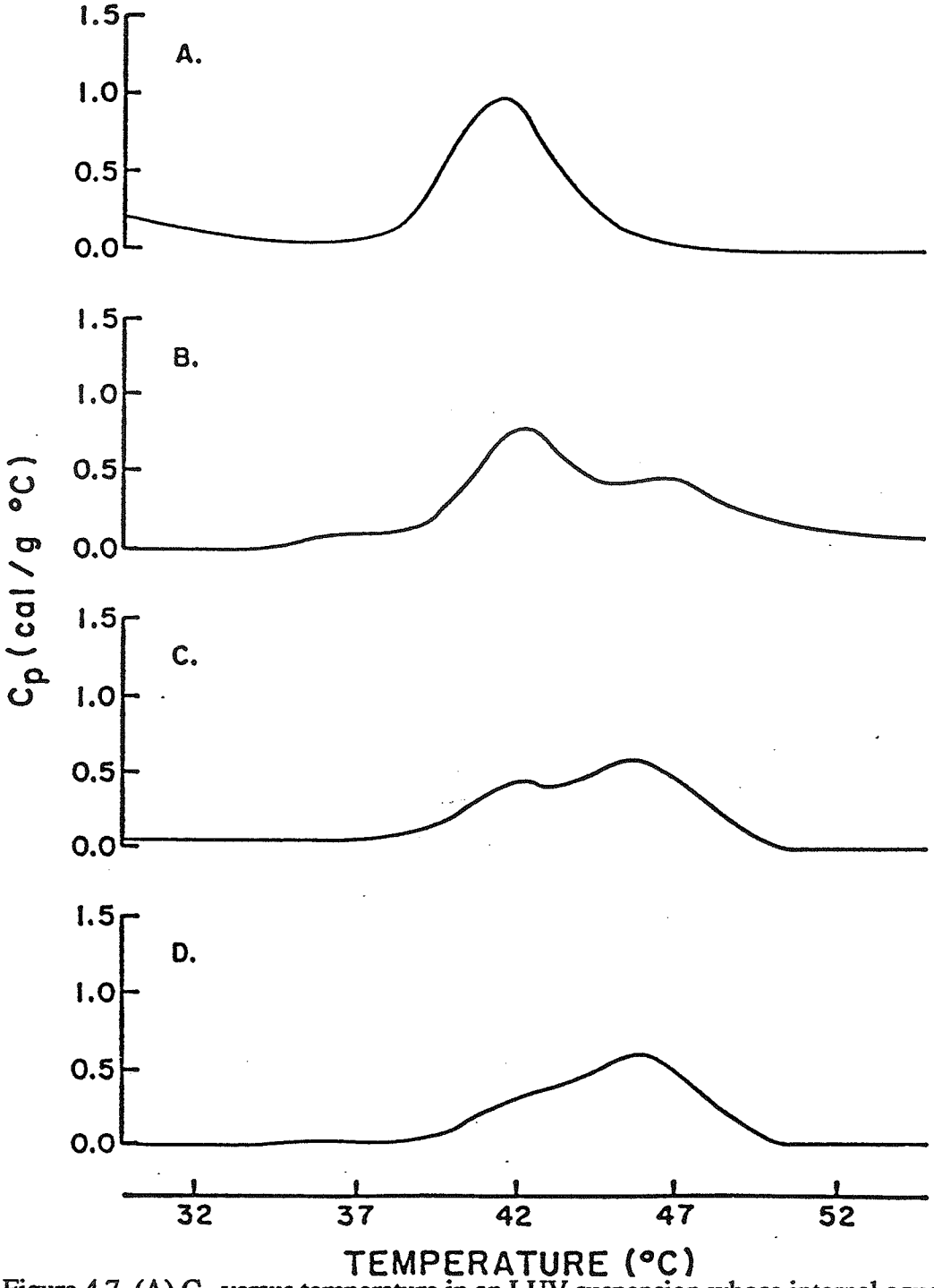

Figure 4.7 (A) C_p versus temperature in an LUV suspension whose internal aqueous phase has a 50 mM EGTA concentration.

(B) The first heating of the LUV suspension in (A) with 8.0 mM $CaCl_2$, as measured by DSC (Note: two peaks).

(C) The fifth heating gives a DSC curve where the first peak is reduced in amplitude while the second peak is increased in amplitude. (Note: the second through fourth heatings indicated the same trend).

(D) The seventh heating of the sample by DSC exhibits further reduction of the lower temperature peak, and further increases in amplitude of the higher temperature peak.

CHAPTER 5

D_2O EXPERIMENTS

5.1. Introduction

In this study, D_2O is used to replace H_2O in the aqueous buffer (in specified proportions) of LUV suspensions in order to investigate the importance of aqueous buffer in the interaction(s) of ultrasound with LUV membranes. The D_2O is used as a specific variation on water structure in order to determine the sensitivity of ultrasonic absorption to perturbations of the membrane-water interface.

In order to study D_2O perturbation of LUV suspensions with a static thermodynamic measure, differential scanning calorimetry (DSC) was also employed. The DSC was peformed because the temperature dependence of $\alpha\lambda$ at ultrasonic frequencies near the relaxation frequency in LUV suspensions is qualitatively like that of excess specific heat, c_p, as determined by DSC.

Electron spin resonance ESR was used as an additional technique to probe changes in the membrane caused by D_2O. The ESR spin probes, such as nitroxides attached to a specific carbon in a stearate molecule, can provide information about the membrane structure and mobility at different depths [Jost et al., 1971]. The spectral features of different nitroxides were used here to probe differences in LUV membranes in the phospholipid headgroup region, at the water-hydrocarbon interface and deep inside the hydrocarbon region.

5.2. Experimental Procedures

5.2.1. Ultrasound Procedure

LUV suspensions were made with varying percentages of H_2O in the aqueous portion replaced by D_2O. With each of the mixtures, D_2O constituted (molar volume) 0, 20, 50, 80, or 100% of the aqueous portion of the suspension. In these experiments, LUVs were prepared in D_2O or H_2O and were subsequently diluted into mixtures of D_2O and H_2O to

give final D_2O:H_2O ratios. The results for these experiments depended only upon the final D_2O:H_2O ratio, and were not significantly affected by the method of LUV preparation. The excess absorption per wavelength per unit concentration, $\alpha\lambda/c$, (c = concentration in g/ml) of these LUV suspensions was determined as a function of temperature and frequency. The temperature was varied from 35° to 46°C, while at each temperature the measurement frequency was varied from 0.64 to 5.2 MHz.

5.2.2. DSC Procedure

The DSC-2 (Perkin-Elmer, St. Louis, MO, USA) was used to obtain the specific heat at constant pressure, c_p, versus temperature on 50 µl samples of LUV suspensions. The suspensions in this study were 25.0 mg/ml phospholipid and the temperature range studied was 295 to 325 K.

5.2.3. ESR Procedure

In order to study more closely the dynamic interaction of D_2O in LUV suspensions with the phospholipid bilayer, LUVs made in D_2O (where D_2O is the only aqueous component of the buffer solution) were investigated with ESR spin label probes. Lipid soluble nitroxides (5-DS, 12-DS, PC-12-DS or CAT_{16}) were added to the membrane at a phospholipid:probe ratio of 100:1 to avoid spin-spin broadening. This was achieved by drying the probe on the bottom and sides of a culture tube (with N_2 gas), and then adding the freshly prepared liposomes and vortexing to ensure complete mixing. The probe partitioned into the organic phase of the LUV suspension, as was seen in the observed ESR signal, indicative of a probe incorporated into the hydrophobic phospholipid bilayer [Jost et al., 1971; Morse, 1985]. The resulting LUV suspensions were then separated into two groups. One group was kept stored under nitrogen (these are referred to as D_2O LUVs). The second group was dialyzed against ordinary hepes buffered saline (buffer) to replace the D_2O with H_2O (referred to as H_2O LUVs). Determinations of the anisotropic maximal splitting, A_{max}, as a measure of phospholipid mobility were made both as a function of aqueous

composition (H_2O versus D_2O in the hepes buffer) and as a function of temperature from 20°C to 48°C. Nitroxide probes are shown in Figure 5.1.

5.3. Results

5.3.1. Ultrasound and DSC Results

5.3.1.1. 95 - 100% D_2O LUV suspensions

Differential scanning calorimetry measurements of LUV suspensions prepared in 95 - 100% D_2O hepes buffer showed a thermotropic phase transition qualitatively very similar to that of standard LUV suspensions, with the exception that the t_m was 43°C compared to 42°C for standard LUV suspensions, as seen in Figure 5.2.

The results of ultrasound experiments in LUV suspensions with varying percentages of D_2O hepes buffer (where H_2O hepes buffer is replaced with D_2O hepes buffer) were as follows. For an LUV supension whose aqueous component consists of 95 - 100% D_2O, the $\alpha\lambda/c$ versus temperature exhibited a shape qualitatively similar to that of a standard LUV curve, with a sharp peak of $\Delta t_{1/2}$ of 1.8 ± 0.1°C (as is seen in LUV suspensions). However, two differences were noted. First, the phase transition temperature, t_m, was increased to 42.9 ± 0.1°C in D_2O preparations, compared to 42.0°C seen in standard LUV suspensions (see Figure 5.3). Second, ΔH_{cal} of this measurement, as determined by the area beneath the $\alpha\lambda/c$ versus temperature curve, was approximately 10 - 20% greater than that normally seen in standard LUV suspensions (see Table 5.2). This was not in agreement with DSC measurements, which showed a non-significant difference in enthalpy between the two types of LUVs (Figure 5.2). This suggests a difference in the enthalpy as determined by ultrasonic absorption measurements as compared to DSC measurements.

5.3.1.2. 80% D_2O LUV Suspensions

Standard LUVs were diluted into D_2O hepes buffer (resulting in at least 80% D_2O aqueous component). A curve close to that of LUVs with 100% D_2O resulted, with a transition temperature of 42.9 ± 0.1°C. A slightly broadened peak ($\Delta t_{1/2}$ = 2.0°C), with a

decreased amplitude (Figure 5.3) was obtained. Note that the enthalpy of the transition, was not significantly decreased compared to 95 - 100% D_2O LUVs (Table 5.2).

5.3.1.3. 50:50 D_2O:H_2O LUV suspensions

The $\alpha\lambda/c$ versus temperature curve for LUVs diluted into a D_2O/H_2O hepes mixture so as to produce a 1:1 D_2O/H_2O (± 5%) ratio for the aqueous component of the suspension, is seen in Figure 5.4. ΔH_{cal} was less than that of standard LUV suspensions. The clearly biphasic nature of this curve suggested two superimposed curves, with peaks at 42.0°C and 43.0°C, each representing decreased cooperativity (compared to standard LUV curves) due to the mixture of two distinct aqueous types. This curve has been decomposed into two curves, as is shown in Figure 5.4. These two peaks may have represented the phase transitions of single phospholipids interacting with H_2O or D_2O molecules, respectively.

However, the possibility also existed that the biphasic nature of the curve in the 1:1 mixture of H_2O and D_2O was dependent upon a partitioning of the two aqueous types to distinct subpopulations of the liposomes. As the liposome preparations were homogeneous in all aspects except for size (as a range of sizes exists for a given liposome suspension) size distributions may account for the biphasic nature of the curves. In order to study this possibility, LUVs of different size populations were studied. The LUVs were made and were then filtered into two groups, those extruded through a 0.2 μm filter and those extruded through a 0.1 μm filter. These LUV suspensions were then (in different experiments) diluted into a mixture of D_2O/H_2O hepes buffer so as to give within 5%, a 1:1 D_2O/H_2O ratio. The results seen in Figures 5.5A and 5.5B and Table 5.2 show that although the $\alpha\lambda/c$ versus temperature curves of these different size LUV populations were slightly different, the clearly biphasic nature of the curve, with a broad maximum at 42.0°C and a sharper peak at 43.0°C was still seen. This suggested that it was D_2O and/or H_2O interacting with individual phospholipids or small groups of phospholipids, that caused a biphasic curve to be seen. However, the distinct peak seen at 42.0°C in the first two preparations was not seen in the

0.1 μm filtered LUVs, suggesting perhaps that some feature of the LUV size may affect slightly their interaction with deuterium oxide.

5.3.1.4. 20% D_2O LUV suspensions

The LUV suspensions prepared such that D_2O made up at least 20% of the aqueous component of the suspension produced ultrasonic $\alpha\lambda/c$ values nearly that of LUVs in 80% D_2O hepes buffer, with a t_m of 42.8 ± 0.2°C (Figure 5.6) and $\Delta t_{1/2}$ = 2.3°C, which was slightly broader than that seen in 100% or 80% D_2O hepes buffer LUV suspensions. The enthalpy, however, was not as large as that seen in pure D_2O LUV suspensions (see Table 5.2). It is important to note that in all of these experiments the relaxation frequency of the phase transition as determined by ultrasound remained 2.1 MHz (see Figure 5.7). This result suggests that D_2O does not change the kinetics of the molecular event that is perturbed by ultrasound.

5.3.2. ESR Results

The broad spectrum in Figures 5.8B - 5.8D are typical for a nitroxide probe immobilized within the membrane [Morse, 1985] while the spectrum in Figure 5.8A is characteristic for rapidly tumbling nitroxides in water. At tempertures below t_m, 12-DS partitioned in both the membrane and in water, giving the free (aqueous) nitroxide spectrum superimposed on the spectrum from the probe in the membrane. These lines caused problems in the estimation of maximum splitting. Moreover, partitioning of 12-DS was different for D_2O compared to H_2O. Therefore, PC-12-DS was used instead, which gave no visible free nitroxide signal. The anisotropic maximal splitting, A_{max}, for different probes within the membrane of LUVs is often used as a measure of the fluidity of the bilayer at different fatty acyl positions [Jost et al., 1971]. The motional anisotropy of the labels is greater for labels whose nitroxide group is placed at the membrane surface than for those labels whose nitroxide group is located within the hydrophobic region of the phospholipid

bilayer, in the order CAT_{16} > 5-DS > PC-12-DS, in agreement with observations for many other membranes [Jost et al., 1971; Morse, 1985]. Thus if D_2O affects membrane structure and mobility in LUV suspensions, ESR probes at different membrane levels may be used to determine the site(s) of that perturbation.

The results of 5-DS experiments at 20°C are given in Figures 5.8C and 5.8D. The experiments at 20°C showed that A_{max} for 5-DS was increased in D_2O LUV suspensions compared to H_2O LUV suspensions. The ESR results showed this trend also with increasing temperature (Table 5.3), although the difference between the A_{max} in D_2O versus H_2O hepes did decrease as the temperature was increased, until at 48.0°C, no significant difference in splitting was observed between the two samples (see Table 5.3). These results suggest that aqueous structure is important in dynamics at or near the water-membrane interface, even to the level of the fifth carbon atom of the fatty acyl chains.

CAT_{16} experiments showed a small difference in A_{max} between D_2O and H_2O LUVs at 20°C (see Figure 5.9) but showed no significant difference in A_{max} in D_2O buffer versus H_2O buffer at higher temperatures, suggesting that the difference in phospholipid mobility at higher than 20°C is not significant in the aqueous portion of the membrane-aqueous interface.

In contrast to the 5-DS, the same experiment using PC-12-DS showed no significant difference in the A_{max} of PC-12-DS in D_2O versus H_2O buffer, suggesting that although aqueous structure is important in determining phospholipid dynamics and structure at the membrane-water interface, it is not important (on ESR timescales of 10^{-8} sec) for phospholipid dynamics deeper in the lipid bilayer.

5.4. Discussion

In order to determine the site of ultrasound interaction in LUV suspensions, different regions of LUV structure are perturbed, and the corresponding changes to the frequency dependence of $\alpha\lambda$ at t_m are observed. The physical propeties of D_2O are only slightly different from those of H_2O (see Table 5.1). However, small differences in molecular

properties may cause a perturbation in the normal aqueous interaction with individual phospholipids. The D_2O is more structured than H_2O and it is known that there exists a hydration shell that interacts with phospholipid headgroups at the membrane-water interface [Merck, 1983]; however, the molecular dynamics of the interction between phospholipids and water molecules has not been described and therefore the effects of D_2O on the dynamics of phospholipid molecules and/or their carbon side chains are not known. It is known that replacement of H_2O by D_2O in specific biological systems has a profound effect on those systems. Specificallly, D_2O is known to depress the excitation-contration coupling in frog skeletal muscle and other experiments have suggested the possibility that D_2O influences the mechanism underlying Ca^{2+} release from the sarcoplasmic reticulum induced by depolarization at the transverse tubules [Sato and Fujino, 1987; Fan et al., 1985]. If D_2O perturbs the LUV bilayer or the lipid bilayer phase transition and also perturbs $\alpha\lambda$ as a function of frequency, then the membrane-water interface could be a site of interaction of ultrasound and LUVs.

It is known that D_2O, as the aqueous component of LUV suspension affects the phospholipid phase transition, as association with D_2O causes at least a subpopulation of the phospholipids to have an increased t_m, to $42.9 \pm 0.1°C$ from 42.0°C. The 1:1 mixtures of H_2O and D_2O clearly create a biphasic nature in the phospholipid phase transiton curve. This is probably due to random association of single phospholipids with D_2O or H_2O molecules, which also results in decreased cooperativity of the two components seen in the transition. These results suggest that the replacement of H_2O with D_2O does cause a change in the LUVs, specifically to their phase transition temperature. It is important to note that the $\alpha\lambda_{max}$ of 2.1 MHz for standard preparation LUV suspensions is not changed with the replacement of H_2O by D_2O in the aqueous buffer of LUV suspensions, suggesting that D_2O does not interact with the site of ultrasound absorption in LUV membranes.

As the activation energy of the phase transition is increased by a substance that should only affect the membrane surface, it is hypothesized tha the structure and mobility of the phospholipids at the membrane-aqueous interface are changed. In order to study the mobility

of the LUV membrane at a specific position at the membrane-aqueous interface, ESR nitroxide probes are used, and should detect any changes in the mobility of the phospholipids caused by the addition of D_2O in LUV suspensions.

The ESR results indicate that D_2O changes the phospholipid side chain mobility near the membrane-water interface (to the level of carbon 5) but that it does not significantly affect side chain mobility in the hydrophobic (at the level of carbon 12) region of the bilayer. The isotropic splitting constant, A_o, for nitroxide in solvent (Figure 5.8A) is dependent only upon the polarity of that solvent, and A_o for nitroxides dissolved in D_2O is the same as in H_2O. Therefore, the difference seen in A_{max} seen in the D_2O and H_2O LUVs is unlikely to originate from the direct interaction of the probe with solvents of different polarity. Furthermore, in LUV suspensions, the difference in A_{max} decreases as temperature increases, suggesting a dependence on some factor other than polarity of the solvent. Therefore it seems that the difference in A_{max} reflects changes in the structure of the bilayer. Greater A_{max} for 5-DS and CAT_{16} in D_2O LUVs as compared to H_2O LUVs indicates a more restricted mobility of the probe, i.e., a less fluid membrane in the polar head group regions.

However, the differences in A_{max} of 5-DS and CAT_{16} in the H_2O and D_2O LUV suspensions could be a consequence of the different water penetration in the LUV bilayer for these two aqueous types, which could occur in addition to the differences in phospholipid mobility. It has been shown that water penetrates into lipid bilayers to a significant distance, so that 5-DS is affected by the aqueous solvent [Griffith et al., 1974]. Increased A_{max} in D_2O LUVs might then indicate increased water penetration, i.e. a more polar environment of the probe. The PC-12-DS is in the nonpolar environment and is not sensitive to water penetration. These effects can be distinguished by recording the spectra at very low temperatures where the effects of motion disappear.

Regardless of the exact origin of the increased splitting for the D_2O LUVs, it can be concluded that the increased splitting reflects changes in the structure of the bilayer. Also,

these changes are significant in the polar headgroup region and extend a few angstroms into the hydrocarbon region, as is seen in the 5-DS spectra.

Based on this information a model for the perturbation and general interaction of D_2O with phospholipids in the LUV membrane may be formulated: It is given that H_2O is situated at the aqueous-membrane interface to allow the most stable energy configuration of the phospholipids and the water molecules and other solvent molecules. The exact nature of this configuration has not been treated but it has been assumed that the dipolar water (1.76 debye) has van der Waals interaction and dipole interaction with the zwitterionic DPPC moiety and with the negatively-charged DPPG headgroups. This configuration allows for a certain mobility (fluidity) of the entire phospholipid moiety, the headgroups, and the hydrocarbon chain near the membrane-water interface in particular. When H_2O is replaced by D_2O, a different molecule with an increased molecular weight and increased dipole moment (1.78 debye), a different low energy configuration at the membrane-water interface must form. It is likely that not only does each D_2O molecule take up a slightly different geometry at the membrane-water interface, but also that the bond strength of the D_2O with those molecules with which it interacts is greater than that of water. This would cause the membrane phospholipids to be more ordered, suggesting a lower mobility at the membrane-water interface (as observed in ESR experiments). It would also suggest that a greater activation energy would be required for the phospholipid gel to liquid phase transition to occur. These effects were observed in these experiments.

In order to investigate further the interaction of D_2O with the lipid bilayer a careful study of the effects of D_2O on a series of doxyl stearate nitroxides (e.g. 5-DS, 7-DS, 9-DS, etc...,) should be performed to provide an estimation of D_2O penetration into the lipid bilayer (as compared to H_2O) and of the magnitude of its effects at different depths of the bilayer. Another useful technique in the study of D_2O effects on the bilayer would be ^{13}C NMR, which would give an estimation of fatty acyl mobility in the bilayer on NMR timescales (10^{-6} to 10^{-8} sec). As there are ^{13}C-labelled lipids, no probe needs to be inserted into the membrane.

Mixtures of D_2O and H_2O in LUV suspensions might also be studied with ESR and NMR in order to determine whether the effects of D_2O on the lipid bilayer are linear with increasing concentration as determined by these techniques. Finally deuterium itself is of interest, as deuterated lipids and proteins are often used in deuterium NMR measurements. It would also be of interest to measure the ultrasonic absorption coefficient per wavelength of specifically-deuterated phospholipids as a function of temperature and frequency and to study these lipids using NMR and ESR as well.

TABLE 5.1

Physical Properties of H_2O and D_2O

	H_2O	D_2O
MW (daltons)	18.016	20.028
C_p (cal/g) (4-25°C)	1.000	1.028
H_f (kcal/mole)	1.436	1.501
Dielectric constant	87.740	78.06
m.p. (°C)	0.0	3.82
b.p. (°C)	100.0	101.42
Critical temperature (°C)	374.2	371.5
density at 25 °C (g/ml)	0.997	1.1044
velocity of sound (m/s) at 20°C	1482.9	1384.2
velocity of sound (m/s) at 40°C	1529.3	1433.1
Index of refraction	1.333	1.3384
Dipole moment (debye)	1.76	1.78

TABLE 5.2

CHARACTERISTICS OF THE LIPID PHASE TRANSITION DETERMINED FROM THE ULTRASOUND ABSORPTION COEFFICIENT MEASUREMENTS IN LUV SUSPENSIONS WITH VARYING PORTIONS OF D_2O

ΔH_{cal} was obtained by comparison of the area under an $\alpha\lambda/c$ versus t(°C) curve of known enthalpy. The Van't Hoff enthalpy was calculated from the width of the ultrasound $\alpha\lambda/c$ peak at one-half its maximum height. The cooperative unit was estimated from the ratio of the Van't Hoff enthalpy to the calorimetric enthalpy. Estimates of error are given for each value.

LUV Composition DPPC:DPPG (4:1 w/w)	0% D_2O	20% D_2O	50% D_2O	50% D_2O	50% D_2O	80% D_2O	100% D_2O
D_2O or H_2O preparation	H_2O	D_2O	D_2O	H_2O	H_2O	H_2O	D_2O
t_m (°C)	42.0 ± 0.1	42.8 ± 0.2	42.0 ± 0.2 43.0 ± 0.1	42.0 ± 0.2 43.0 ± 0.1	43.0 ± 0.2	42.8 ± 0.2	42.9 ± 0.1
$\Delta t_{1/2}$ (°C)	1.6 ± 0.2	2.3 ± 0.2	--------	--------	--------	2.0 ± 0.2	1.7 ± 0.2
ΔH_{VH} (kcal/mole)	428 ± 21	299 ± 15	--------	--------	--------	344 ± 17	405 ± 21
ΔH_{cal} (kcal/mole)	7.5 ± 0.2	6.3 ± 0.6	6.2 ± 0.6	7.6 ± 0.8	7.6 ± 0.8	9.4 ± 0.9	9.7 ± 0.9
Cooperative Unit Size	57 ± 4	48 ± 4	--------	--------	--------	37 ± 3	42 ± 4

TABLE 5.3

ESR DATA

A_{max} of 5-DS in LUVs in D_2O buffer are compared to LUVs in H_2O buffer, as a function of temperature, below and above the phase transition temperature of the LUV suspensions. The estimate of error of these measurements is 0.3 gauss.

t(°C)	A_{max} (H_2O LUVs) (gauss)	A_{max} (D_2O LUVs) (gauss)
22	59.7	62.3
25	58.0	60.0
29	57.8	59.1
33	55.9	57.6
39	48.6	49.5
42	43.2	43.9
43	-----	43.0
44	41.7	42.2
48	41.3	41.3

NITROXIDES

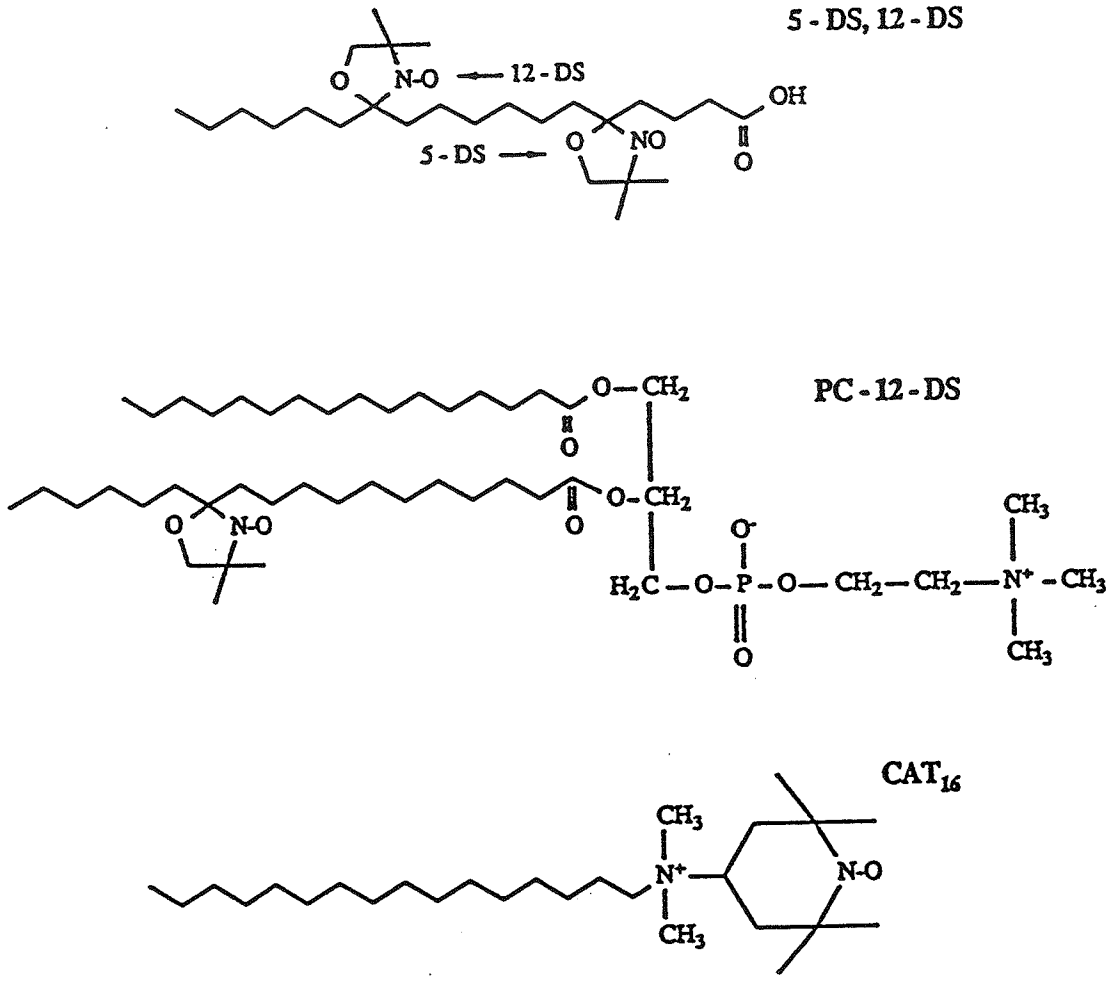

Figure 5.1 The structures of the nitroxide-labelled molecules used in this study:
5-DS: 4,4-dimethyl-oxazolidine-N-oxyl derivative of 5-ketostearic acid
PC-12-DS: 1-palmitoyl-2-(12-doxyl stearoyl)phosphatidylcholine
CAT16: 2,2,6,6-tetramethylpiperidine-N-oxyl-4-[N,N dimethyl-N-hexaolecyl-ammonium].

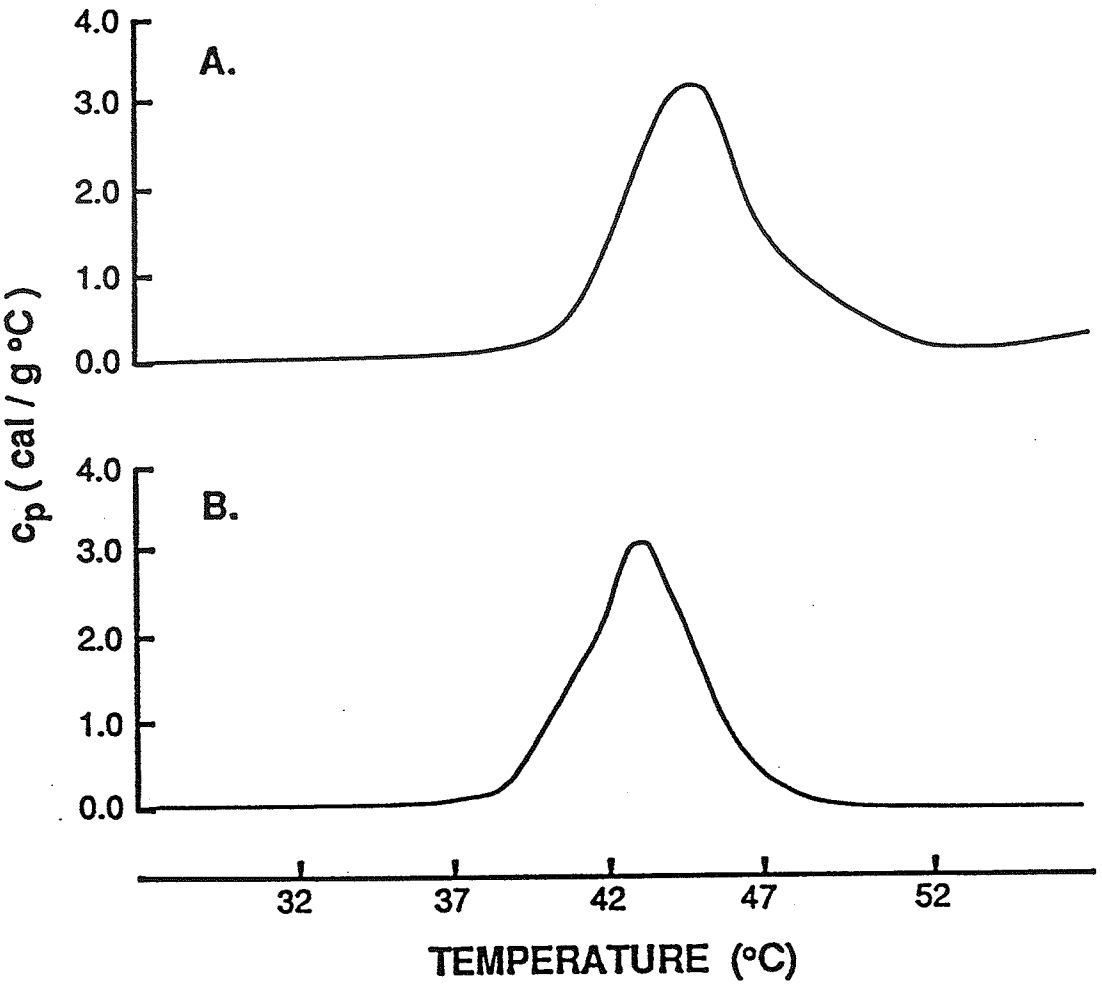

Figure 5.2 DSC measurement of c_p versus temperature (°C) of LUVs in:
A. 100% D_2O buffer (t_m = 43 °C)
B. 100% H_2O buffer (t_m = 42 °C)

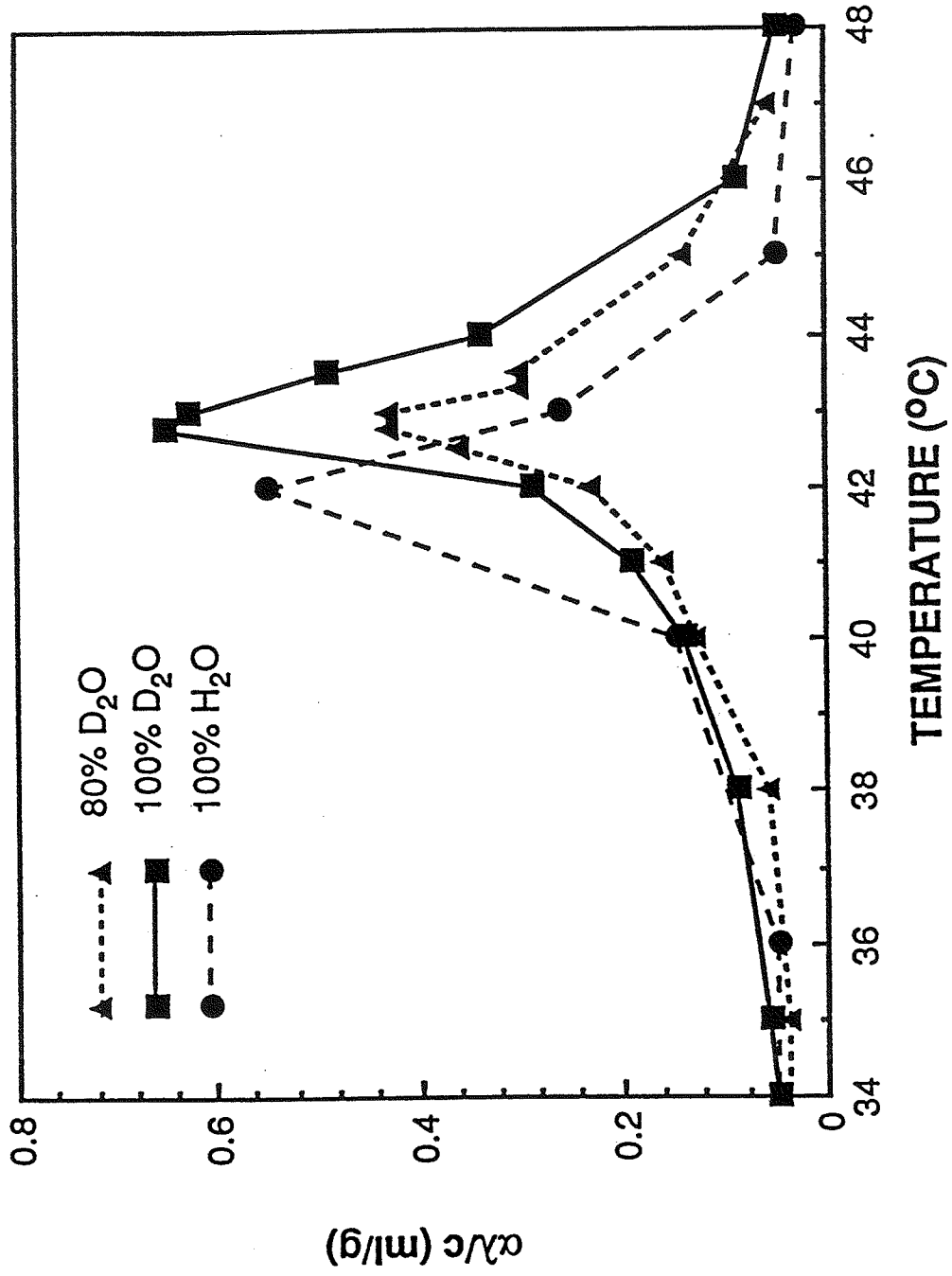

Figure 5.3 Effects of D_2O addition on $\alpha\lambda/c$ versus temperature (°C) at 3.1 MHz for LUVs in 100% H_2O, 100% D_2O, and 80% D_2O. The estimated error in $\alpha\lambda/c$ is 0.01 ml/g.

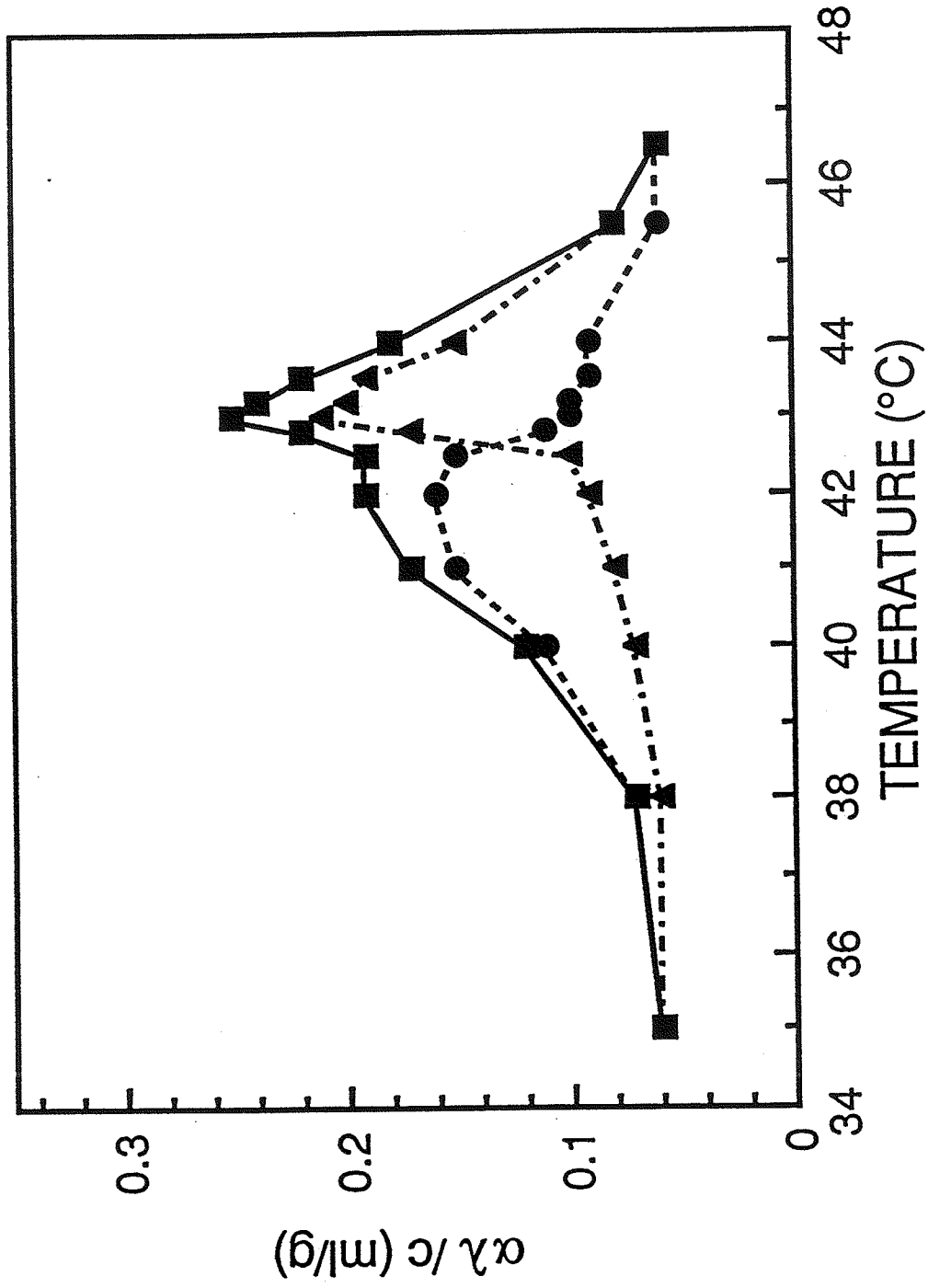

Figure 5.4 The solid line represents $\alpha\lambda/c$ versus temperature of LUVs in 1:1 D_2O:H_2O buffer. The broken lines represent two simulated peaks, at 42.0°C and 43.0°C, respectively.

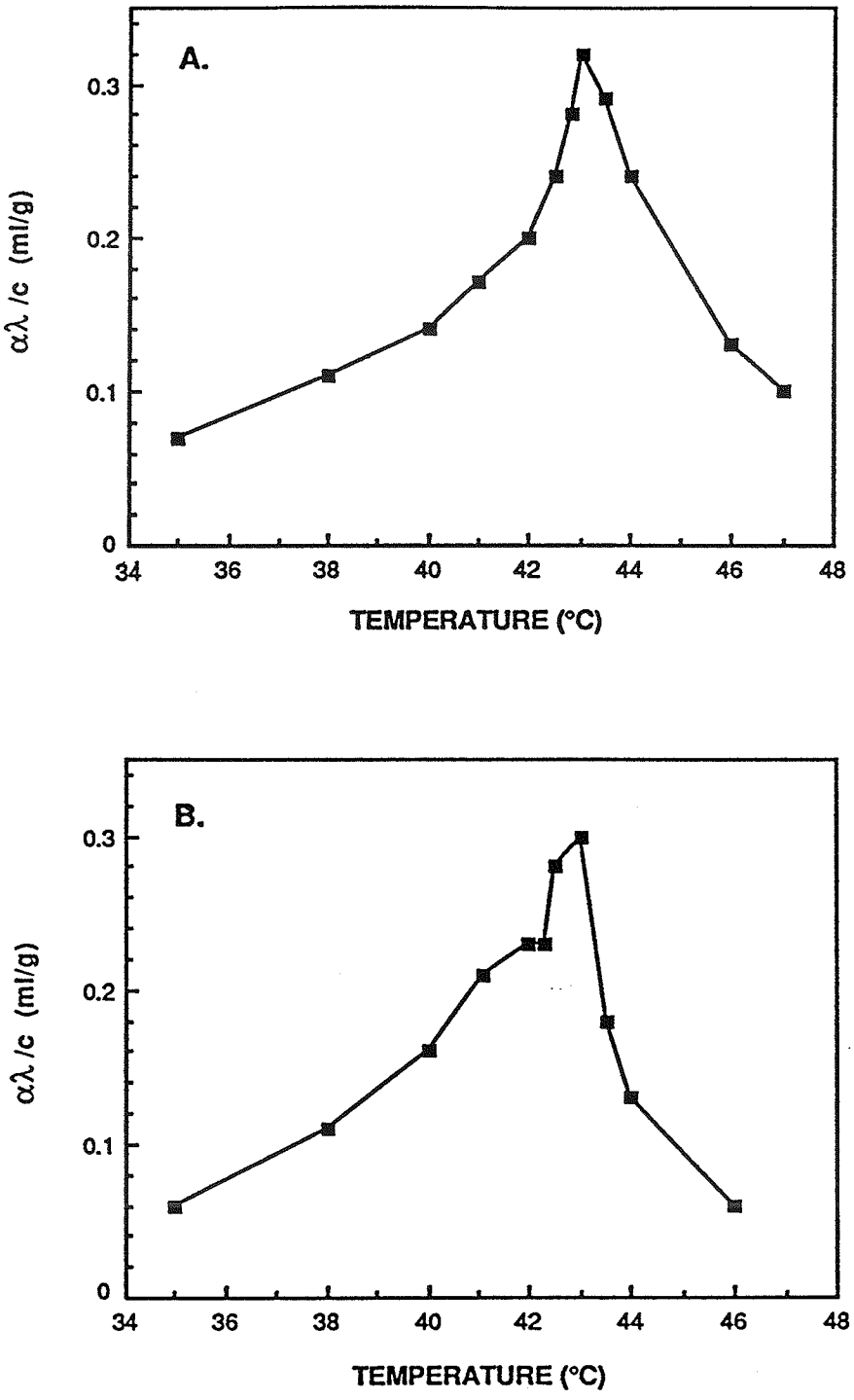

Figure 5.5 $\alpha\lambda/c$ versus temperature in:
A. 0.1 μm filtered LUVs in 1:1 D_2O:H_2O hepes buffer.
B. 0.2 μm filtered LUVs in 1:1 D_2O:H_2O hepes buffer.

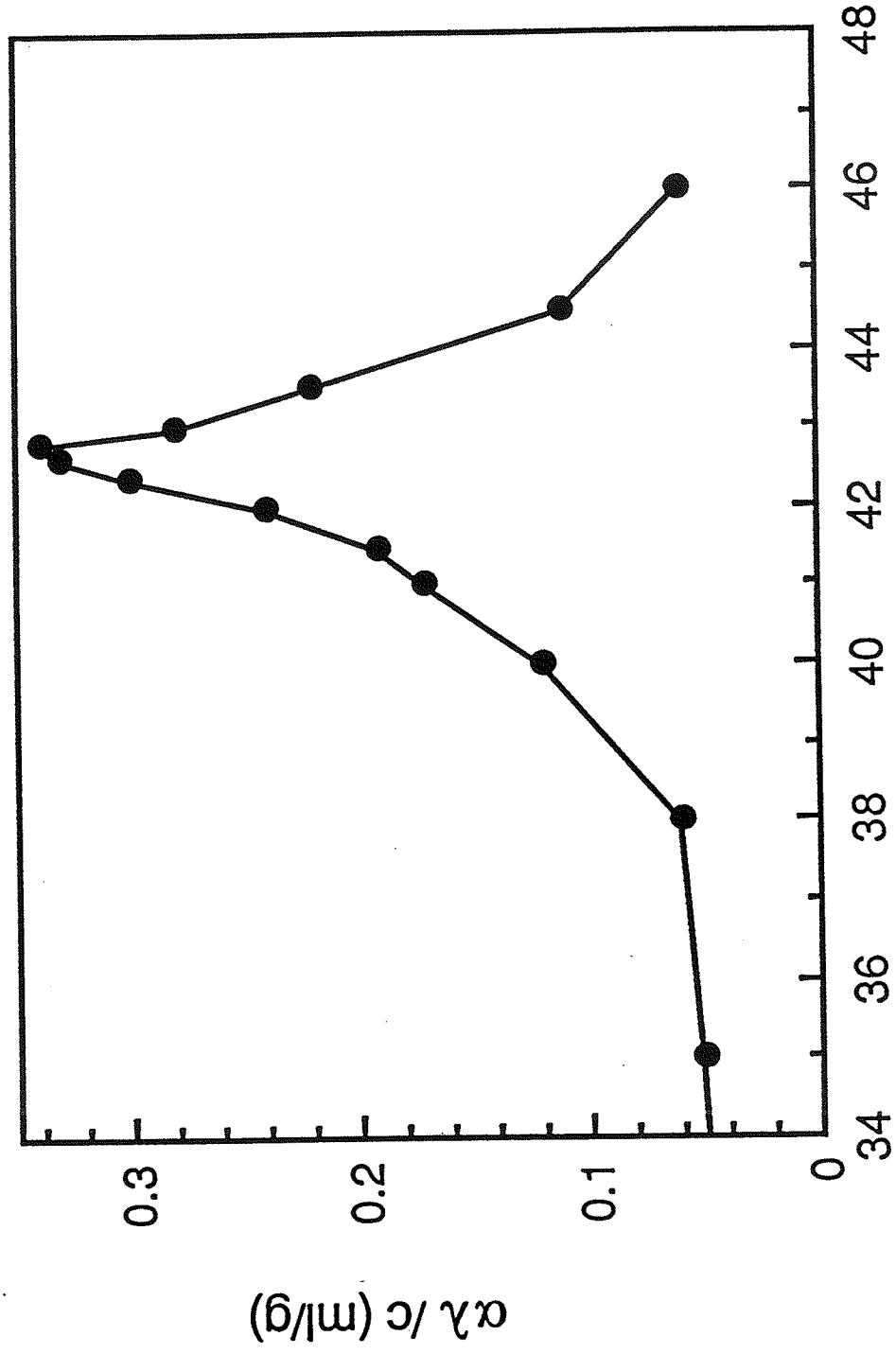

Figure 5.6 $\alpha\lambda/c$ versus temperature of LUVs in 20% D_2O buffer.

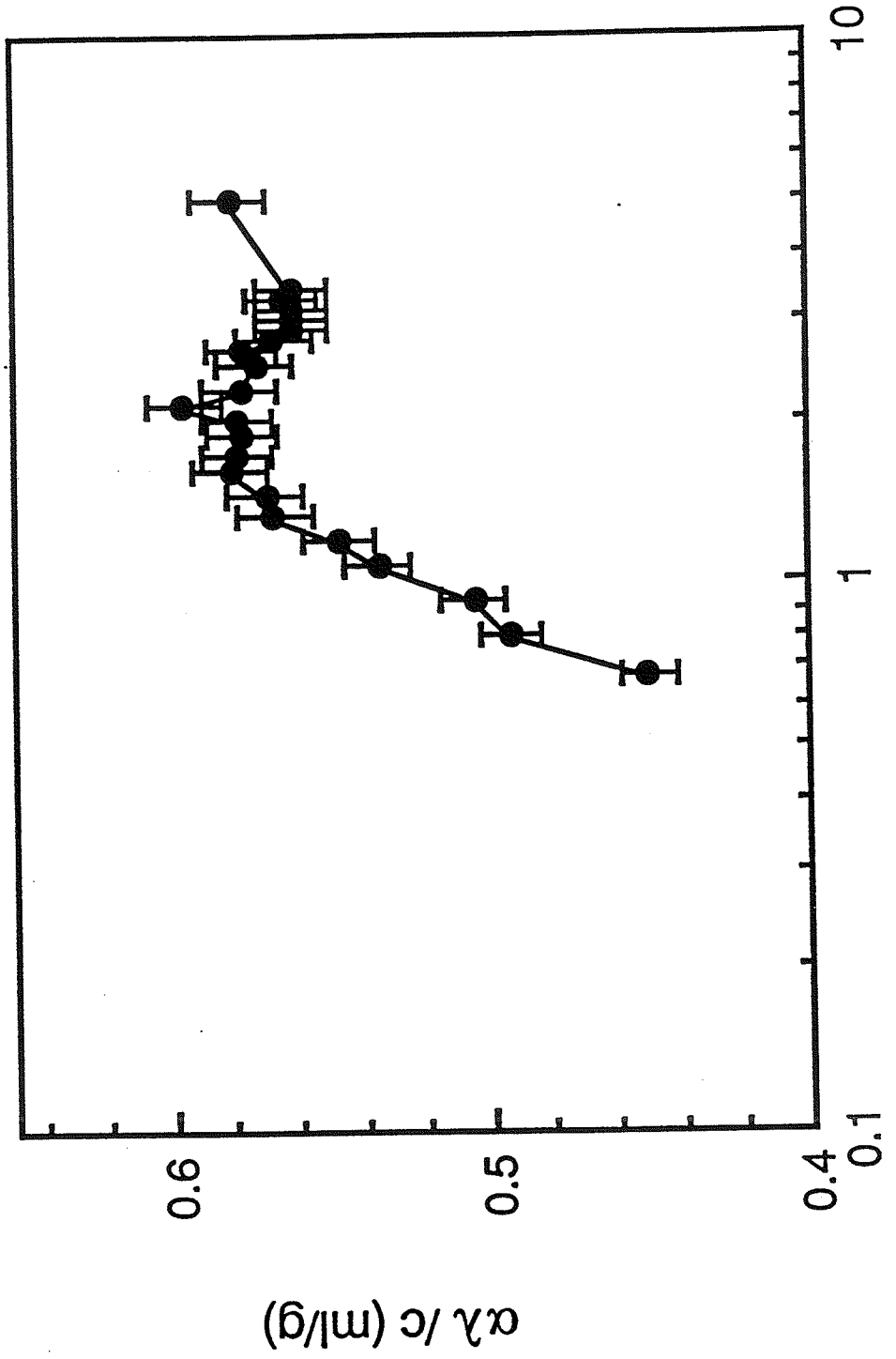

Figure 5.7 $\alpha\lambda/c$ versus frequency of LUVs in 100% D_2O buffer.

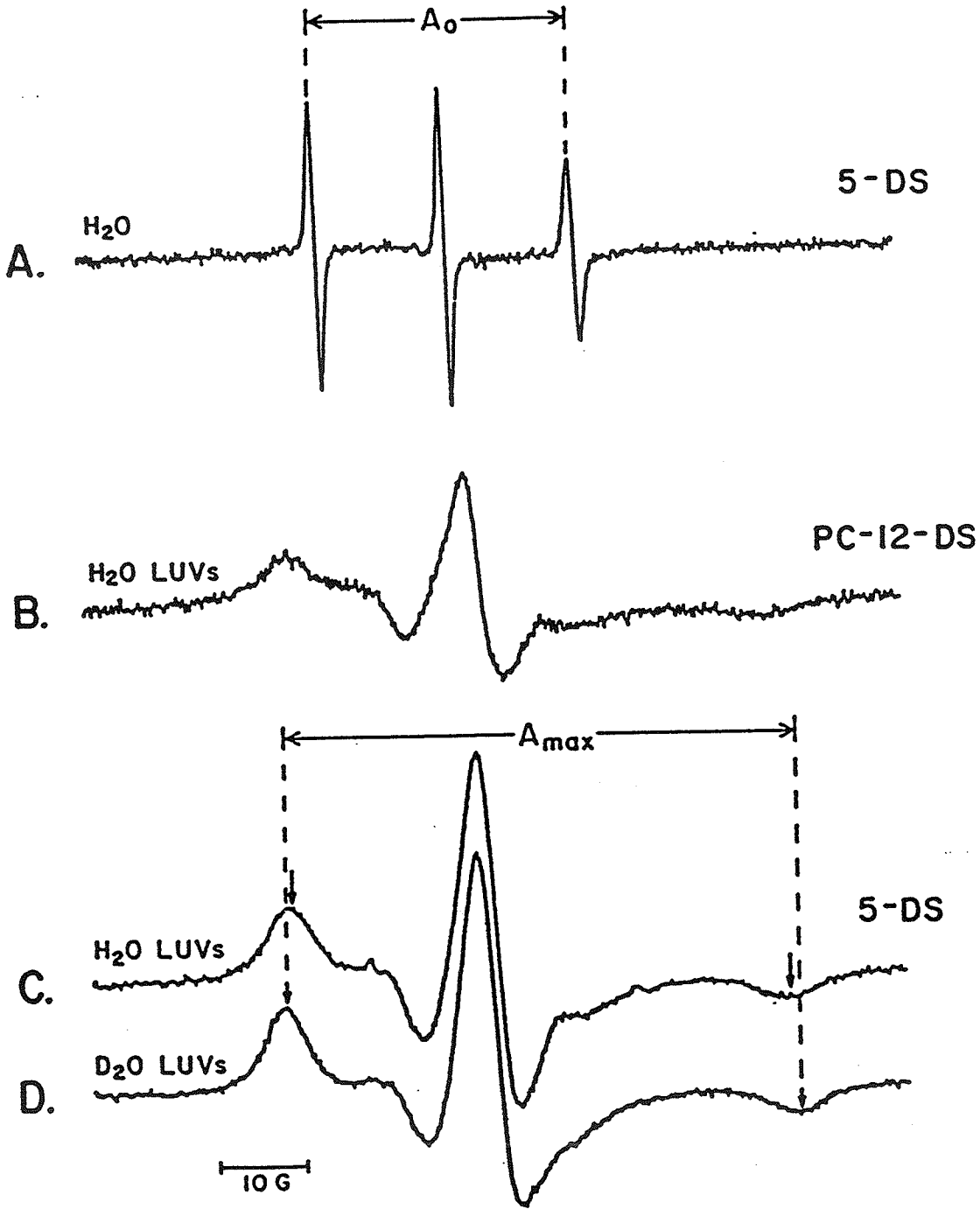

Figure 5.8 ESR spectra showing:
A. A_o of free nitroxides in solution
B. A_{max} of nitroxides in membranes
C. A_{max} of 5-DS in LUVs at 20°C in H_2O hepes buffer
D. A_{max} of 5-DS in LUVs at 20°C in D_2O hepes buffer

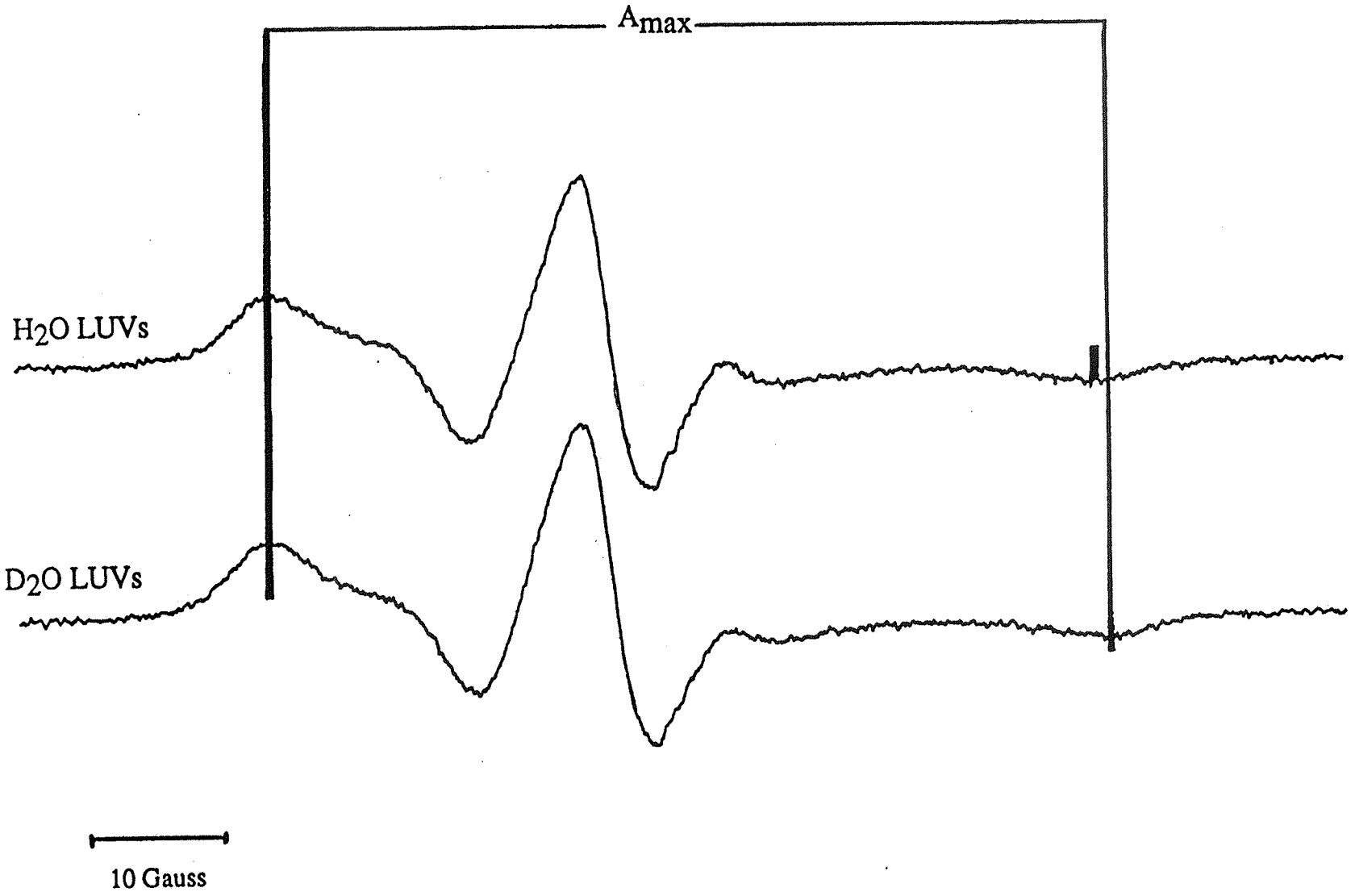

Figure 5.9 ESR spectrum of CAT_{16} in H_2O LUV and D_2O LUV suspensions.

CHAPTER 6

A23187 AND DEUTERATED PHOSPHOLIPID EXPERIMENTS

6.1. Introduction

In order to ascertain the nature of the interaction of ultrasound with biological membranes, agents with specific partitioning properties can be incorporated into LUV suspensions. These agents should affect membrane dynamics at their site of interaction with the membrane, and these perturbations, if of a large enough amplitude may be detected as changes in the ultrasonic absorption coefficient per wavelength, as a function of temperature and/or frequency. This depends upon the specific ultrasonic interaction with the membrane at the site of perturbation and also depends upon the event perturbed occurring on a timescale that can be detected by ultrasound. The absence of a change in $\alpha\lambda$ as a function of temperature and especially frequency is then probably due to a failure of one of the aforementioned criteria, and may be an indication that the interaction of the ultrasound with biological membranes is not at a tested site.

The A23187 is a small molecular weight Ca^{2+} ionophore (523.6 daltons) that is well known to partition into the hydrophobic region of the phospholipid bilayer [Houslay and Stanley, 1982]. It is soluble in organic solvents such as chloroform, DMSO, and ethanol, and is insoluble in water. The A23187 is a carrier ionophore specific for divalent cations with its affinity for $Mn^{2+} > Ca^{2+} > Mg^{2+}$. It forms a complex of two molecules in order to transport divalent cations across a membrane.

As mentioned in Chapter 1, other molecules known to partition into the hydrophobic lipid bilayer have been incorporated into LUVs, viz., cholesterol, and gramicidin. The incorporation of these two substances has shown different effects on $\alpha\lambda/c$ as a function of frequency and temperature. Specifically, the incorporation of cholesterol into LUV membranes increasingly broadened the $\alpha\lambda/c$ versus temperature curve, probably as a result of decreasing the cooperativity of the phase transition. It is not clear that cholesterol's addition changed $\alpha\lambda_{max}$ as a function of frequency until at 50 mole % cholesterol the $\alpha\lambda/c$ versus

temperature and frequency peaks were no longer apparent. This may indicate that cholesterol does not interact in a dynamic manner with the specific molecular event causing ultrasonic absorption in the bilayer.

The incorporation of gramicidin into the phospholipid bilayer of LUV suspensions gave different results. While the phase transition was broadened and ΔH decreased as a function of concentration of gramicidin, as was seen with cholesterol, the frequency of maximum $\alpha\lambda$ for 5 mole % gramicidin incorporation was shifted from 2.1 MHz to 0.75 MHz [Strom Jensen et al., 1984]. This indicates that (1) ultrasound is sensitive to changes in the phase transition and (2) that the incorporation of gramicidin changes the relaxation kinetics of the event that couples with ultrasound. This further suggests that it is a dynamic interaction between ultrasound and the phosopholipid molecules that is changed by the incorporation of molecules that change the rate of an event that occurs in the lipid bilayer. It is possible that A23187, as a transport molecule acting in the lipid bilayer, could also affect the kinetics of the event responsible for the relaxational absorption of ultrasound.

Deuterated phospholipids are also of interest in the determination of the site of ultrasound interaction with LUV membranes. Specifically, it is hypothesized that this site of interaction is with the hydrophobic fatty acyl side chains of the phospholipid molecule. Therefore, a perturbation of the fatty acyl side chains may lead to a perturbation of the relaxation kinetics of the molecular event that interacts with ultrasound, as determined by $\alpha\lambda$ as a function of temperature and frequency. Phospholipids were obtained in which all of the hydrogens of the fatty acyl side chains had been replaced by deuterium (referred to per-deuterated phospholipid). This results in a phospholipid whose molecular weight is increased by approximately 60 Daltons (796.54 compared to 734.05) and whose ΔH and t_m are slightly decreased, compared to ordinary DPPC [Guard-Friar et al., 1985]. It is hypothesized that this perturbation of the phospholipid structure, specifically in the region of the fatty acyl side chains, will perturb $\alpha\lambda$ as a function of frequency at t_m of the LUV suspension.

6.2. Procedure

As described in Section 3.1.2.3., A23187 LUVs were prepared by the reverse phase evaporation method of Szoka and Papahadjopoulos [1976] as modified by Magin and Weinstein [1982]. The only exception in the preparation was that in the organic phase (lipid + chloroform + ether) at the beginning of the reverse phase evaporation process, dried A23187 was included, in such quantities as to result in 1, 2, or 5 mole percent LUVs. The incorporation of the A23187 did not obviously change the preparation of the liposomes and a stable suspension of liposomes, as determined by consistency and stability over three days in 9°C dark dialysis was observed. In each case, after dialysis, the LUV suspension at 25 mg/ml was directly used for DSC experiments and a portion of the original sample was diluted to 2 mg/ml in hepes buffer for ultrasound experiments. The DSC experiments gave a determination of specific heat, c_p, versus temperature (295 - 325 K) and were performed to (1) compare the A23187 LUV DSC trace to standard LUV DSC traces and, (2) to determine any changes, e.g. t_m, ΔH, etc., caused by the addition of A23187 to the LUVs. Ultrasound experiments consisted of an $\alpha\lambda/c$ determination over the temperature range 35° - 46°C, a complete frequency scan (0.6 - 5.1 MHz) being performed at each temperature.

Deuterated LUV suspensions were prepared in the same manner as standard LUV suspensions, except that a certain portion of the phospholids was replaced by deuterated phospholipid. In these preliminary experiments specific portions of the DPPC fraction of the phospholipids were replaced by 50% and 100% deuterated DPPC. The DPPG was retained as its negative charge causes LUVs to repel one another, therefore ensuring stability of the LUV suspension. DSC experiments gave a determination of c_p versus temperature in these suspensions, to determine the viability of the LUV suspensions and to determine approximately the changes in t_m and ΔH of these suspensions, compared to normal LUV suspensions. Ultrasound determinations of $\alpha\lambda/c$ as a function of temperature (30° - 45°C) and frequency (0.6 - 5.2 MHz) were performed for each of these suspensions.

6.3. A23187 Results

6.3.1. 1 mole % A23187 LUVs

6.3.1.1. DSC measurements

The DSC showed that 1 mole percent A23187 LUVs gave a basically standard LUV curve with a slightly increased t_m (see Figure 6.1). Otherwise no differences between these and standard LUVs were noted.

6.3.1.2. Ultrasound experiments

One mole percent A23187 LUVs gave an $\alpha\lambda/c$ versus temperature peak that was only slightly different from that of standard LUV suspensions. The only differences, as seen in Figure 6.2., were that the amplitude of the peak was higher, ΔH as determined by ultrasound was increased, t_m was shifted by 0.2°C to 42.2°C and $\Delta t_{1/2}$ was slightly decreased as compared to standard LUVs. Only small differences were expected as the phospholipid:A23187 ratio was 100:1.

Most striking, however, was $\alpha\lambda/c$ as a function of frequency at t_m (see Figure 6.3). One mole percent A23187 LUVs had an $\alpha\lambda/c$ versus frequency peak that was shifted to lower frequencies, with a maximum at 1.55 MHz (Figure 6.3). This indicated that the presence and/or activity of A23187 in LUV membranes perturbed the event to which ultrasound couples. This effect also definitely pointed to a membrane interaction, as the LUV structure was maintained with the addition of A23187, as determined by DSC, and as the phase transition properties of the suspension were otherwise only slightly perturbed by the addition of A23187.

6.3.2. 2 mole % A23187 LUVs

6.3.2.1. DSC measurements

Two mole percent A23187 LUVs in suspension (25 mg/ml phospholipid) showed a thermotropic phase transition similar to that of standard LUVs in suspension; the t_m of these LUVs was slightly increased from a normal t_m of 42°C to 42.2°C, and the amplitude of c_p

was increased slightly, as seen in Figure 6.1. These data suggested that 2 mole % A23187 LUVs were thermodynamically not perturbed greatly in structure from standard LUV preparations.

6.3.2.2. Ultrasound experiments

Two mole percent A23187 LUVs gave an $\alpha\lambda/c$ versus temperature curve that again was similar to that of standard LUVs, but which showed an increased amplitude and increased ΔH, slight broadening ($\Delta t_{1/2}$ = 2.0°C), as expected with a decreased cooperativity, and a slight increase in t_m to 42.3°C (see Figure 6.4). This suggested that the A23187 decreased the cooperativity of the lipid bilayer phase transition, as evidenced by broadening of the $\alpha\lambda/c$ versus temperature curve, and that A23187 enhanced the ultrasonic absorption of the phospholipid bilayer phase transition. Note that the presence of A23187 alone was probably not causing simply an offset of $\alpha\lambda/c$, as the baseline (measured ± 5°C from t_m) had the same value (0.06 ± 0.01 ml/g) as was seen in standard LUV suspensions.

As was observed with 1 mole % A23187 LUVs, $\alpha\lambda_{max}$ of 2 mole % A23187 LUVs at t_m was shifted to 1.55 MHz (Figure 6.5). This further suggested that individual A23187 molecules interacted in a dynamic manner with phospholipid molecules to change the kinetics of the molecular event to which ultrasound couples. As two $\alpha\lambda$ peaks as a function of frequency, representing two populations of lipid, were not seen in either case, it is probable that the interaction of A23187 molecules with individual populations of phospholipid molecules occurred on a fast enough time scale to allow any signal from two populations of lipid to be observed as an averaged signal for ultrasound timescales.

6.3.3. 5 mole % A23187 LUVs

6.3.3.1. DSC measurements

Five mole percent A23187 LUVs in suspension resulted again, in a c_p versus temperature curve similar to that of standard LUVs in suspension. The t_m and ΔH were not changed appreciably from 1 or 2 mole % A23187 LUVs (Figure 6.1).

6.3.3.2. Ultrasound experiments

Ultrasound experiments on 5 mole % A23187 LUVs in suspension (1 mg/ml) showed a dramatically different determination of $\alpha\lambda/c$ as a function of temperature and especially of frequency. As seen in Figure 6.6, $\alpha\lambda/c$ was greatly increased, especially at low frequencies, and in fact at frequencies from 0.58 - 1.27 MHz, was above the normal baseline throughout the temperature range studied. At higher frequencies (2 - 5 MHz), $\alpha\lambda/c$ versus temperature was qualitatively like that of an LUV curve, but with a significantly higher amplitude of $\alpha\lambda/c$ compared to standard LUV suspensions. Note also that t_m was slightly increased, to 42.3°C, and that the peak was broadened ($\Delta t_{1/2}$ = 2.2°C), which is reasonable as the incorporation of one A23187 molecules for every 20 phospholipid molecules should affect the cooperative unit of the transition. A peak in $\alpha\lambda$ as a function of frequency at t_m could not be found within the operating frequency range as $\alpha\lambda$ increased with decreasing frequency, suggesting that $\alpha\lambda_{max}$ was probably at a frequency lower than that of the low frequency limit of this interferometer (see Figure 6.7).

6.4. Deuterated LUV Results

6.4.1. 50% deuterated DPPC LUV Suspensions

6.4.1.1. DSC measurements

DSC results showed a broadened transition with t_m at 40°C compared to standard LUVs whose t_m is 42°C (see Figure 6.8). However, ΔH was not decreased in this LUV suspension. In 100% per-deuterated DPPC liposomes, a decrease in t_m was observed in Guard Friar et al., [1984], but the ΔH of the transition was decreased in these liposomes.

6.4.1.2. Ultrasound experiments

Ultrasound experiments on LUV suspensions with 50% of the DPPC per-deuterated showed an $\alpha\lambda/c$ versus temperature curve qualitatively like that of a standard LUV suspension, but with two major differences (see Figure 6.9). The first difference was that

the transition temperature of the suspension was 40.8°C, compared with 42.0°C for standard LUV suspensions. Second, the $\alpha\lambda$ versus frequency curve at t_m no longer showed a sharp peak at 2.1 MHz. As seen in Figure 6.10, these LUVs showed a high $\alpha\lambda/c$ at low frequencies, indicating a decreased relaxation frequency. A slight increase in $\alpha\lambda$ at 2.1 MHz was still observed, but was low in amplitude and was broadened out over a wide range of frequencies. This was perhaps due to the DPPC (50%) and DPPG (100%) which had not been deuterated. These results suggest that the deuterated DPPC LUVs, with their heavier side chains, had a perturbed $\alpha\lambda_{max}$, suggesting that the site of the interaction of ultrasound and LUV suspensions is in the hydrophobic phospholipid side chains.

6.4.2. 100% deuterated DPPC LUV Suspensions

6.4.2.1. DSC measurments

The DSC results with these LUV suspensions show a broadened transition compared to standard LUVs as well as a decreased t_m of 39°C (Figure 6.8). This was observed also by Guard-Friar et al., [1985] in 100% per-deuterated DPPC LUVs, where t_m was decreased to 36°C and ΔH was decreased.

6.4.2.2. Ultrasound experiments

Ultrasound experiments on (DPPC:DPPG) LUVs with 100% per-deuterated DPPC showed a low enthalpy and broadened transition curve of $\alpha\lambda/c$ versus temperature, with a main peak at 39.0°C and a small peak at 37.5°C (see Figure 6.11). At t_m, $\alpha\lambda$ as a function of frequency no longer showed a peak at 2.1 MHz (see Figure 6.12). Rather, the 2.1 MHz peak was broadened over the frequency spectrum with indications of peaks at 0.75, 2.25, and 2.95 MHz. These results indicate that deuteration of DPPC fatty acyl side chains changes the rate of the molecular event to which ultrasound couples and that this coupling is within or is directly related to the phospholipid side chains of the LUV bilayer.

6.5. Discussion

The incorporation of A23187 into the phospholipid bilayers of LUVs results in a change in $\alpha\lambda$ as a function of frequency, at the phospholipid phase transition temperature. The incorporation of 1 and 2 mole % A23187, as shown in DSC measurements perturbs only slightly the thermotropic phase transition exhibited by LUVs in suspension. The phase transition temperature is perturbed only slightly without any significant change in ΔH of the transition, as determined by DSC. In contrast, ultrasound experiments show an increasing area under the $\alpha\lambda/c$ versus temperature curve with increasing A23187 concentration, and show that $\alpha\lambda_{max}$, as a function of frequency changes to 1.55 MHz. This peak is presumably shifted from the 2.1 MHz relaxation frequency seen in standard LUV suspensions, as that peak is no longer observed. These data suggest that A23187, in the hydrophobic region of the phospholipid bilayer, changes the relaxation rate of the molecular event responsible for ultrasound absorption in LUV suspensions. These data further suggest that the relaxational absorption of ultrasound at the phase transition temperature in LUV suspensions is due to ultrasound coupling to molecules of the hydrophobic bilayer, whose chemical or conformational state is related to the lipid bilayer phase transition.

In 5 mole % A23187 LUVs in suspension, $\alpha\lambda/c$ as a function of temperature and especially frequency is changed significantly (Figure 6.7). This also suggests a perturbation of the ultrasonic interaction with the LUV suspension. However, at such high A23187 concentrations, the A23187 itself may be absorbing ultrasound significantly. Analysis of $\alpha\lambda/c$ as a function of temperature, at different frequencies has shown that at low frequencies (0.58 - 1.27 MHz) $\alpha\lambda/c$ is high even at 38.0°C and rises slowly until, near t_m, it increases dramatically and remains the same over approximately 1.0°C, above which temperature it decreases again to a 0.37 ml/g baseline, and remains there to 46.0°C (see Figure 6.6). At frequencies above 1.55 MHz, $\alpha\lambda/c$ versus temperature is qualitatively like that of standard LUV suspensions, except for the slight increase in $\alpha\lambda$, t_m and the decreased cooperativity of the transition. These data suggest that the A23187 itself (at high concentrations), or an

A23187-phospholipid complex, absorbs ultrasound in a different manner (at low frequencies) than does the phospholipid membrane.

The results of LUV experiments with per-deuterated DPPC show that $\alpha\lambda$ as a function of frequency at t_m can be perturbed with the increased mass in the phospholipid side chains. This suggests that perturbation at this level changes the rate of the molecular event in LUV suspensions to which ultrasound couples.

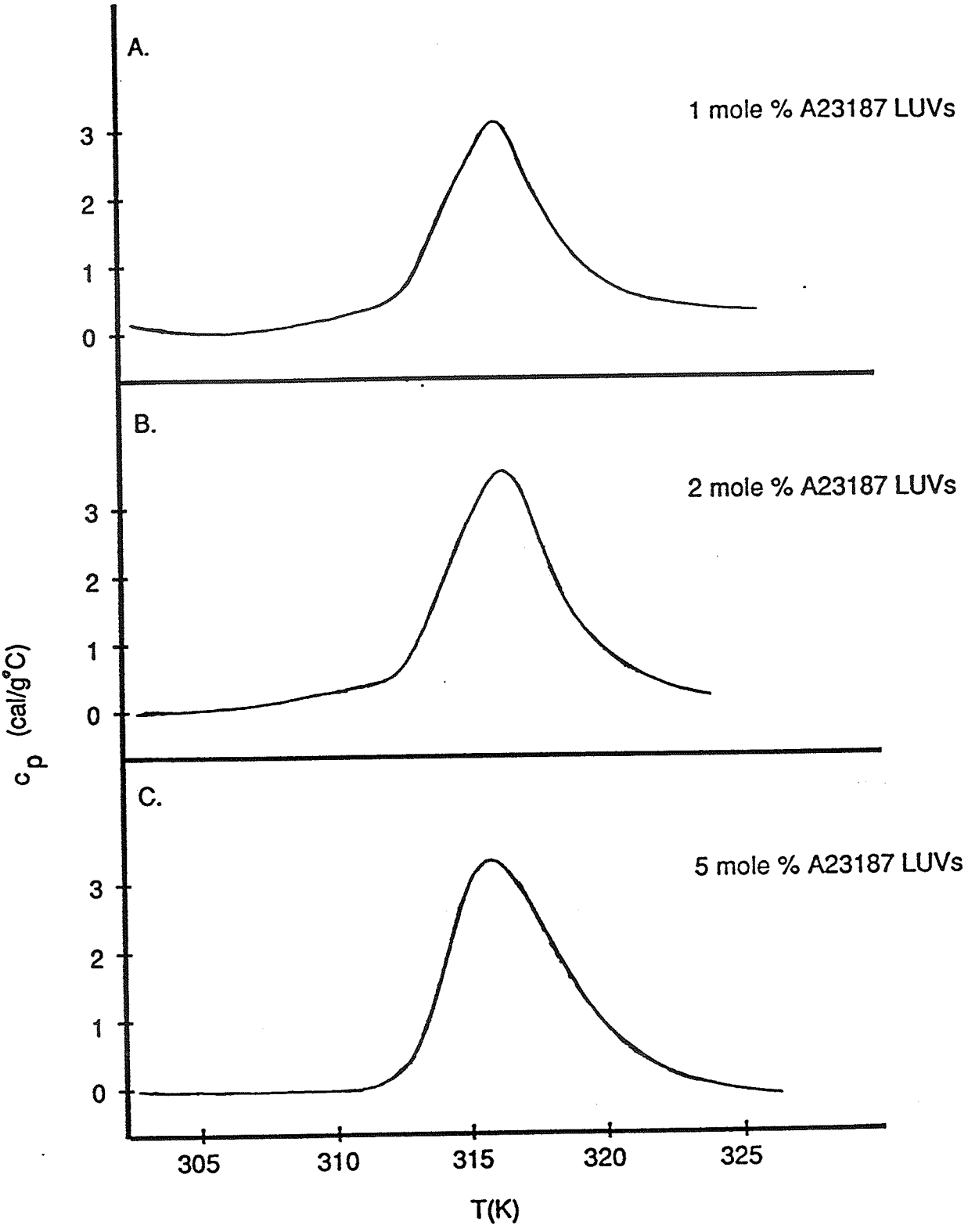

Figure 6.1 c_p versus T(K) in LUV suspensions with 1, 2 and 5 mole % A23187.

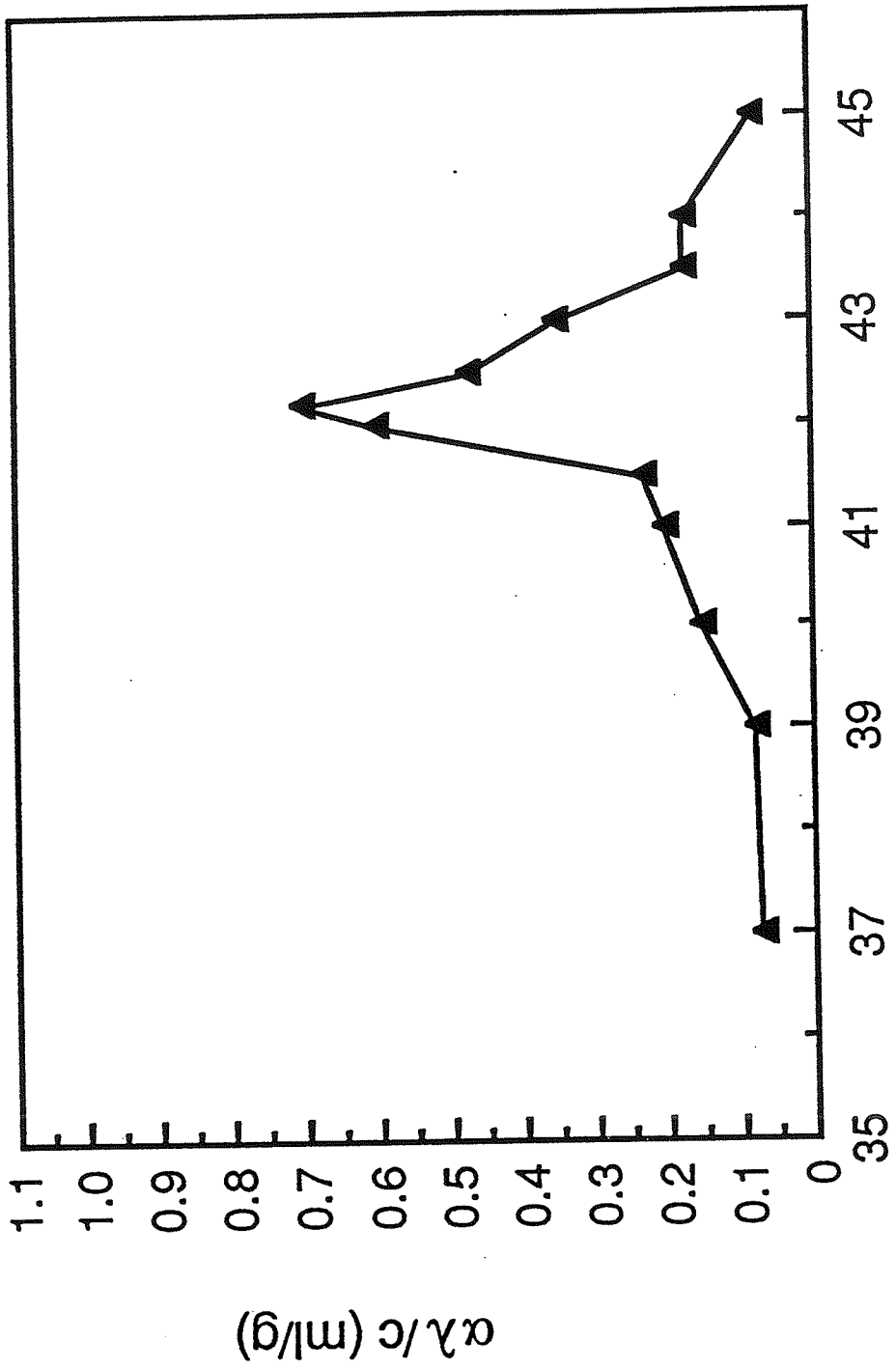

Figure 6.2 αλ/c versus temperature (°C) in 1 mole % A23187 LUV suspensions.

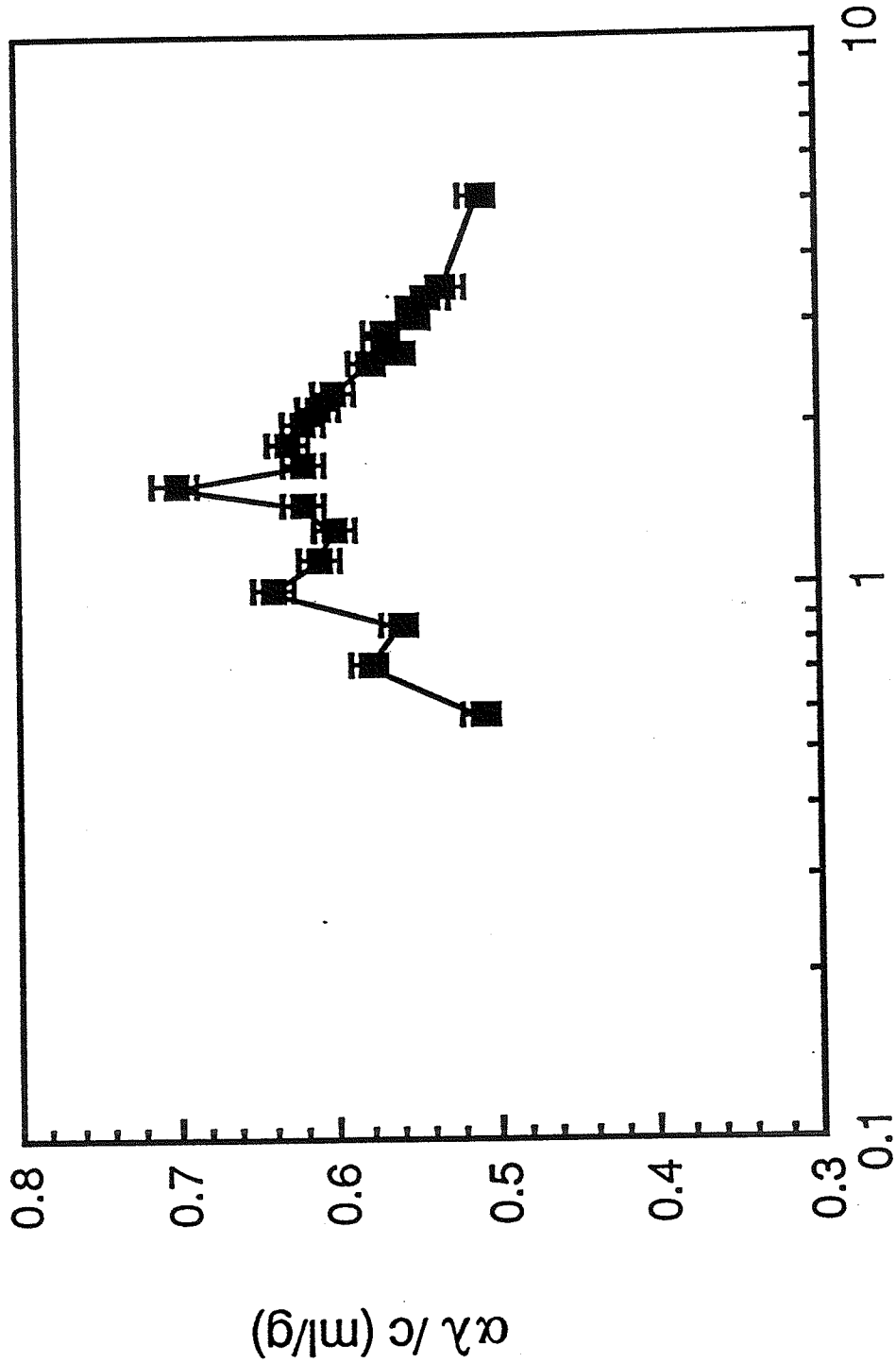

Figure 6.3 $\alpha\lambda/c$ versus frequency in 1 mole % A23187 LUV suspensions at t_m.

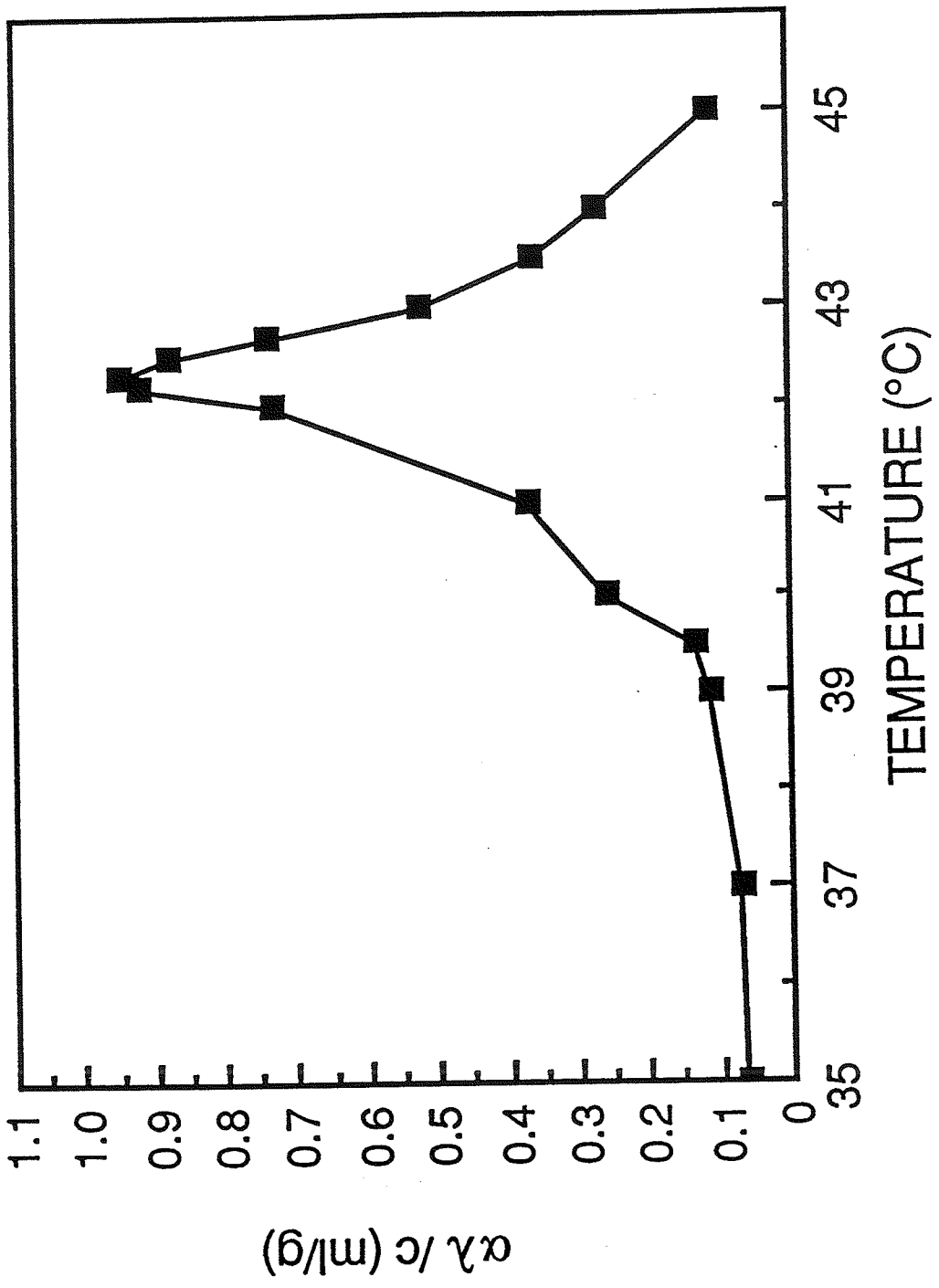

Figure 6.4 αλ/c versus temperature in 2 mole % A23187 LUV suspensions.

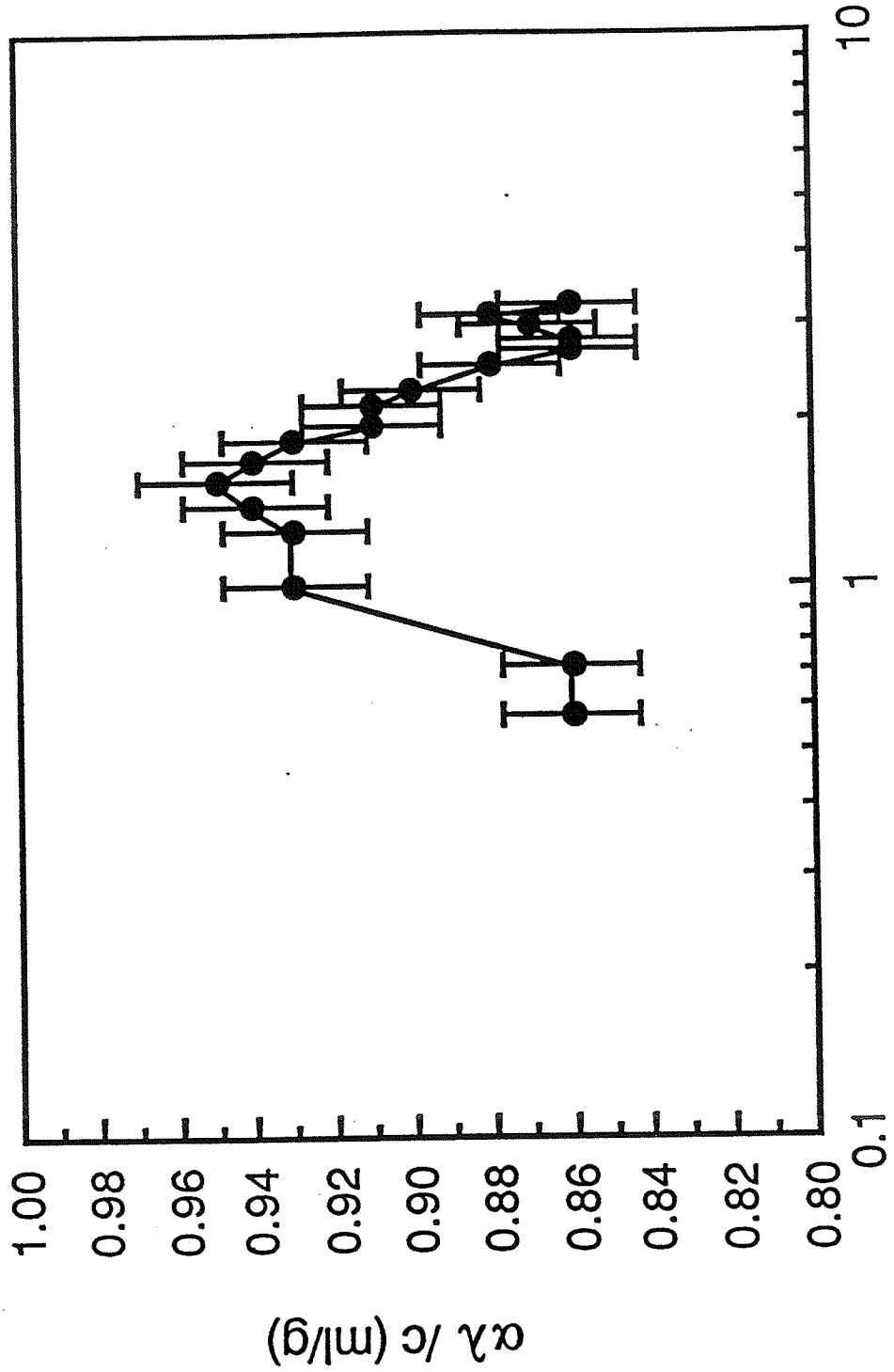

Figure 6.5 $\alpha\lambda/c$ versus frequency in 2 mole % A23187 LUV suspensions at t_m.

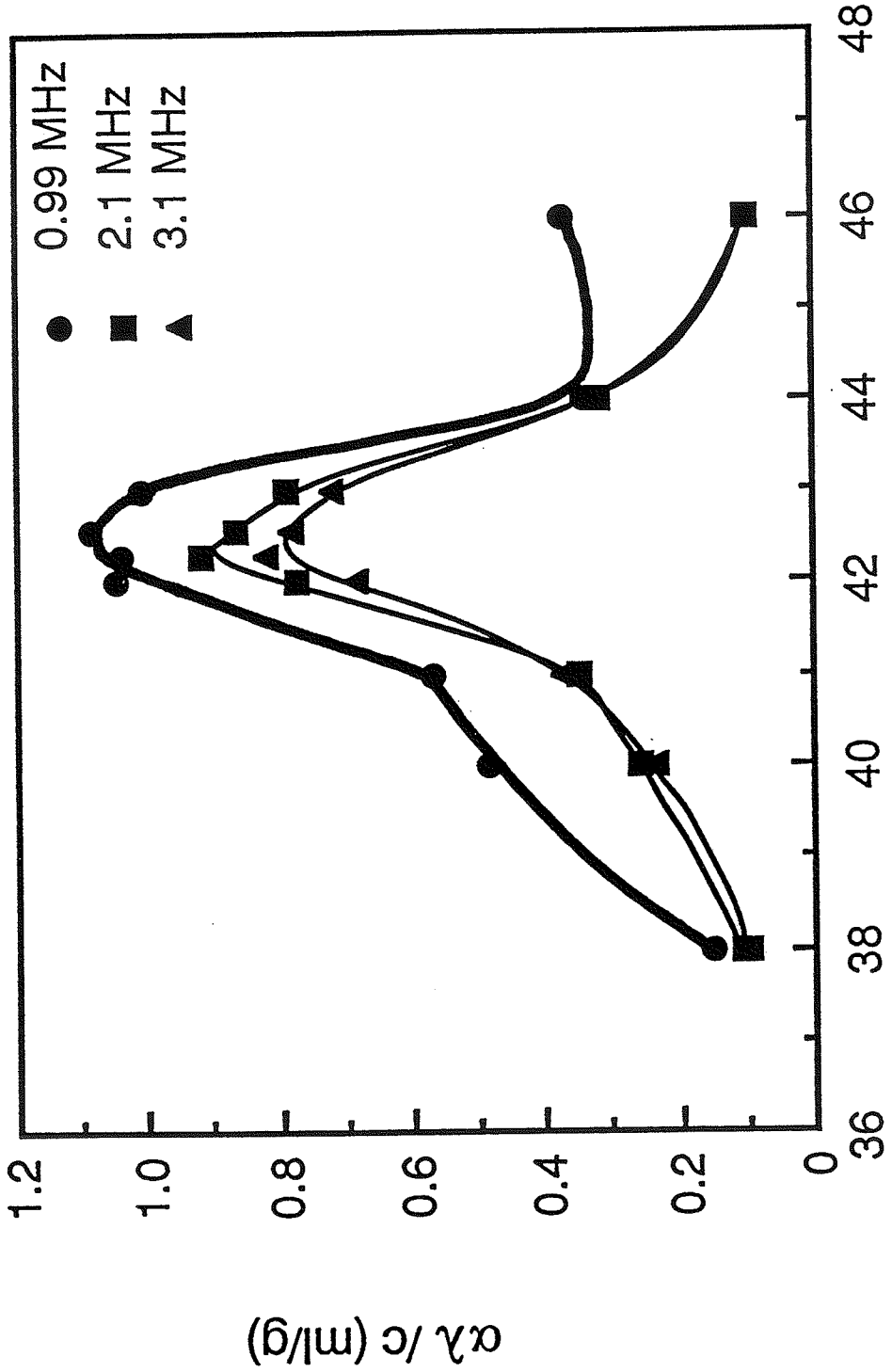

Figure 6.6 $\alpha\lambda/c$ versus temperature (°C) in 5 mole % A23187 LUV suspensions.

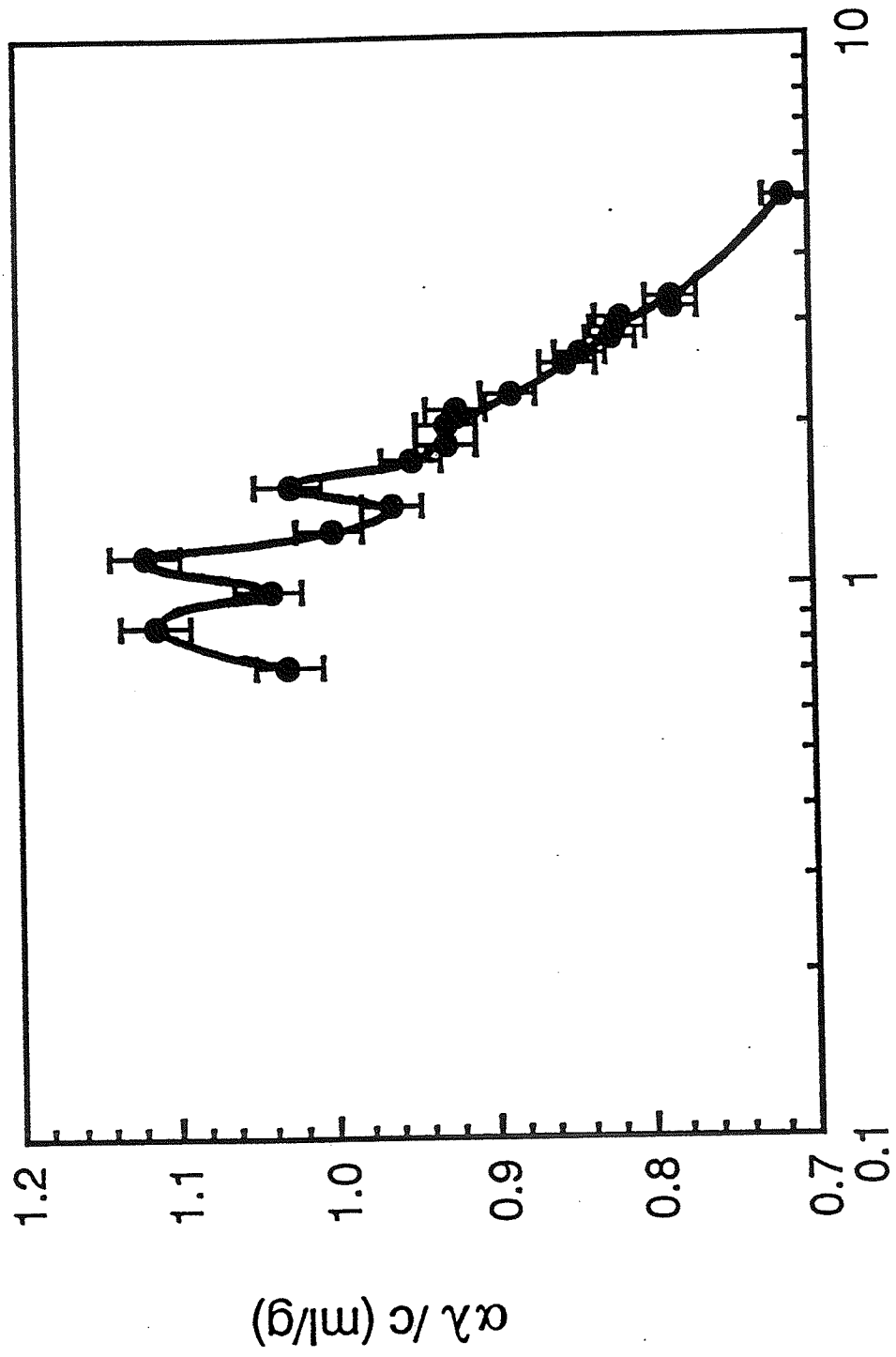

Figure 6.7 $\alpha\lambda/c$ versus frequency in 5 mole % A23187 LUV suspensions at t_m.

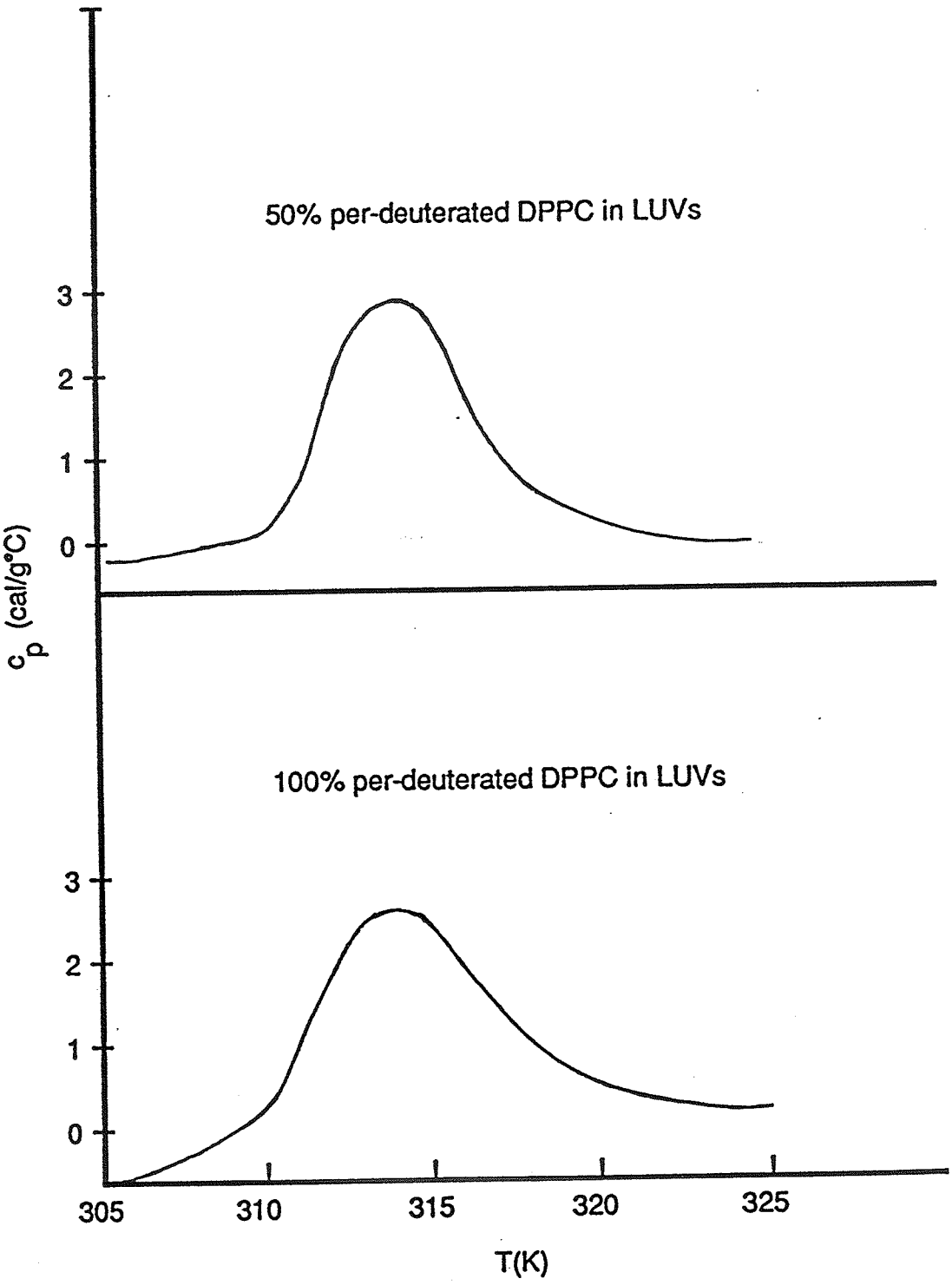

Figure 6.8 c_p versus T(K) in LUV suspensions with 50% and 100% per-deuterated DPPC.

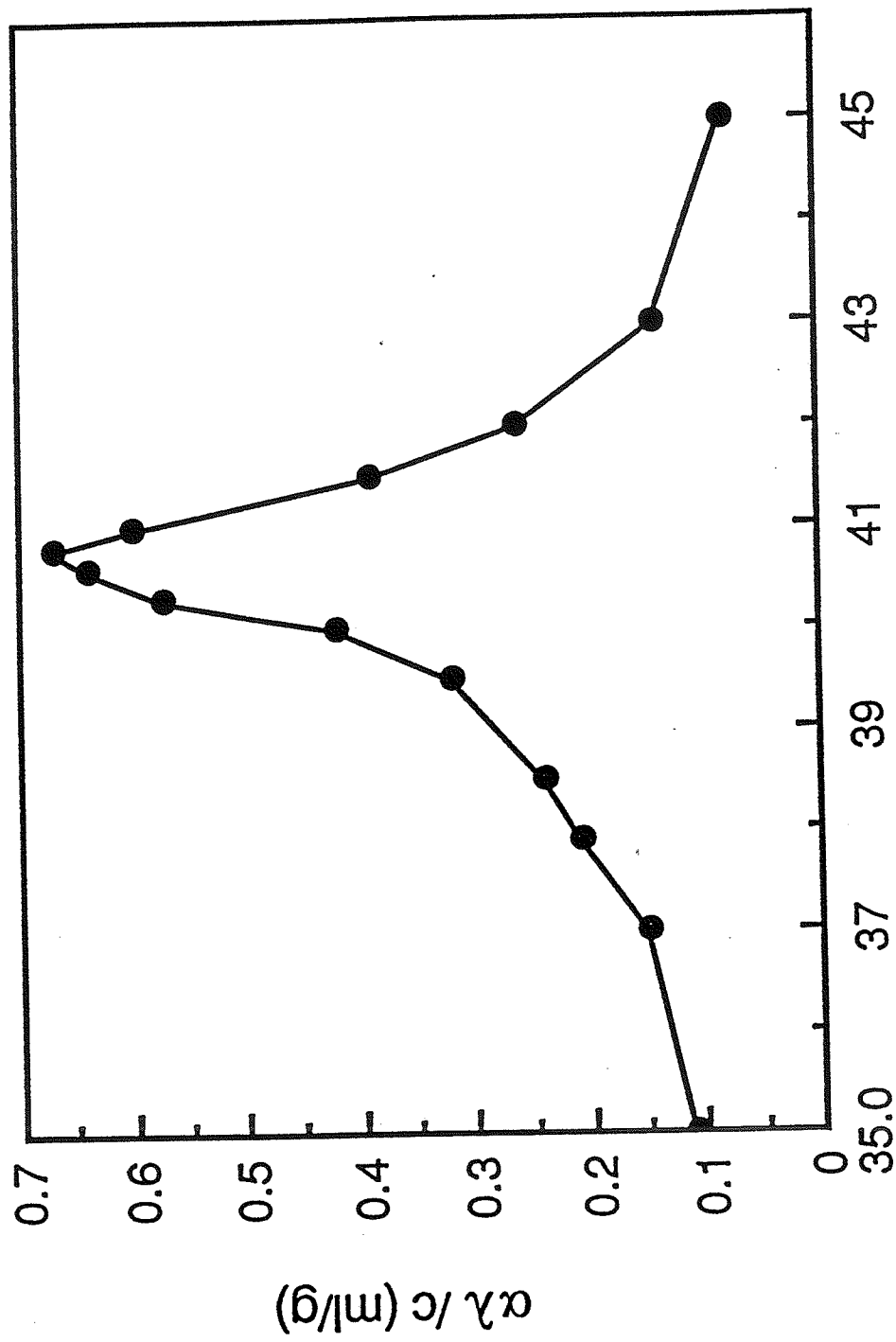

Figure 6.9 $\alpha\lambda/c$ versus temperature (°C) in LUV suspensions with 50% per-deuterated DPPC.

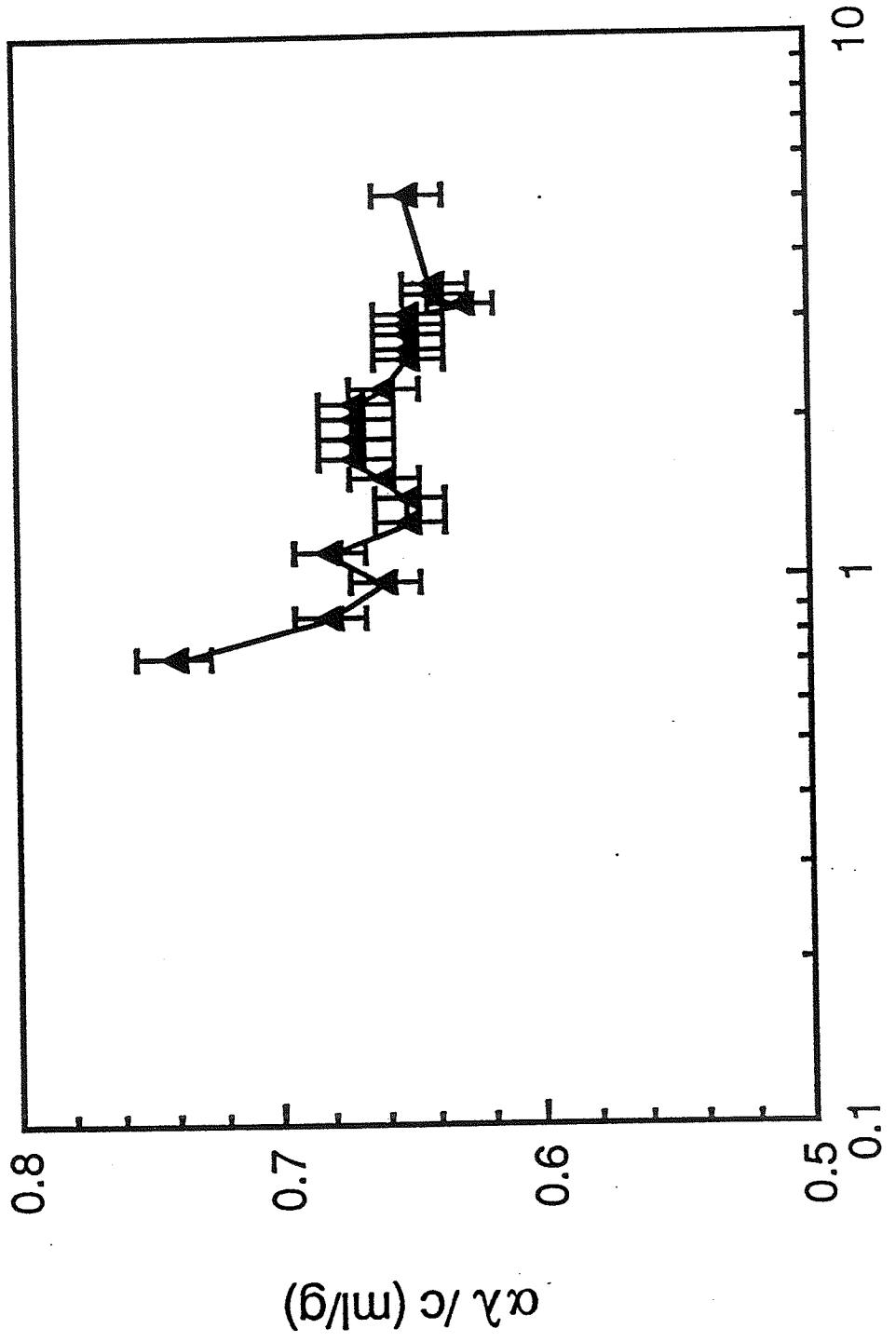

Figure 6.10 $\alpha\lambda/c$ versus frequency in LUV suspensions with 50% per-deuterated DPPC, at t_m.

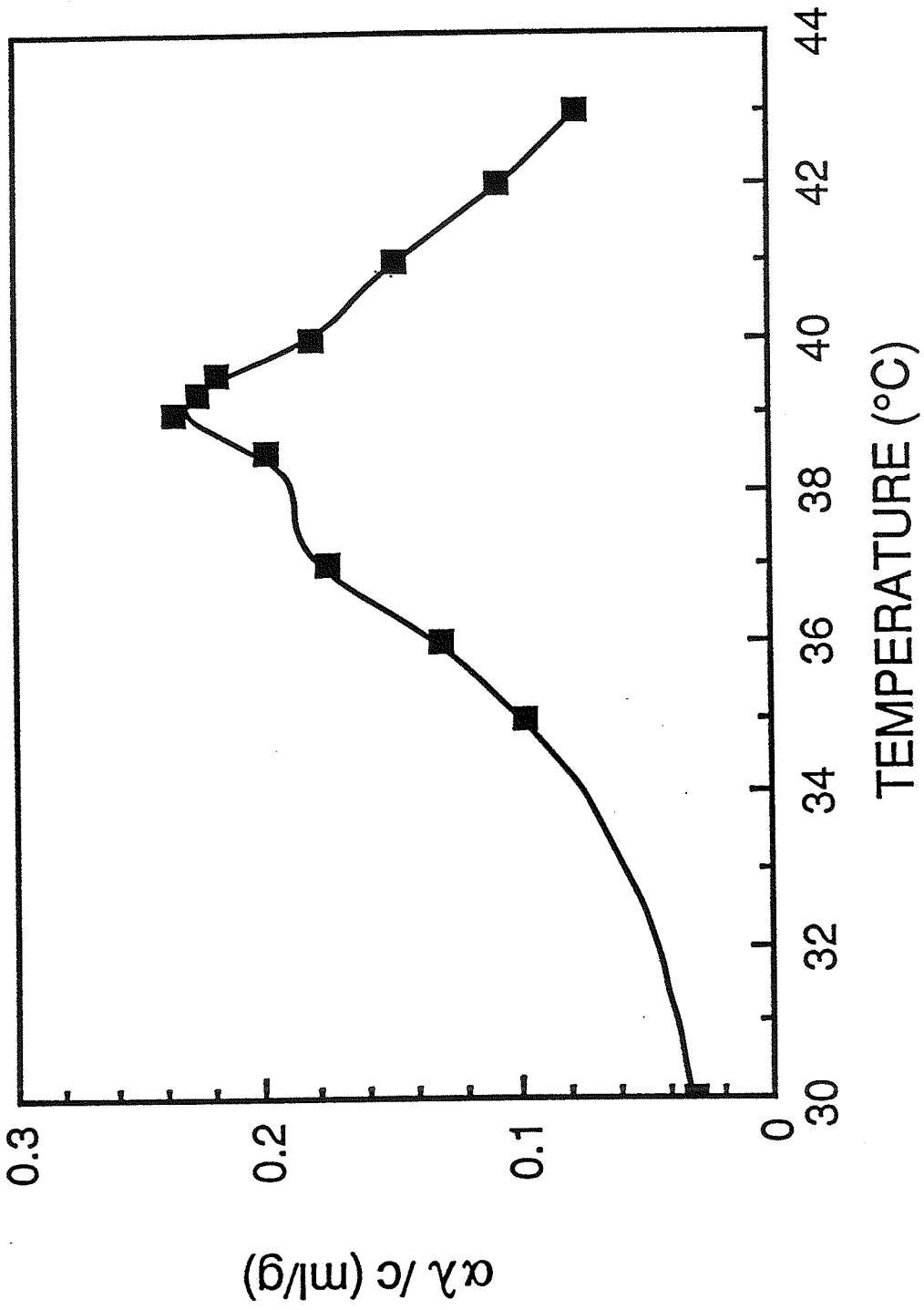

Figure 6.11 αλ/c versus temperature (°C) in LUV suspensions with 100% per-deuterated DPPC.

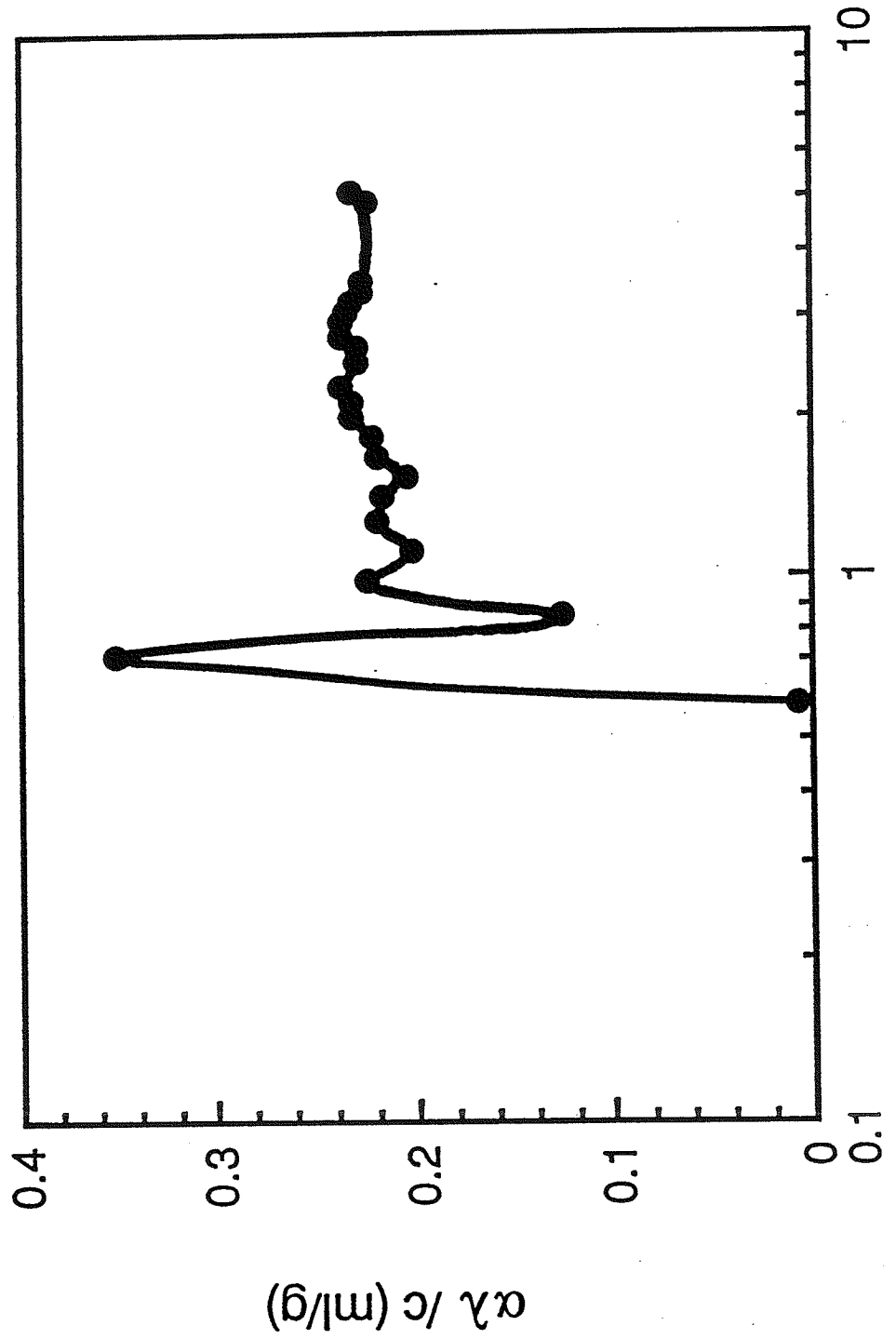

Figure 6.12 $\alpha\lambda/c$ versus frequency (°C) in LUV suspensions with 100% per-deuterated DPPC, at t_m.

CHAPTER 7

CONCLUSIONS AND REMARKS

The data presented in Chapters 4, 5, and 6 allow conclusions to be drawn regarding the interaction of ultrasound with LUVs in aqueous suspension. First, from perturbing different aspects of the LUV suspension, it is found that $\alpha\lambda/c$ as a function of temperature is sensitive to any change in the phospholipid bilayer phase transition. That is, any agent that changes the phase transition temperature of the LUV suspension, or the cooperativity of the phospholipid phase transition, contributes to a change in $\alpha\lambda_{max}$ as a function of temperature, both in the temperature of the peak and in the broadness of the $\alpha\lambda/c$ versus temperature curve, as indicated by $\Delta t_{1/2}$. This is the case with divalent cations (Chapter 4) and with deuterium oxide (Chapter 5). In both of these studies, the perturbing agent changes t_m and $\Delta t_{1/2}$ of the lipid bilayer phase transition to some extent. However $\alpha\lambda_{max}$ at t_m of these LUV suspensions is not changed from its value of 2.1 MHz, for standard LUV suspensions. These results suggest that while the character of the phase transition could be changed, the relaxation time of the event to which ultrasound couples is not changed by these perturbing agents, which act at the polar headgroups and at the membrane-aqueous interface, respectively. It is therefore reasonable to conclude that the site of the observed ultrasonic interaction is not at the level of the polar headgroups or membrane-aqueous interface.

The hydrophobic ionophore A23187, however, should affect $\alpha\lambda/c$ as a function of frequency given two requirements: (1) that ultrasound interaction with the LUVs is at the level of the hydrophobic bilayer and, (2) if the incorporated A23187 can perturb that molecular event to affect its relaxation time. As ultrasound is sensitive to changes in the cooperative unit of the lipid bilayer phase transition, and if the hypothesis that ultrasound interacts with the hydrophobic region of the lipid bilayer is valid and is dependent upon the melting of single phospholipid molecules or the cooperative melting event between a small number of phospholipid molecules, then A23187 insertion between phospholipid fatty acyl chains may be able to perturb the rate of such a molecular event. As seen in Chapter 6, the

inclusion of A23187 in the phospholipid membrane of LUVs did perturb $\alpha\lambda/c$ as a function of frequency at t_m, even without a significant perturbation to the lipid bilayer phase transition, as determined by DSC measurements. These data suggest that the ultrasound must be sensitive to small perturbations of the hydrophobic region of the phospholipid bilayer.

One and 2 mole % A23187 in LUVs increase the amplitude of $\alpha\lambda/c$ slightly, but the increase in $\alpha\lambda/c$ is seen only near t_m, suggesting that it is still the lipid bilayer phase transition and events tied to it that cause the absorption of ultrasound energy. If an $\alpha\lambda/c$ offset was observed at all temperatures, then the change in $\alpha\lambda/c$ as a function of frequency might simply have been a combination of the ultrasound absorption of phospholipid plus A23187.

Five mole percent A23187 in LUV suspensions presents a different picture. Although the lipid bilayer phase transition is still easily detectable by $\alpha\lambda/c$ versus temperature, a high $\alpha\lambda/c$, at low frequencies, over the entire temperature range indicates that the A23187 itself absorbs at these frequencies of ultrasound, to alter the spectrum obtained. The spectrum is thus a superposition of at least two spectra with the possible inclusion of more spectral components due to specific ionophore-phospholipid or ionophore-ionophore complexes.

Finally, a more subtle perturbation of the LUV suspension is needed in order to identify better the site of ultrasound interaction with LUVs in suspension. In this work, phospholipid with deuterated side chains are employed (Chapter 6). That is, the excess mass of deuterated fatty acyl side chains could definitely affect the rate of any conformational change (cooperative or not) in them, and this perturbation is a subtle one as no probe or protein is added. Preliminary work shows that $\alpha\lambda/c$ as a function of frequency is changed in such an LUV suspension, and is highly suggestive that the fatty acyl side chains are involved in the relaxational absorption of ultrasound by LUVs at t_m.

Possible candidates for the event to which ultrasound is coupling, given these studies, include: (1) ultrasound coupling to the rate of the molecular event of melting itself, (2) ultrasound coupling to a melting of a specific number of molecules as a cooperative group,

(3) ultrasound coupling to a sequence of trans to gauche conformational changes down the length of a given fatty acyl side chain, and (4) ultrasound coupling to movement or repacking of the phospholipid fatty acyl side chains related to, but not defining, the melting event.

Experiments to specify further the site of ultrasound interaction with the LUV membrane include: (1) ultrasound determinations of $\alpha\lambda/c$ versus temperature and frequency in LUVs, where deuteration of specific sites on the fatty acyl side chains of phospholipids has taken place, in order to specify a more exact site of ultrasound interaction with the bilayer, (2) the use of longer or shorter fatty acyl side chains in LUVs, and (3) the inclusion in this system of proteins, lipid mixtures, etc., which may be studied in order to investigate further the interaction of ultrasound with more biologically relevant membranes, and to study the ultrasound absorption of proteins within a membrane.

REFERENCES

Bartlett, G.R. (1959). "Phospholipid determination for column chromatography", J. Biol. Chem., 234, 466 - 468.

Chan, H. (1986). unpublished data.

Chaussy, C., Schmiedt, E., Jocham, D., Schueller, J., Brandl, H., and Liedl, D. (1984). "Extracorporeal shockwave lithotripsy for treatment of urolithiasis", Urology, 23, Suppl. 5, 59 - 66.

CRC Handbook of Chemistry and Physics (1987). 68th edition, p. F40, CRC Press, Inc., Cleveland, OH.

Cullis, P.R. and Hope, M.J. (1985). in Biochemistry of Lipids and Membranes, (Vance, D. E. and Vance, J.E., eds.), pp. 25 - 72, Benjamin-Cummings Publ. Co., Inc., Reading, MA.

Dunn, F., Edmonds, P.D. and Fry, W.J. (1969). "Absorption and dispersion of ultrasound in biological media", in Biological Engineering, 6th edition (Schwan, ed.), pp. 205 - 332, McGraw-Hill, New York.

Dunn, F. and O'Brien, W.D., Jr. (1976). Ultrasonic Biophysics, Dowden, Hutchinson and Ross, Inc., Stroudsberg, PA.

Eggers, F. and Funck, Th. (1976). "Ultrasonic Relaxation Spectroscopy in Liquids", Naturwissenschaften, 63, 280 - 285.

Eggers, F., Funck, Th. and Richmann, K.H. (1978). "Improved Ultrasonic Resonator for Liquid Samples", Acustica, 40, 273 - 275.

Eigen, M. and de Maeyer, L. (1963). "Relaxation Methods", in Technique of Organic Chemistry, vol. VIII pt. 2, (Weissberger, A., ed.), Interscience, New York.

Fan, S-F, Dewey, M.M., Colflesh, D. and Chu, B. (1985). "The effects of deuterium oxide on the active cross-bridge motion of thick filaments isolated from striated muscle of Limulus", Biochim. Biophys. Acta., 830, 333 - 336.

Gamble, R.C., and Schimmel, P.R. (1978). "Nanosecond Relaxation Processes of Phospholipid Bilayers in the Transition Zone", Proc. Nat'l. Acad. Sci., 75, 3011 - 3014.

Griffith, O.H., Dehlinger, P.J. and Van, S.P. (1974). "Shape of the Hydrophobic Barrier of Phospholipid Bilayers", J. Memb. Biol., 15, 159 - 192.

Guard-Friar, D., Chen, C.H., and Engle, A.S. (1985). "Deuterium Isotope Effect on the Stability of Molecules: Phospholipids", J. Phys. Chem., 89, 1810 - 1813.

Hall, L. (1948). "The Origin of Ultrasonic Absorption in Water", Phys. Rev., 73, 775 - 781.

Hammes, G.G. and Roberts, P.B. (1970). "Ultrasonic Attenuation Measurements in Phospholipid Dispersions", Biochim. Biophys. Acta., 203, 220 -227.

Harkness, J.E. and White, R.D. (1979). "An Ultrasonic Study of the Thermotropic Transition of Dipalmitoyl Phosphatidylcholine", Biochim. Biophys. Acta., 552, 450 - 456.

Herzfeld, K.F. and Litovitz, T.A. (1959). Absorption and Dispersion of Ultrasonic Waves, Academic Press, New York.

Hirai, N. and Eyring, H. (1958). "Bulk Viscosity of Liquids", J. Appl. Phys., 29, 810 - 816.

Houslay, M.D. and Stanley, K.K. (1982). in Dynamics of Biological Membranes, pp. 281 - 322, John Wiley & Sons, New York.

IEEE Centennial Issue (1984). IEEE Trans. Sonics and Ultrasonics, 31, 536 - 669.

Jost, P., Libertini, L., Herbert, V.L. and Griffith, O.H. (1971). "Lipid Spin Labels in Lecithin Multilayers. A Study of Motion Along Fatty Acid Chains", J. Mol. Biol., 59, 77 - 98.

Kossoff, G. and Fukuda, M., eds., (1984). Ultrasonic Differential Diagnosis of Tumors, Igaku-Shoin, New York.

Labhardt, A. and Schwarz, A. (1976). "A High Resolution and Low Volume Ultrasonic Resonator Method for Fast Chemical Relaxation Measurements", Berlin Bunsenges, 80, 83 - 92.

Lamb, J. (1965). "Thermal Relaxation in Liquids", in Chp. 4 of Physical Acoustics, vol. II, (Mason, W.P., ed.), pp. 203 - 279, Academic Press, New York.

Litovitz, T.A. and Davis, C.M., (1965). "Structural and Shear Relaxation in Liquids", in Chp. 5 of Physical Acoustics, vol. II (Mason, W.P., ed.), pp. 282 - 348, Academic Press, New York.

Magin, R.L. and Niesman, M.R. (1984). "Temperature dependent Permeability of Large Unilamellar Liposomes", Chem. Phys. Lipids, 34, 245 - 256.

Magin, R.L. and Weinstein, J.N. (1984). in Liposome Technology, vol. III, (Gregoriadis, G., ed.), pp. 137 - 156, CRC Press, Inc., Boca Raton, FA.

Maynard, V.M. (1984). Ultrasonic Absorption by Liposomes Near the Phase Transition as a Function of Diameter, Ph.D. Thesis, University of Illinois.

Maynard, V.M., Magin, R.L., Dunn, F. (1985). "Ultrasonic Absorption and Permeability for Liposomes Near Phase Transition", Chem. Phys. Lipids, 37, 1 - 12.

Mitaku, S. and Okano, K. (1981). "Ultrasonic Measurements of Two-Component Lipid Bilayer Suspensions", Biophys. Chem., 14, 147 - 158.

Mitaku, S. and Sakka, T. (1987). in Ultrasonic Spectroscopy and its Applications to Materials Science, (Wada, Y., ed.), pp. 253 - 257, Japan.

Morse, P.D. II, (1985) in Structure and Properties of Cell Membranes, vol. III, (Benga, G., ed.), pp. 196 - 220, CRC Press Inc., Boca Raton, FL.

Muhleisen, M., Probst, W., Hayashi, K., and Rohmann, H. (1983). "Calcium Binding to Liposomes Composed of Negatively Charged Lipid Moieties", Japan J. Exp. Med., 53, 103 - 107.

Nagle, J.F. (1973). "Theory of Biomembrane Phase Transitions", J. Chem. Phys., 58, 252 - 264.

O'Brien, W.D., Jr., Erdman, J.W., Jr., and Hebner, T.B. (1988). "Ultrasonic propagation properties (@ 100MHz) in excessively fatty rat liver", J. Acoust. Soc. Am., 83(3), 1159 - 1166.

Olerud, J.E., O'Brien, W.D., Jr., Riederer-Henderson, M.A., Steiger, D., Forster, F.K., Daly, C., Ketterer, J. and Odland, G.F. (1987). "Ultrasonic assessment of skin and wounds with the scanning laser acoustic microscope", J. Invest. Dermatol., 88, 615 - 623.

Papahadjopoulos, D., Nir, S., and Ohki, S. (1972). "Permeability properties of phospholipid membranes: effects of cholesterol and temperature", Biochim. Biophys. Acta., 266, 561 - 583.

Papahadjopoulos, D., Portis, A.and Pangborn, W. (1978). in Liposomes and Their Uses in Biology and Medicine, vol. 308 (Papahadjopoulos, D., ed.), pp. 50 - 66, New York Academy of Sciences, New York.

Sano, T., Tanaka, J., Yasunaga, T. and Toyoshima, Y. (1982). "Studies on the Phase Transition in Single Lamellar Liposomes. 5. The Rapid Process of the Phase Transition.", J. Phys. Chem., 86, 3013 - 3016.

Sato, Y. and Fujino, M. (1987). "Inhibition of Arsenazo III Ca Transient with Deuterium Oxide in Frog Twitch Fibers at a Resting Sarcomere Length", Japan J. Physiol., 37, 149 - 153.

Strom-Jensen, P.R., Magin, R.L. and Dunn, F. (1984). "Ultrasonic Evidence for Structural Relaxation in Large Unilamellar Liposomes", Biochim. Biophys. Acta., 769, 179 - 186.

Szoka, F., Jr., and Papahadjopoulos, D. (1978). Procedure for Preparation of Liposomes with Large Internal Aqueous Space and High Capture by Reverse-Phase Evaporation", Proc. Nat'l. Acad. Sci. USA, 75, 4194 - 4198.

Vidaver, G.A. and Lee, J.W. (1983). "Rapid Stopping of A23187 action by phosphatidylcholine", FEBS Letters, 155 no. 1, 117 - 119.

VITA

Loralie Dawn Ma was born November 5, 1964, in Carbondale, Illinois. She entered the Early Admissions program at the University of Illinois, at Urbana-Champaign, in August, 1981. Ms. Ma completed her Bachelor of Science degree in biophysics in January, 1985 and at that time began her graduate studies in biophysics at the University of Illinois (U-C). She has held a Research Assistantship in the Department of Electrical and Computer Engineering since that time. In September, 1985, she entered the Medical Scholars Program at the University of Illinois and has completed her first year of medical school. Ms. Ma is a member of the American Medical Association (Medical student section).